PHOTOGRAPH THIS SHEET

LEVEL

INVENTORY

AD-A995210

DTIC ACCESSION NUMBER

AFSWP-121, Interim Rpt.-Part I
Contract DA-49-129-ENG-119

DOCUMENT IDENTIFICATION

Oct '51

DISTRIBUTION STATEMENT A
Approved for public release;
Distribution Unlimited

DISTRIBUTION STATEMENT

ACCESSION FOR
NTIS GRA&I
DTIC TAB
UNANNOUNCED
JUSTIFICATION

BY
DISTRIBUTION /
AVAILABILITY CODES

DIST	AVAIL AND/OR SPECIAL
A/1	

DISTRIBUTION STAMP

Released

DTIC COPY INSPECTED

UNANNOUNCED

DTIC
ELECTE
JUL 5 1984
S D
D

DATE ACCESSIONED

DATE RETURNED

84 07 05 003

DATE RECEIVED IN DTIC

REGISTERED OR CERTIFIED NO.

PHOTOGRAPH THIS SHEET AND RETURN TO DTIC-DDAC

OCTOBER 1951

INTERIM REPORT - PE-1

HE TESTS — OPERATION JANGLE

[PROJECT 1.(9)]

PREPARED FOR

OFFICE OF THE CHIEF OF ENGINEERS

DEPARTMENT OF THE ARMY

WASHINGTON, D. C.

Contract DA-49-129-eng-119

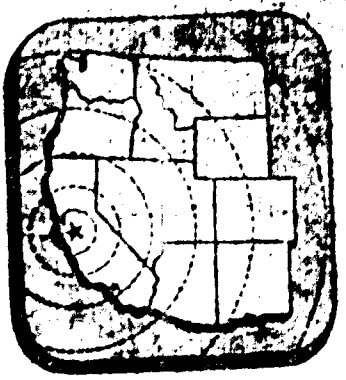

STANFORD RESEARCH INSTITUTE

STANFORD, CALIFORNIA

October 1951

Interim Report

HE TESTS - OPERATION JANGLE
Project 1(9)

by

E. B. Doll and D. C. Sachs

STANFORD RESEARCH INSTITUTE Project 424, WALRUS
Contract Project DA-49-129-Eng-119

Prepared for

OFFICE OF THE CHIEF OF ENGINEERS
WASHINGTON, D. C.

Approved:

E. B. Doll
Chairman, Department of Applied Physics
Stanford Research Institute

Ralph A. Krause
Director of Research
Stanford Research Institute

Copy No. 12

[redacted]

TABLE OF CONTENTS

[redacted]

[redacted]

TABLE OF CONTENTS

FIGURES

[redacted]

[redacted]

TABLE OF CONTENTS

TABLES

APPENDIX

[redacted]

[redacted]

October 5, 1951

STANFORD RESEARCH INSTITUTE

Interim Report

HE TESTS - OPERATION JANGLE

I. INTRODUCTION

This Interim Report describes the results of free-earth acceleration, earth pressure, and air-blast measurements made during the four HE (High Explosive - TNT) tests of OPERATION JANGLE. These tests were performed during August and September, 1951 at the Nevada Proving Ground of the Atomic Energy Commission (Site Mercury, Yucca Flat). The report covers the following subjects:

A. Description of the tests.

B. Description of the instrumentation.

C. Partial results in tabular and graphical form, including individual transient gage records.

D. Preliminary discussion of results with some general comments.

Because of the complexity and the amount of data obtained, this Interim Report covers only the information considered to be of immediate importance and which could be summarized or analyzed quickly. In particular, the following data are omitted from this report:

1. Auxiliary earth-pressure measurements.*

2. Free earth accelerations other than those at five-foot gage depths.

3. Earth pressures as measured by Carlson-Wiancko diaphragm-type gages (in cooperation with the Sandia Corporation).

4. Permanent displacement of concrete monuments adjacent to accelerometers.

5. Transient free-earth velocities and displacements as might be obtained by integration of accelerometer records.

A total of 264 transient gage records were obtained on the four tests, of which the results of 196 channels are presented in this Interim Report. It is intended that the Final Report will describe all tests conducted and it will report all results obtained. There is some possibility that integrations will be made of some of the free-earth acceleration records.

---

* The only earth-pressure measurements reported are those obtained with gages in holes five feet deep and filled to the top with an Aquagel solution.

[redacted]

[redacted]

A. General Description of Tests

The four explosions with which this report is concerned were as follows:

Test Number	Pounds of TNT W	$W^{1/3}$	Depth of Charge ft.	λ_c	Date
HE-1	2,560	13.8	1.9	0.135	August 25, 1951
HE-2	40,000	34.2	4.7	0.135	September 3, 1951
HE-3	2,560	13.8	6.9	0.5	September 15, 1951
HE-4	2,560	13.8	-1.9	-0.135	September 9, 1951

The explosive charges were composed of 100-pound TNT blocks stacked to approximate a sphere. The lines of gages were perpendicular to one of the flatter sides of the stack. On HE-1 and HE-2 the charge depth was such that the top of the charge was essentially flush with the ground surface. On HE-4 no excavation was made for the charge, and the bottom of the TNT sphere was flush with the ground surface (surface shot). The charge depth was measured to the center of the charge, and λ_c represents the ratio of the charge depth in feet to the cube root of the pounds of TNT.

The gage patterns were arranged as nearly as possible in a radial line from ground zero. In each test the free-earth accelerometers were installed on a radial line, and the distance between gage holes at any one radius was approximately three feet. The gage lines for HE-1, HE-3, and HE-4 were parallel and approximately 30 degrees from the gage line for HE-2. Figure 1 illustrates the general test area and gage-line layout for the four tests.

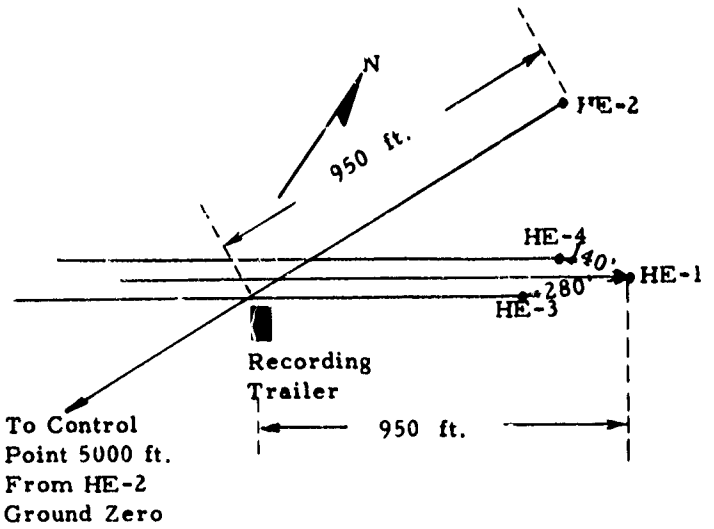

Figure 1. General Test Area and Gage-Line Layout

[redacted]

[redacted]

For all practical purposes, the test area was flat. The soil appeared to consist of extremely fine, powder-like sand mixed with some gravel. Below the surface there were one or more streaks of localized "Caliche" deposits*. The sub-surface soil was tightly packed, very dry, and extremely porous. There was no water table and the bed-rock was at a depth of about 1,000 feet. Preliminary seismic survey data gave the following results for the seismic velocity and soil constant**.

Depth ft.	Seismic Velocity f.p.s.	Soil Constant lbs./in.^{2}
0 - 100	3,000	8,400
100 - 350	4,000 - 4,500	15,000 - 19,000
350 - 1,000	5,000 - 5,500	23,000 - 28,000

A complete geological survey of the test site has been conducted by another agency, but this information is not available for inclusion in this Interim Report.

B. Purpose of the Tests

The four tests were conducted for the following principal purposes:

1. To establish a better basis for the prediction of corresponding phenomena from anticipated larger explosions under similar conditions at the same test site.

2. To establish correlation between future explosion tests at this site with similar tests conducted at the Dugway Proving Ground.

3. To obtain additional information on air-earth energy coupling as a function of the charge depth.

4. To obtain additional information in the general field of underground explosion phenomena with respect to such things as attenuation characteristics, wave forms, and scale and model laws.

C. Instrumentation Plan

It has been found convenient, in working with explosion phenomena, to describe distances in terms of the total energy contained in the explosion. The parameter λ is defined as follows: $R = \lambda W^{1/3}$, where R is a distance measured in feet and W is the weight of explosive in equivalent

---

* Hard, cemented conglomerate of geologically recent origin.

** Soil constant is used as defined in OSRD Report No. 6645, "Final Report on Effects of Underground Explosions," by C. W. Lampson.

[redacted]

pounds of TNT. This term, λ, is used frequently in this report. For HE-1, HE-3, and HE-4, λ values may be converted to feet by multiplying by 15.8. For HE-2 the multiplication factor is 34.2.

In general, the region of military interest in underground explosions does not extend beyond λ = 10. However, measurements at much greater distances are frequently desirable to assist in the prediction of similar effects for still larger charges. For this reason, the single radial gage lines used for each of the four tests extended to a distance of approximately 2,000 feet, although most of the instrumentation was confined to the region of λ less than 10. The free-earth accelerometers were located five feet below the surface, and two components of acceleration were determined at each gage station -- vertical and horizontal radial. The earth-pressure measurements were made at a depth of five feet, whereas the air-pressure measurements were made at a height of 14 inches above the ground surface.

The instrumentation pattern used for each test is evident in the tables of test results.

II. INSTRUMENTATION*

A. General System

The gages used to measure acceleration, hydrostatic pressure, and air pressure all contain the same variable-reluctance transducer element. For all practical purposes, these gages are electrically identical, differing only in the mechanism used to actuate the basic displacement transducer element (Figure 2). Rotation of the armature, A, increases one inductance while it decreases the other, introducing an inductance unbalance.

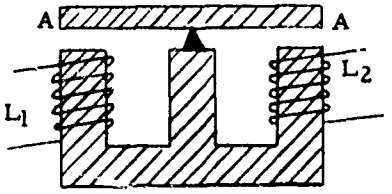

Figure 2. Basic Variable-Reluctance Element

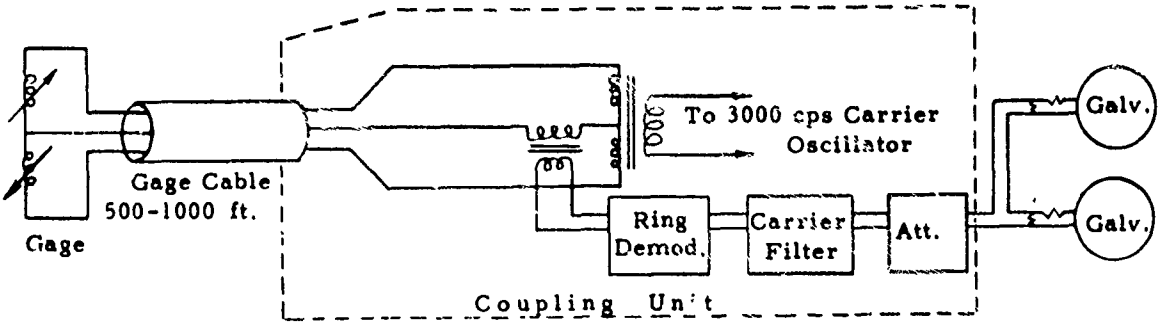

Figure 3. Typical Gage Channel

Figure 3 illustrates one complete gage channel. The variable-reluctance gage is connected to the coupling and control circuit by a three-conductor shielded microphone cable 500-1,000 feet in length. Carrier energy at 3,000 cps is supplied to the gage from a very low impedance source. The signal produced by the gage inductance unbalance is fed to a conventional ring demodulator, and the demodulated output contains the original signal frequencies from zero to an upper cut-off frequency determined either by the gage or by the carrier frequency. The over-all system is essentially linear to 150 per cent of gage rating.

The demodulated output current (7ma. into 85 ohms at gage rating) of the ring demodulator is more than sufficient for the operation of the galvanometer element of a conventional re-

* The pressure gages and accelerometers were manufactured by the Wiancko Engineering Company, and the recording oscillographs were made by the William Miller Corporation, both of Pasadena, California.

cording optical oscillograph. For this reason no vacuum tube amplifiers are required; in fact the output level is sufficient to permit the use of dual recording galvanometers, whereby the signal current is divided between two galvanometers of different effective sensitivities. These sensitivities were selected so that the gage produced two recorded traces with a constant amplitude ratio of about six to one. If the phenomenon to be recorded is appreciably higher than anticipated, the low sensitivity trace yields a usable record, whereas for low signals the high sensitivity trace is useful. Because of the extremely low noise level of this gage system (probably 60 to 100 db below rated output), this dual recording technique gives a great dynamic range for a single gage a feature of particular value in measuring underground explosion phenomena where predicted magnitudes are quite uncertain.

A single 3,000 cps regulated vacuum tube oscillator is used to supply a coupling unit feeding 12 gage channels. Six such units were used, providing a total of 72 gage channels, of which 60 were connected to dual recording galvanometers and 12 to single galvanometers. A total of 132 active galvanometer traces were available for each test, although all channels were not used on every test. These galvanometers were contained in five oscillographs, each producing records on sensitive paper 12-inches wide. The six carrier oscillators were synchronized to prevent background interference due to intercarrier beats.

The five recording oscillographs (or cameras), the six 12-channel variable-reluctance gage coupling units, the six carrier power oscillators, and miscellaneous control circuits were mounted in a small recording trailer designed for remote operation. This trailer was placed in a fixed protective shelter which was located 630 to 950 feet from the ground zeros. This unattended recording station permitted the use of much shorter gage cables, thus improving the gage performance while effecting great savings both in the cost of gage cable and in the labor of laying and picking up the cable for each test. The recording trailer was operated through a single multi-conductor control cable connected to the central control point used for firing in each of the four tests. The control point was approximately 5,000 feet from ground zero. Under automatic operation a calibration signal was introduced into each recording channel when the recording cameras were started.

B. Earth Acceleration

The basic variable-reluctance transducer element is converted to a linear accelerometer by the addition of a mass to one side of the armature with a suitable restoring spring. Accelerometers having the following nominal rated outputs and natural frequencies were used:

Rated Output (G units)	Natural Frequency (Damped) (cycles per second)
30	190
5	80
1	45
0.5	26

The damping of each accelerometer was adjusted to 60-70 per cent of critical at 70° F, which corresponded quite closely to the ground temperature at the five-foot gage depth used.

The recording galvanometers used for each accelerometer depended both on the gage rating and on the anticipated value of acceleration. However, in each case the galvanometers were adjusted to 70-80 per cent of critical damping and the galvanometer natural frequency was well above that of the associated accelerometer. It may be assumed that the upper frequency response limit of each accelerometer gage channel was determined by the accelerometer used.

For the measurement of earth acceleration, two mutually perpendicular gages were mounted in a single canister as shown in Figure 4. Suitable damping was provided by wooden blocks inside the canister to eliminate ringing upon shock excitation. The average canister density was adjusted to be approximately equal to the soil in which it was placed.

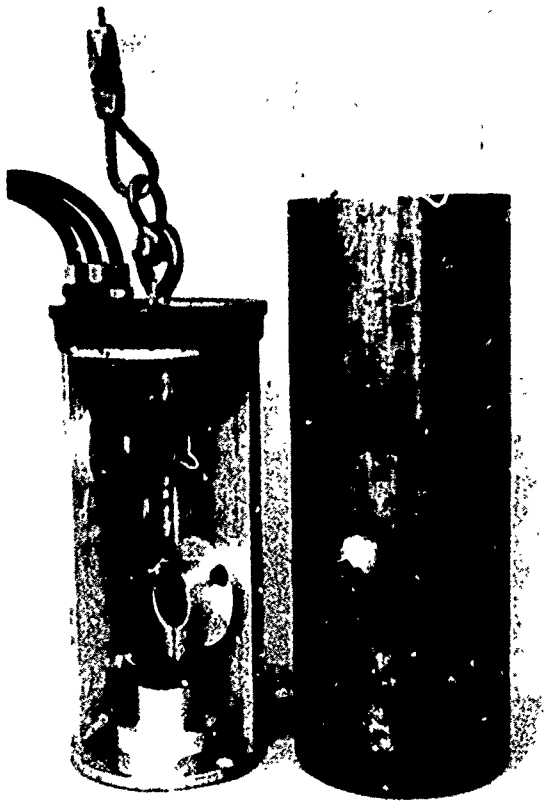

Figure 4. Earth-Acceleration Canister

Each canister was installed and oriented at the bottom of a hole in the ground six inches in diameter, at a nominal gage depth of five feet. On the HE-1 and HE-2 tests the canisters were cemented in the holes with calseal, a quick-setting gypsum cement. Some holes were then filled and packed with dirt and others were left open. No difference was detected in the accelerometer output attributed to air blast.

Because of the very extensive effort involved in the recovery of the cemented canisters as well as unavoidable damage to them, a single additional test canister was installed by careful tamping with damp earth on HE-2. There were no significant differences between the records obtained from this unit and those obtained from a cemented canister located alongside. Hence it was decided that tamped damp earth could be used for the accelerometer installations on HE-3 and HE-4. After the earth around the canister was tamped, the gage holes were filled and tamped with additional earth. On both HE-3 and HE-4, a single canister was cemented for control purposes.

Since each accelerometer gage channel has a static response, it was possible to calibrate the gages by rotation in the earth's gravitational field just prior to installing the canister in the hole, with all connections made to the gage cable and recording channel to be used for the explosion test.

C. Earth Pressure

The basic variable-reluctance transducer element is converted to a hydrostatic-pressure gage by fastening the armature to a slightly twisted Bourdon tube. The gage is filled with oil to give 60 to 70 per cent of critical damping at 70° F, and the gage is intended for use immersed in similar oil. Behind the Bourdon tube is a controlled "air-bubble," followed by a "porous plug" having a time-constant of 15 minutes to 2 hours, which permits the relief of a true static pressure.

Figure 5. Earth-Pressure Gage

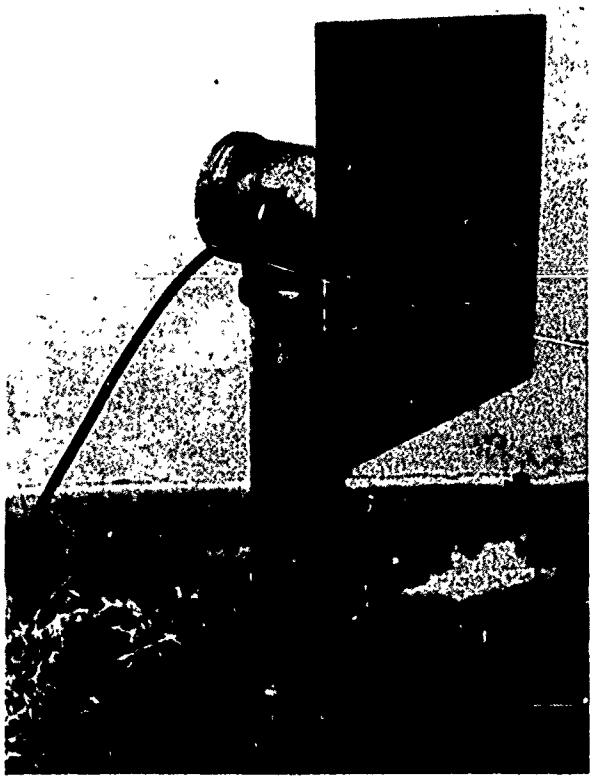

Figure 6. Air-Blast Pressure Gage

An earth-pressure gage is shown in Figure 5. The pressure gage is placed in a five-inch diameter, flexible Neoprene bag which is filled with oil having the proper viscosity for damping at the operating temperature. This gage then measures the hydrostatic pressure of the oil contained in the closed Neoprene bag.

Hydrostatic pressure gages having nominal ratings of 100, 10, and 1 psi were utilized. The rise times of the gages were such that the ultimate high-frequency response was determined by

the particular recording galvanomenters used. All recording galvanomenters were adjusted to 70-80 per cent of critical damping, and galvanometers having natural frequencies of 120, 230, and 340 cps were included. Examination of the pressure records shows very few instances of frequency components approaching 100 cps.

All ground pressure data included in this report were obtained with the oil bag located near the bottom of a five-foot hole six inches in diameter. Each hole was filled to the top with a thin solution of Aquagel. The Aquagel solution was adjusted to minimize the loss of liquid into the surrounding porous earth. The holes were examined immediately after each test, and in no case had the liquid level dropped more than a few inches.

D. Air-Blast Pressure

The basic variable-reluctance transducer element is converted to an air-pressure gage by fastening the armature to a slightly twisted Bourdon tube. A "porous plug" having a time constant of 30-90 seconds is used for static equilibrium. Silicone grease in the armature gap along with acoustic damping gives a net damping of 60-70 per cent of critical. The rise time of the gages used was approximately 0.0003 second, and hence the over-all rise time of each air-blast channel was determined by the single 340 cps recording galvanometer used for all air-blast measurements at 70 per cent of critical damping.

The air-blast was measured by mounting an air-pressure gage flush with the surface at the center of a 12-inch by 12-inch by 0.5-inch steel plate. This steel plate was then mounted vertically in a radial plane passing through ground zero as shown in Figure 6. The gage center was approximately 14 inches above the ground surface.

It is worth noting that the air-blast measurements were of a secondary nature and that it was not possible to provide a smooth, hard blast line for this measurement.

III. RESULTS

The following tables present summary results obtained from the four tests. In general, each gage channel gave a complex record of amplitude versus time. The description of such a complex curve by a few numbers is necessarily incomplete, and sometimes misleading. For a better understanding of the results, the reader is referred to the Appendix where the individual gage records are presented.

Figure 7 shows the explosive charge position with respect to the ground surface for each test.*

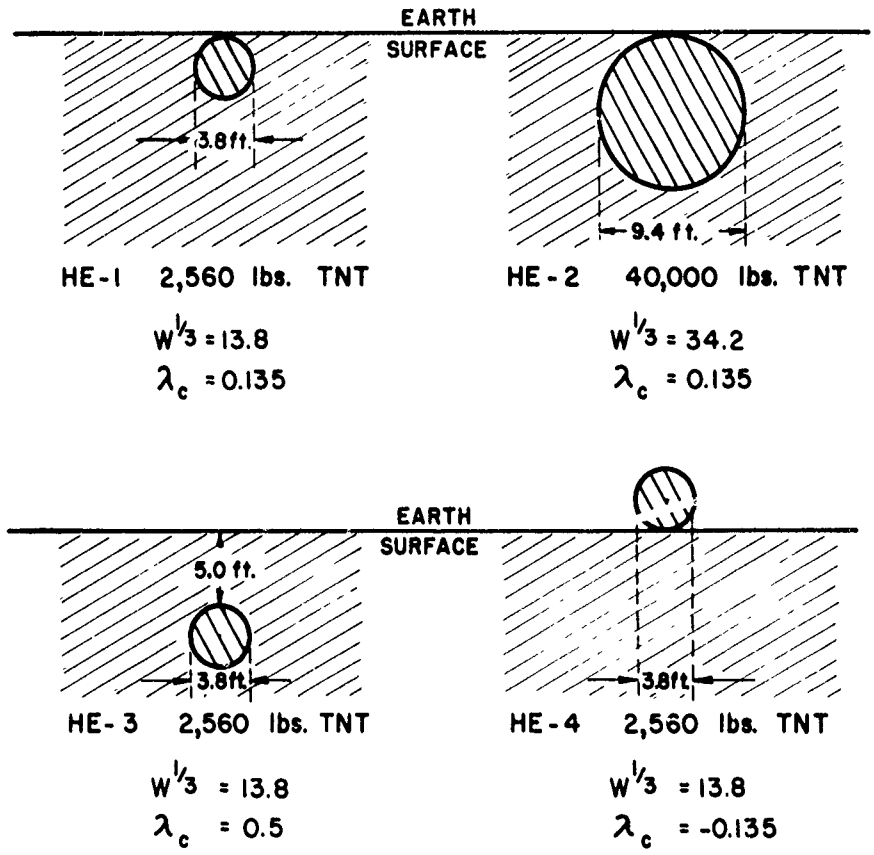

Figure 7. Explosive Charges

* See Page 2 for a description of each test.

The following terminology is used in the tables:

Earth Acceleration - gage depth five feet.
Horizontal - (H) - horizontal radial component (longitudinal) - positive is outward.
Vertical - (V) - vertical component - positive is upward.

Earth Pressure - (P) - gage depth five feet - holes five feet deep filled with Aquagel solution - positive for increasing pressure.

Air-Blast - (B) - side-on - gage height 14 inches - positive for increasing pressure.

Gage Code No. - for identification purposes - indicates gage position on gage line and identifies records in Appendix.

Gage Rating - (G units or psi) - for accelerometer this determines gage channel high frequency response.*

Radius - horizontal distance from ground zero to gage location.
R - feet
λ - from $R = \lambda W^{1/3}$, where W is charge weight in equivalent pounds of TNT.

Arrival Time - (sec.) - time of first arrival of any signal at gage. Zero time determined from first interruption in the firing line to the electric blasting cap used for detonating each charge.

First Peak - (G units or psi) - amplitude of first peak recorded. In general this describes the first significant peak as determined from a study of all records of one kind from a single test. It appears that this is the only amplitude measurement that can be measured on all records with a reasonable assurance of its being derived from the same driving and transmission functions. Except as otherwise noted, the first peak was positive.

First Pulse Duration - (sec.) - elapsed time between arrival time and first zero crossover. In some cases the crossover used was dependent upon study of all records of one kind from a single test.

Max. Pos. Peak - (G units or psi) - maximum positive peak, regardless of when it occurred.

Max. Neg. Peak - (G units or psi) - maximum negative peak, regardless of when it occurred.

---

* See Page 6 for accelerometer natural frequencies.

[redacted]

TABLE I

HE-1 EARTH ACCELERATION
(Gage Depth = 5 Feet)

Gage Code No.	Gage Rating (G)	Radius ft.	Radius λ	Arrival Time (sec.)	First Peak (G)	First Pulse Duration (sec.)	Max. Pos. Peak (G)	Max. Neg. Peak (G)
			HORIZONTAL					
2H	30	28.4	2.08	.008	11.3	.016	11.9	7.5
3H	30	34.0	2.49	.009	7.2	.019	13.5	6.8
4H	40	41.0	3.0	.010	4.3	.017	7.0	6.0
5H	30	49.5	3.62	.013	3.3	.019	8.5	6.6
6H	5	58.8	4.3	.014	2.9	.023	3.6	4.3
7H	5	71.1	5.2	.017	3.2	.025	4.1	4.5
8H	5	85.5	6.25	.020	2.3	.021	2.8	2.6
9H	5	102.5	7.5	.027	1.9	.017	1st	2.9
10H	1	123	9.0	.032	1.3	.018	1st	2.0
11H	0.5	148	10.8	.036	0.67	.022	1st	0.60
12 H	0.5	178	13.0	.041	0.50	.029	1st	0.59
13 H	1	217	15.9	.051	0.34	.022	1st	0.56
14 H	1	262	19.2	.061	0.24	.031	--	--
15 H	0.5	314	23.0	.069	0.14	.033	--	--
16 H	0.5	378	27.6	.088	0.062	.024	--	--
17 H	0.5	542	39.6	.123	0.073	.038	--	--
18 H	0.5	788	57.5	.186	0.044	.046	0.057	0.059
19 H	0.5	1025	75.0	.255	0.043	.050	0.13	0.14
20 H	0.5	1480	108.0	.383	0.025	.052	0.045	0.059
			VERTICAL					
2V	30	28.4	2.08	.009	1.3	.012	7.7	3.3
3V	30	34.0	2.49	.009	2.6	.017	5.0	3.6
4V	30	41.0	3.0	.010	1.8	.022	3.0	4.4
5V	30	49.5	3.62	.013	0.92	.018	5.9	5.8
6V	5	58.8	4.3	.015	0.74	.021	1.2	2.9
7V	5	71.1	5.2	.018	0.49	.016	4.8	0.58
8V	5	85.5	6.25	.021	0.67	.017	3.8	2.1
9V	5	102.5	7.5	.026	0.32	.015	1.3	1.2
10V	1	123	9.0	.033	0.25	.017	0.51	0.58
11V	0.5	148	10.8	.036	0.10	.021	0.46	0.55
12V	0.5	178	13.0	.043	0.13	.019	0.31	0.27
13V	1	217	15.9	.051	0.079	.019	0.25	0.22
14V	1	262	19.2	.061	0.080	.014	--	--
15V	0.5	314	23.0	.071	0.030	.027	0.15	0.16
16V	0.5	378	27.6	.085	0.016	.029	0.083	0.076
17V	0.5	542	39.6	.128	0.0084	.034	0.068	--
18V	0.5	788	57.5	.186	0.0097	.056	0.046	0.042
19V	0.5	1025	75.0	.265	0.012	.043	0.067	0.048
20V	0.5	1480	108.0	.388	0.010	.044	0.034	0.020

[redacted]

[redacted]

TABLE II

HE-1 EARTH PRESSURE
(Gage Depth = 5 Feet)

Gage Code No.	Gage Rating (psi)	Radius ft.	Radius λ	Arrival Time (sec.)	First Peak (psi)	First Pulse Duration (sec.)	Max. Pos. Peak (psi)	Max. Neg. Peak (psi)
3PF	100	34.0	2.49	.011	5.7	.036	6.1	2.4
6PF	10	58.8	4.3	.016	1.5	.026	2.4	1.5

TABLE III

HE-1 AIR-BLAST PRESSURE
(Gage Height = 14 Inches)

Gage Code No.	Gage Rating (psi)	Radius ft.	Radius λ	Arrival Time (sec.)	First Peak (psi)	First Pulse Duration (sec.)
3B	10	34.0	2.49	.018	13.3	.012
6B	10	58.8	4.3	.032	11.4	.019
9B	10	102.5	7.5	.061	6.4	.024
12B	10	178	13.0	.118	4.2	.036
15B	10	314	23.0	.225	2.0	.040
17B	10	542	39.6	.413	0.89	.054
19B	10	1025	75.0	.824	0.36	.056

[redacted]

[redacted]

TABLE IV

HE-2 EARTH ACCELERATION
(Gage Depth = 5 Feet)

Gage Code No.	Gage Rating (G)	Radius ft.	Radius λ	Arrival Time (sec.)	First Peak (G)	First Pulse Duration (sec.)	Max. Pos. Peak (G)	Max. Neg. Peak (G)
			HORIZONTAL					
32H	30	71.1	2.08	.015	8.0	.037	1st	2.2
33H	30	85.5	2.49	.019	4.2	.030	1st	2.8
34H	5	102.5	3.0	.024	2.9	.035	1st	2.7
35H	5	123	3.62	.031	2.5	.038	1st	3.7
36H	5	148	4.3	.038	2.0	.037	1st	4.8
37H	5	178	5.2	.046	1.3	.038	1st	2.5
38H	5	217	6.35	.058	0.90	.040	1.4	2.1
39H	5	262	7.66	.070	0.60	.041	1.4	1.2
40H	5	314	9.2	.088	0.45	.045	0.70	0.85
41H	5	378	11.1	.106	0.31	.046	1.3	0.29
42H	1	512	15.0	.145	0.18	.057	0.49	0.22
43H	1	788	23.0	.252	0.12	.052	0.17	0.18
44H	1	1025	30.0	.327	0.050	.056	0.055	0.10
45H	0.5	1480	43.3	.456	0.036	.053	0.040	0.064
			VERTICAL					
32V	30	71.1	2.08	.016	1.3	.015	7.0	13.0
33V	30	85.5	2.49	.021	1.3	.020	3.15	5.6
34V	5	102.5	3.0	.025	1.0	.030	9.2	4.4
35V	5	123	3.62	.035	0.63	.032	7.6	5.5
36V	5	148	4.3	.041	0.39	.030	3.0	6.5
37V	5	178	5.2	.050	0.34	.031	2.1	4.2
38V	5	217	6.35	.062	0.13	.030	2.5	2.9
39V	5	262	7.66	.080	0.080	.027	2.0	2.2
40V	5	314	9.2	.095	0.063	.032	1.0	1.0
41V	5	378	11.1	.115	0.040	.037	1.5	1.4
42V	1	512	15.0	.155	0.043	.033	1.1	1.0
43V	1	788	23.0	.257	0.035	.047	0.30	0.19
44V	1	1025	30.0	.330	0.038	.050	0.22	0.13
45V	0.5	1480	43.3	.456	0.040	.050	0.070	0.10

[redacted]

[redacted]

TABLE V

HE-2 EARTH PRESSURE
(Gage Depth = 5 Feet)

Gage Code No.	Gage Rating (psi)	Radius ft.	Radius λ	Arrival Time (sec.)	First Peak (psi)	First Pulse Duration (sec.)	Max. Pos. Peak (psi)	Max. Neg. Peak (psi)
31P	100	58.8	1.72	.014	24.2	.053	1st	4.9
32P	100	71.1	2.08	.017	14.2	.068	1st	4.8
33P	100	85.5	2.49	.019	6.5	.062	1st	2.8
34P	10	102.5	3.0	.024	5.4	.068	1st	3.4
36P	10	148	4.3	.037	2.9	.032	9.2	2.6
38P	1	217	6.35	.057	1.1	.033	3.0	1.7
41P	1	378	11.1	.104	0.13	.042	>0.87	1.1

TABLE VI

HE-2 AIR-BLAST PRESSURE
(Gage Height = 14 Inches)

Gage Code No.	Gage Rating (psi)	Radius ft.	Radius λ	Arrival Time (sec.)	First Peak (psi)	First Pulse Duration (sec.)
33B	100	85.5	2.49	.037	21.4	.034
36B	10	148	4.3	.075	13.4	.053
38B	10	217	6.35	.119	10.1	.062
41B	10	378	11.1	.237	5.1	.082
42B	10	512	15.0	.342	3.3	.095
44B	10	1025	30.0	.763	1.35	.130

[redacted]

[redacted]

TABLE VII

HE-3 EARTH ACCELERATION
(Gage Depth = 5 Feet)

Gage Code No.	Gage Rating (G)	Radius ft.	Radius λ	Arrival Time (sec.)	First Peak (G)	First Pulse Duration (sec.)	Max. Pos. Peak (G)	Max. Neg. Peak (G)
			HORIZONTAL					
52H	30	28.4	2.08	.007	36.9	.015	1st	13.0
53H	30	34.0	2.49	.009	13.9	.018	1st	7.2
54H	30	41.0	3.0	.010	8.2	.019	1st	5.9
55H	30	49.5	3.62	.013	7.3	.019	7.6	5.0
56H	30	58.8	4.3	.015	5.5	.019	8.0	3.7
57H	30	71.1	5.2	.018	5.4	.017	1st	2.7
58H	5	85.5	6.25	.022	4.0	.018	1st	2.7
59H	5	102.5	7.5	.025	4.3	.018	1st	2.5
60H	5	148	10.8	.034	1.7	.022	1st	1.7
61H	5	178	15.9	.041	1.1	.025	1st	1.2
62H	5	314	23.0	.071	0.38	.021	0.52	0.44
63H	1	542	39.6	.127	0.12	.043	0.37	0.22
64H	0.5	1340	98.2	.342	0.037	.055	0.065	0.084
			VERTICAL					
52V	30	28.4	2.08	.008	20.2	.022	1st	4.3
53V	30	34.0	2.49	.008	4.4	.040	4.6	3.0
54V	30	41.0	3.0	.010	4.3	.018	6.1	1.5
55V	30	49.5	3.62	.014	2.2	.018	8.5	2.2
56V	30	58.8	4.3	.015	1.5	.019	7.0	1.7
57V	30	71.1	5.2	.018	1.6	.017	1st	1.4
58V	5	85.5	6.25	.020	1.5	.019	1st	1.0
59V	5	102.5	7.5	.025	0.80	.018	1.3	0.76
60V	5	148	10.8	.035	0.35	.015	0.83	0.48
61V	5	178	15.9	.042	0.25	.018	0.81	0.35
62V	5	314	23.0	.071	0.084	.024	0.20	0.25
63V	1	542	39.6	.127	0.0089	.036	0.16	0.10
64V	0.5	1340	98.2	.355	0.012	.044	0.029	0.032

[redacted]

[redacted]

TABLE VIII

HE-3 EARTH PRESSURE
(Gage Depth = 5 Feet)

Gage Code No.	Gage Rating (psi)	Radius ft.	Radius λ	Arrival Time (sec.)	First Peak (psi)	First Pulse Duration (sec.)	Max. Pos. Peak (psi)	Max. Neg. Peak (psi)
51P	100	23.5	1.72	.006	146	.028	1st	5.0
52P	100	28.4	2.08	.007	44	.030	1st	4.1
53P	100	34.0	2.49	.009	26.6	.028	1st	3.6
54P	100	41.0	3.0	.010	8.3	.026	1st	2.8
55P	100	49.5	3.62	.013	8.0	.028	1st	2.1
56P	10	58.8	4.3	.014	3.3	.021	5.0	2.1
57P	10	71.1	5.2	.018	3.4	.017	4.7	2.5
58P	10	85.5	6.25	.020	3.0	.020	5.3	2.3
59P	10	102.5	7.5	.026	1.3	.020	1.9	2.1
60P	10	148	10.8	.034	1.1	.021	1.4	1.2
61P	1	178	15.9	.040	1.1	.020	2.8	1.8
62P	1	314	23.0	.068	0.36	.029	0.98	0.82
63P	1	542	39.6	.122	0.056	.038	0.79	0.43

TABLE IX

HE-3 AIR-BLAST PRESSURE
(Gage Height = 14 Inches)

Gage Code No.	Gage Rating (psi)	Radius ft.	Radius λ	Arrival Time (sec.)	First Peak (psi)	First Peak Duration (sec.)	Max. Pos. Peak (psi)	Pos. Phase Duration (sec.)	Max. Neg. Peak (psi)
52B	10	28.4	2.08	.022	1.2	.011	4.2	.027	1.1
54B	10	41.0	3.0	.033	0.82	.008	4.2	.029	1.1
56B	10	58.8	4.3	.047	0.57	.009	3.8	.029	0.94
58B	10	85.5	6.25	.070	0.41	.007	3.1	.029	0.74
60B	10	148	10.8	.124	none	--	2.0	.030	0.41
61B	10	178	15.9	.148	none	--	1.4	.031	0.36
62B	10	314	23.0	.260	none	--	0.73	.032	0.18
63B	10	542	39.6	.453	none	--	0.43	.039	0.12

[redacted]

[redacted]

TABLE X

HE-4 EARTH ACCELERATION
(Gage Depth = 5 Feet)

Gage Code No.	Gage Rating (G)	Radius ft.	Radius λ	Arrival Time (sec.)	First Peak (G)	First Pulse Duration (sec.)	Max. Pos. Peak (G)	Max. Neg. Peak (G)
			HORIZONTAL					
72H	30	28.4	2.08	.007	6.2	.009	6.4	7.5
73H	30	34.0	2.49	.008	10.6	.004	13.4	12.0
74H	30	41.0	3.0	.009	10.0	.006	1st	8.4
75H	30	49.5	3.62	.010	6.0	.005	6.7	7.4
76H	5	58.8	4.3	.012	3.1	.005	4.0	5.2
77H	5	71.1	5.2	.015	2.0	.005	1st	2.1
78H	5	85.5	6.25	.018	1.5	.008	1.7	2.1
79H	5	102.5	7.5	.023	1.9	.008	1st	3.0
80H	5	148	10.8	.034	0.69	.015	1st	0.92
81H	5	178	15.9	.041	0.50	.016	0.92	0.61
82H	5	314	23.0	.068	0.12	.024	0.19	0.21
83H	1	542	39.6	.125	0.030	.039	0.13	0.15
84H	0.5	1480	108	.380	0.015	.039	0.018	0.040
			VERTICAL					
72V	30	28.4	2.08	.007	-29.0	.005	23.2	1st
73V	30	34.0	2.49	.008	-25.8	.006	26.2	1st
74V	30	41.0	3.0	.010	-23.5	.005	16.4	1st
75V	30	49.5	3.62	.011	-14.8	.009	16.5	1st
76V	5	58.8	4.3	.012	-10.2	.008	9.1	1st
77V	5	71.1	5.2	.016	-5.8	.008	4.0	1st
78V	5	85.5	6.25	.019	-5.[illegible]	.005	3.7	1st
79V	5	102.5	7.5	.024	0.24	.006	3.7	4.2
80V	5	148	10.8	.034	0.49	.013	1.8	1.5
81V	5	178	15.9	.040	0.14	.011	0.90	1.3
82V	5	314	23.0	.067	0.019	.021	1.4	0.44
83V	1	542	39.6	.125	0.0045	.027	0.23	0.16
84V	0.5	1480	108	.388	0.006	.042	0.034	0.022

[redacted]

[redacted]

TABLE XI

HE-4 EARTH PRESSURE
(Gage Depth = 5 Feet)

Gage Code No.	Gage Rating (psi)	Radius ft.	Radius λ	Arrival Time (sec.)	First Peak (psi)	First Pulse Duration (sec.)	Max. Pos. Peak (psi)	Max. Neg. Peak (psi)
71P	100	23.5	1.72	.005	19.7	.049	1st	2.4
72P	100	28.4	2.08	.006	27.4	.060	1st	3.4
73P	10	34.0	2.49	.007	17.0	.041	1st	3.3
74P	10	41.0	3.0	.008	15.2	.041	1st	2.2
75P	10	49.5	3.62	.010	12.9	.044	1st	2.1
76P	10	58.8	4.3	.012	7.4	.045	1st	2.0
77P	10	71.1	5.2	.014	13.3	.044	1st	2.5
78P	10	85.5	6.25	.018	1.9	.044	6.8	2.3
79P	1	102.5	7.5	.022	1.4	.046	5.1	1.8
80P	1	148	10.8	.034	0.56	.014	2.9	1.4
81P	1	178	15.9	.040	0.64	.014	3.0	1.4
82P	1	314	23.0	.068	0.094	.021	2.0	1.1
83P	1	542	39.6	.124	0.015	.055	0.88	0.68

TABLE XII

HE-4 AIR-BLAST PRESSURE
(Gage Height = 14 Inches)

Gage Code No.	Gage Rating (psi)	Radius ft.	Radius λ	Arrival Time (sec.)	First Peak (psi)	First Pulse Duration (sec.)
72B	100	28.4	2.08	.003	106*	--*
74B	100	41.0	3.0	.006	85**	--**
76B	100	58.8	4.3	.011	19.0	.020
78B	100	85.5	6.25	.019	13.4	.006
80B	10	148	10.8	.056	6.2	.040
81B	10	178	15.9	.077	3.9	.043
82B	10	314	23.0	.184	1.8	.049
83B	10	542	39.6	.369	1.0	.056

* Questionable. Cable torn loose from gage shortly after air-blast arrival.
** Questionable. Gage record failed to return to zero following passage of air-blast.

[redacted]

IV. PRELIMINARY ANALYSIS AND COMMENTS

A. General

For this Interim Report the preliminary analysis of results is confined largely to the amplitude of the first significant peaks of earth acceleration, earth pressure, and air-blast pressure, with some consideration given to the arrival time of earth acceleration. A more detailed analysis must give consideration to may other factors. A more comprehensive analysis of the results will be a principal subject of the Final Report. In the meantime, the reader is referred to the Appendix. This Appendix consists of copies of the actual gage records, as recorded, presenting earth acceleration, earth pressure, and air-blast pressure as functions of time. These 196 records contain a wealth of information concerning wave form variation as a function of distance, frequency content as a function of charge size, late arrival earth phenomena, and other interesting characteristics.

For most purposes it is believed that the first significant peak of earth acceleration and earth pressure is of principal importance. In most cases, the first peak is also the maximum peak in the region of military interest, λ less than 10. An examination of all the records of one phenomenon from a single test shows that the first cycles of earth acceleration and earth pressure have wave forms which vary little with the radial distance from ground zero. Later cycles and peaks show a marked variation with distance, and little correlation appears possible at first glance. It would appear that the first cycle of these phenomena result from the same driving and transmission functions, whereas these characteristics become more complex for later excitations. Since absolute maximum amplitudes are of importance in the design of instrumentation, they have been included in the preceding tables. Where the maximum peak of earth acceleration is not the first peak, it is generally of less duration than the first peak, and very likely has less military significance than the relatively long first peak.

Due to the shallow charge burial used for these tests, the air-blast induced pronounced earth effects. This report is concerned principally with those earth effects produced directly by the action of the explosive forces on the surrounding earth, rather than the earth effects induced near the earth surface by the passage of the air-blast wave. The separation of the air-blast induced ground effects was not particularly difficult for the records of HE-2 and HE-3, whereas some difficulty was experienced on HE-1. Since HE-4 was a surface burst, the air-blast was much greater than for the other tests, while the direct ground effects were somewhat less. The high air-blast propagation velocity due to the strong over-pressure permitted the air-blast effects to arrive at many gage stations either before or coincident with the direct ground effects, making interpretation extremely difficult. This accounts for the large negative first peaks of vertical earth acceleration on HE-4. In general, all HE-4 first peak data to about $\lambda = 10$ are probably not representative of the true earth effects caused by the explosion forces.

In the graphs presented in this report, the first peaks of horizontal earth acceleration, vertical earth acceleration, and earth pressure have been plotted as functions of λ for the four tests. The symbol, λ, is defined by $R = \lambda W^{1/3}$, where R is the radial horizontal distance, in feet, between ground zero and the gage, and W is the weight of the explosive charge in pounds of TNT. To aid in making comparisons between tests, the same attenuation law has been assumed for a single phenomenon on all tests, where a reasonable fit to the experimental data was achieved. It is worth noting that, with the exception of HE-4 (where the air-blast induced earth

effects were dominant for λ less than 10), either an inverse square law or an inverse cube law of attenuation was satisfactory for both earth acceleration and earth pressure.

Reference to the test description* shows that HE-1 and HE-2 were fired under identical scaled conditions with a scale factor of 2.5. Model law and scaling considerations are confined to these two tests. HE-3 and HE-4 used an explosive charge identical to that used for HE-1, but with different charge positions relative to the ground surface. For consideration of the effect of charge depth on air and earth effects, HE-1, HE-3, and HE-4 are used.

B. Horizontal Earth Acceleration - First Peak (Gage Depth 5 Feet)

Attention is directed to Figures 8, 9, and 10. In the region of $\lambda = 4.5 \pm 1.5$ there is a distinct irregularity in each curve. For values of λ less than about 3, an inverse cube attenuation law appears to hold, while for values of λ greater than about 6, an inverse square law fits.

In the region where the attenuation appears to follow an inverse square law for HE-1 and HE-2, the model law holds extremely well for the first peak of the horizontal earth acceleration. In fact, on a scale basis (scale factor 2.5) the difference between the two curves in this region is entirely negligible and well within the probable error of locating a line through the experimental points on either graph. Where the attenuation appears to follow an inverse cube law, HE-2 is about 50 per cent greater than HE-1 when the appropriate scaling factor is applied.

The steps in the attenuation curves also appear to follow the model law for HE-1 and HE-2. This is indeed interesting, since these steps seem to be a characteristic of this phenomenon rather than of the medium. However, these are probably insufficient data to permit firm conclusions.

By comparison of HE-1, HE-3, and HE-4 in the region beyond the step in the attenuation curves (λ greater than about 5), the effect of charge depth on the horizontal earth acceleration is estimated to be:

Test	λ_c**	Effect Relative to Surface Burst (HE-4)
HE-4	-0.135	1.0
HE-1	0.135	1.4
HE-3	0.5	2.3

C. Vertical Earth Acceleration - First Peak (Gage Depth 5 Feet)

Attention is directed to Figures 12, 13, and 14 for HE-1, HE-2, and HE-3. For HE-1 and HE-2 an inverse square attenuation law fits well out to a distance of about 500 feet ($\lambda = 35$ for HE-1 and $\lambda = 14$ for HE-2). A step is evident in the HE-3 curve, and an inverse square law applies from $\lambda = 5$ to 500 feet ($\lambda = 35$).

---

* See Page 2.

** Charge burial depth in terms of λ. See Page 2.

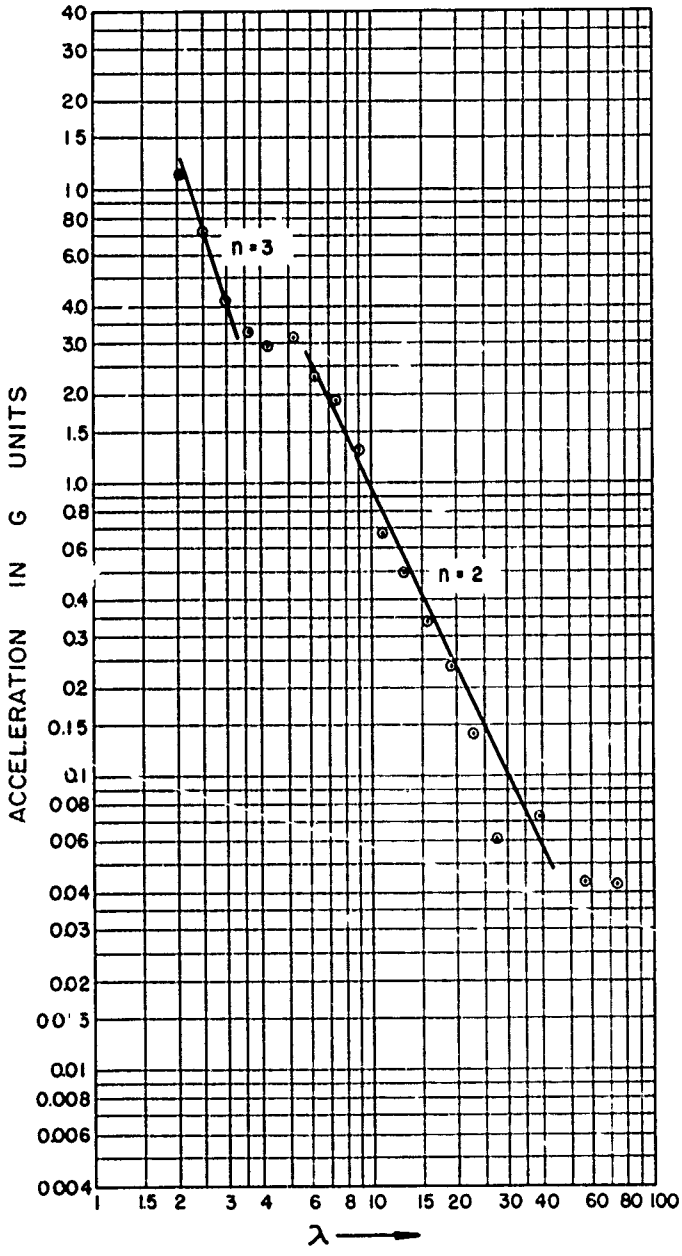

FIGURE 8
HORIZONTAL EARTH ACCELERATION - FIRST PEAK
HE - 1

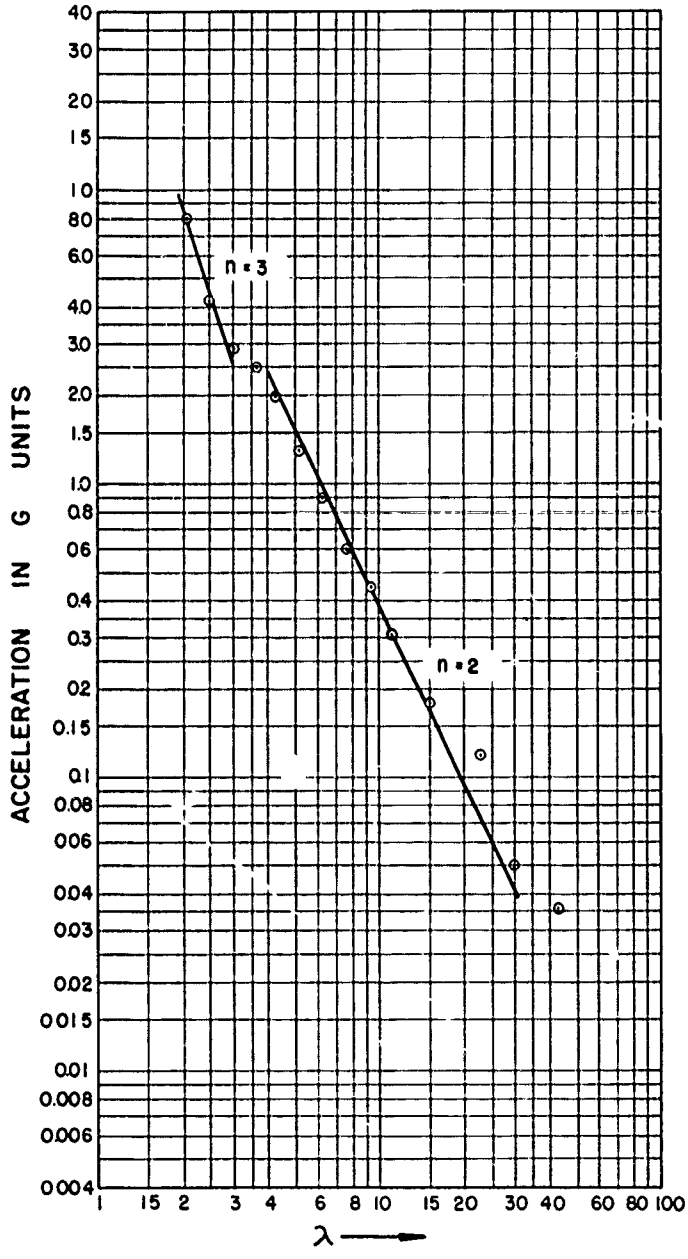

FIGURE 9
HORIZONTAL EARTH ACCELERATION - FIRST PEAK
HE - 2

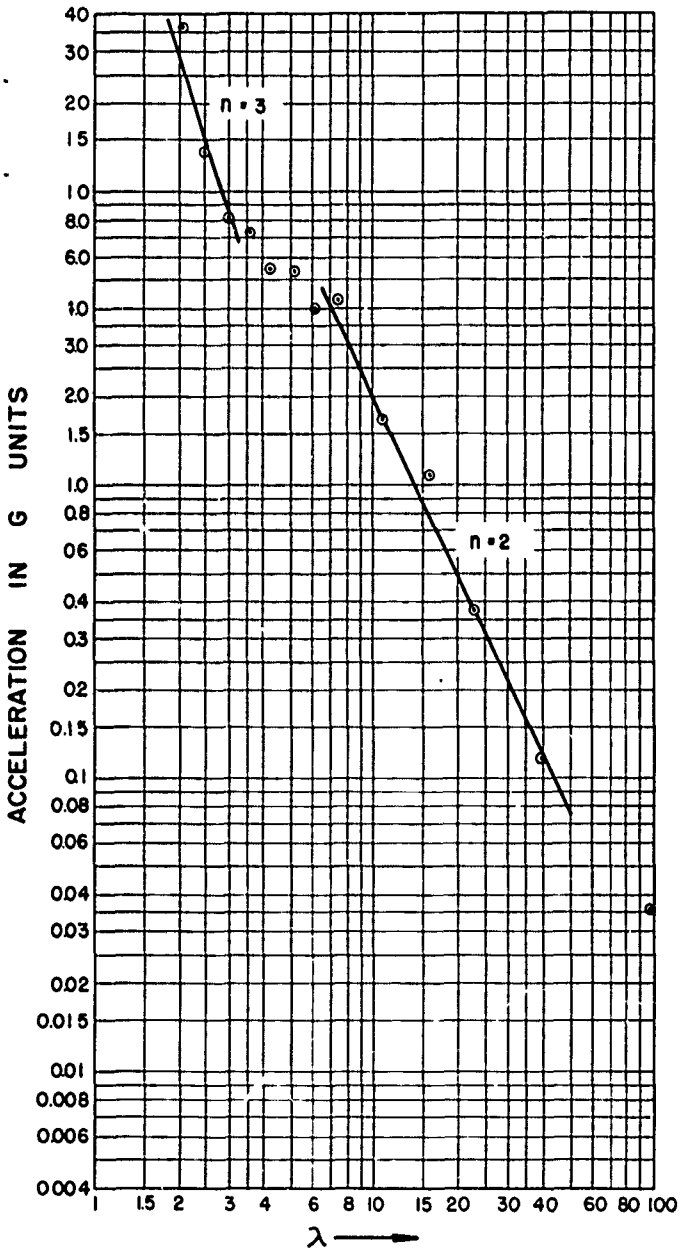

FIGURE 10
HORIZONTAL EARTH ACCELERATION - FIRST PEAK
HE-3

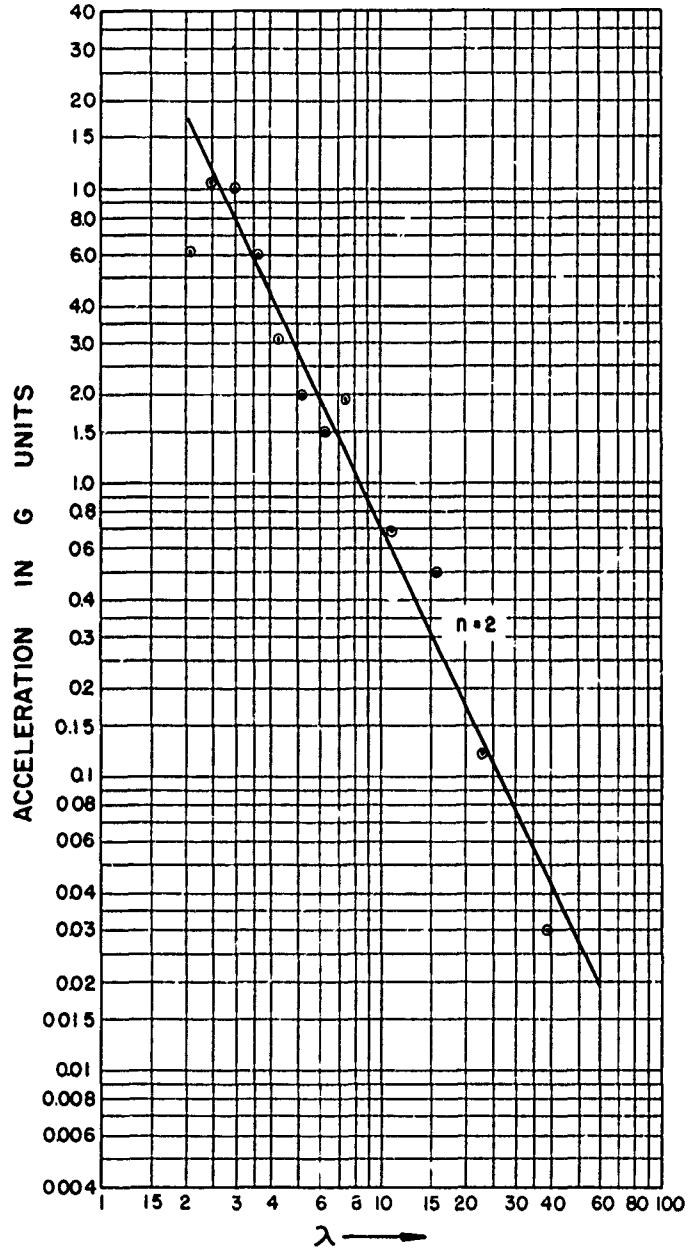

FIGURE 11
HORIZONTAL EARTH ACCELERATION - FIRST PEAK
HE-4

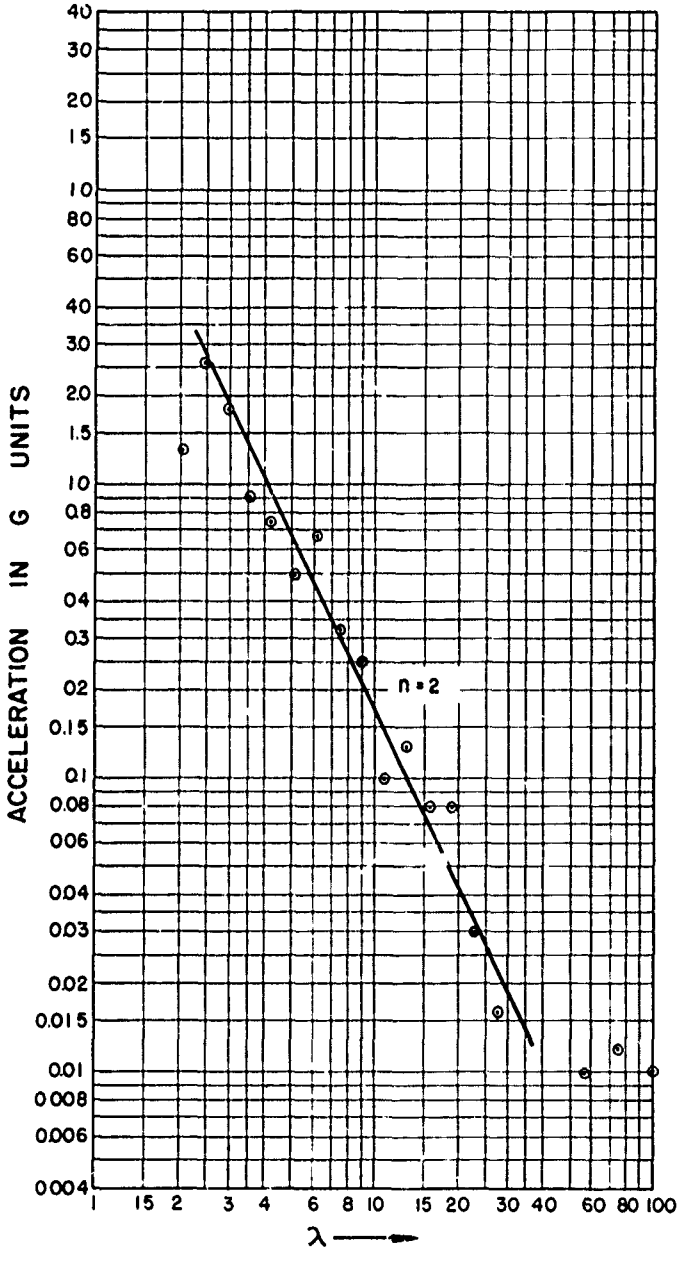

FIGURE 12
VERTICAL EARTH ACCELERATION - FIRST PEAK
HE-1

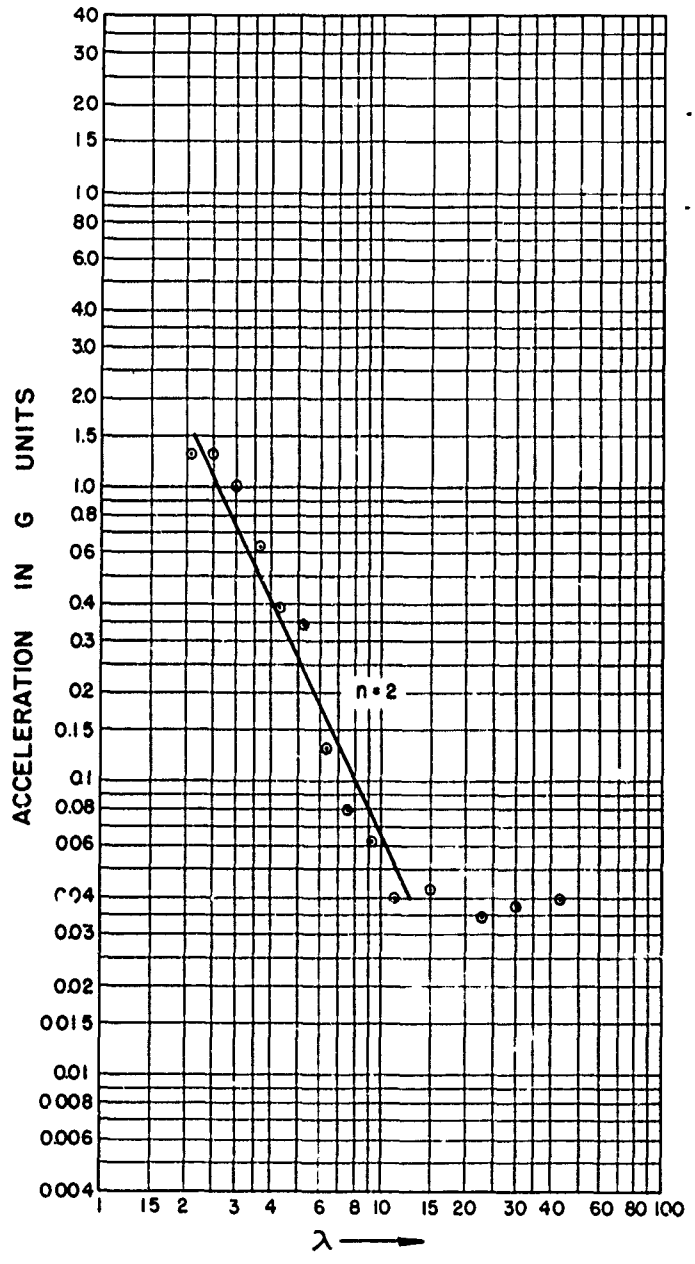

FIGURE 13
VERTICAL EARTH ACCELERATION - FIRST PEAK
HE-2

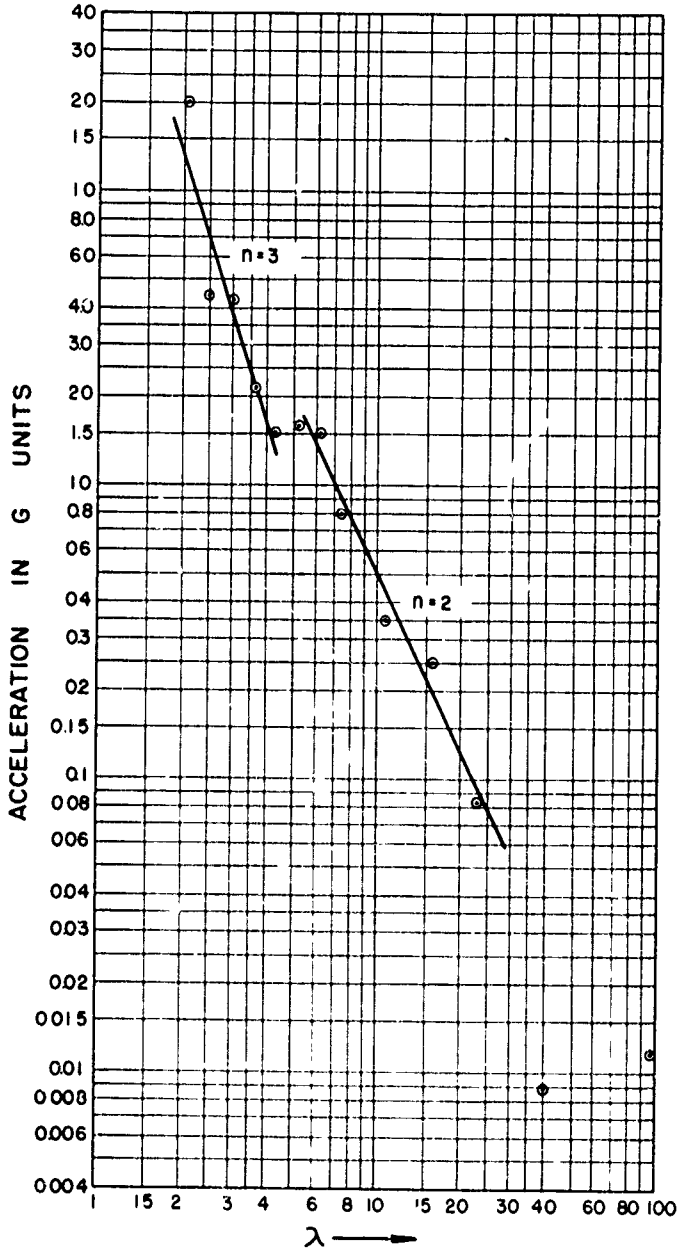

FIGURE 14
VERTICAL EARTH ACCELERATION - FIRST PEAK
HE - 3

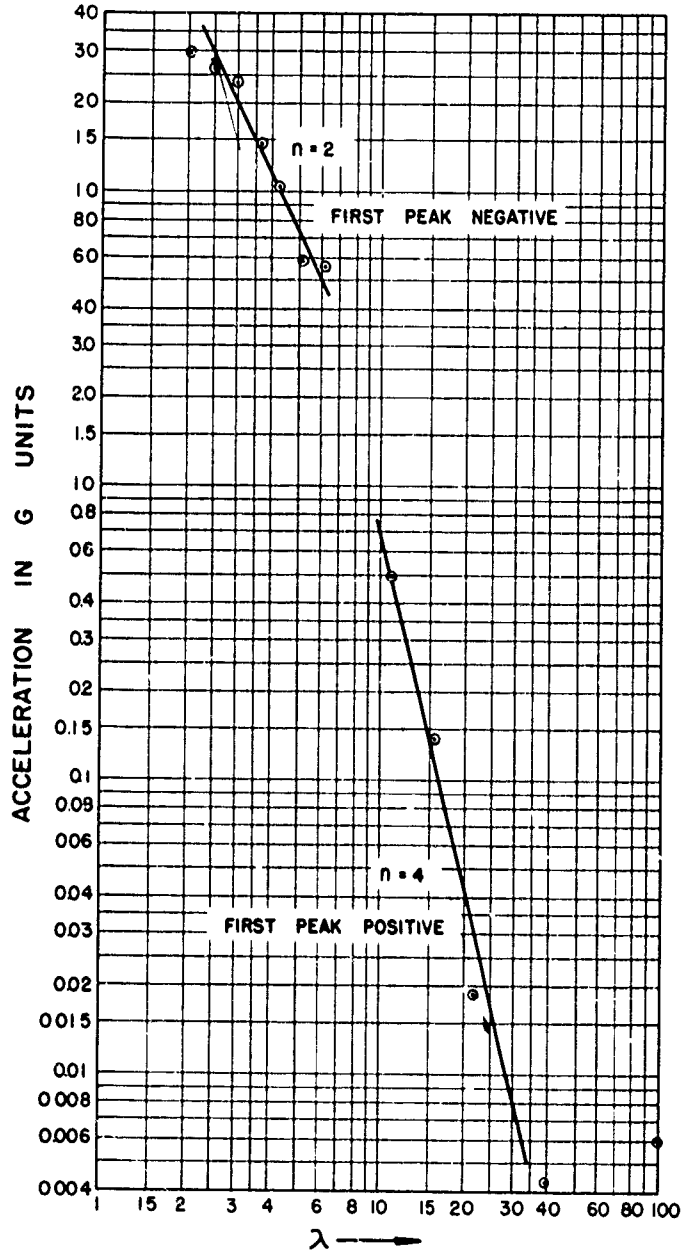

FIGURE 15
VERTICAL EARTH ACCELERATION - FIRST PEAK
HE - 4

For HE-1 and HE-2 the model law holds extremely well for the first peak of the vertical earth acceleration within the probable error of locating a line through the experimental points on either graph. However, beyond 500 feet, the vertical earth-acceleration curves appear to flatten out for both tests. This effect definitely does not scale and is probably due to a characteristic of the medium. A disturbing conclusion is reached if these data are extended to large charges where this flattening could occur in the region of military interest.

On HE-4 the air-blast had such a pronounced effect on the vertical earth acceleration that no comparison has been made between HE-4 and the other tests. Figure 15 and the gage records under HE-4 -- Vertical Earth Acceleration -- in the Appendix clearly show this air-blast effect. Out to the region of about $\lambda = 8$ the first peaks were clearly negative, whereas beyond $\lambda = 10$ the first peaks were positive. The inconsistant attenuation characteristic (inverse fourth power) does not permit a direct comparison to the other tests.

It is estimated that the vertical earth acceleration for HE-3 was about three times greater than that for HE-1. For the horizontal earth acceleration this effect of depth ratio ($\lambda_c = 0.5$ vs. $\lambda_c = 0.135$) was about two.

For HE-1 and HE-2 ($\lambda_c = 0.135$) the first peaks of the horizontal earth acceleration are about six times the similar peaks of the vertical earth acceleration in the region where the inverse square attenuation law applies. For HE-3 ($\lambda_c = 0.5$) this ratio is about four.

D. Earth Pressure - First Peak

All earth-pressure measurements included in this report were obtained from gages located near the bottom of holes five feet deep. These holes were filled to the top with an Aquagel solution. In terms of λ the gage depth was $\lambda_g = 0.36$ for HE-1, HE-3, and HE-4 and $\lambda_g = 0.14$ for HE-2. Lampson's work* utilized a gage depth of $\lambda_g = 1.5$ for similar measurements using smaller explosive charges. Two additional measurements on HE-2 at a gage depth of 17 feet ($\lambda_g = 0.5$) gave first peaks about three times greater than those obtained at five feet ($\lambda_g = 0.14$). It is clear that there is insufficient information to isolate the effect of depth on the phenomenon being measured and the effect of the liquid column height on the gage coupling to the earth. It is suspected that the liquid column had a significant effect for these relatively shallow (scale) depths. Accordingly, any scale comparisons between HE-1 and HE-2 would be suspicious.

At the time of the HE-1 test a different method was used to couple the gage to the earth for earth-pressure measurements. On HE-1 only two earth-pressure gages were installed in holes filled to the top with an Aquagel solution. Following HE-1, in conferences with representatives of Program One of OPERATION JANGLE, the Ballistic Research Laboratories and the Naval Ordnance Laboratory, it was decided to use liquid filled holes for earth-pressure measurements. It was further decided that the principal measurements would be made at a depth of five feet for logistic reasons, in spite of the indication from Lampson's work that much greater hole depths were desirable.

Figure 16 shows a graph of the first peaks of the two HE-1 earth-pressure measurements, while Figures 17, 18, and 19 show the corresponding information for HE-2, HE-3, and HE-4.

---

*OSRD Report No. 6645, "Final Report on Effects of Underground Explosions," by C.W. Lampson.

HE-1 gave insufficient data to plot a curve, and the line shown in Figure 16 is scaled from HE-2. For HE-2 and HE-3 an inverse cube attenuation law applies, although a step appears in the attenuation curve for HE-3. On HE-4 the air-blast had a very marked effect on the earth pressure measured. In fact, the first peaks of earth pressure measured out to about $\lambda = 6$ on HE-4 appeared to follow the same attenuation law as the air-blast maximum peak pressures.

Reference to the gage records in the Appendix shows that the earth-pressure measurements obtained on the close-in gages (to about $\lambda = 3$) consist of a single positive pulse, followed by a long negative phase. At greater distances additional positve pulses appear while at still greater distances an oscillatory condition develops where the late peaks are many times greater than the first peak.

E. Air-Blast Pressure

Examination of the air-blast records in the Appendix shows that, with the exception of HE-3, a single peak sharp-front air-blast pressure record was obtained. HE-3, which used a much deeper charge than the other tests, shows the familiar double shock observed on similar tests at Dugway.* However, the peak air-blast pressures for HE-3 are considerably greater than those for the similar Dugway tests. Furthermore, the ratio between the maximum peak and the first peak is greater for HE-3 than for the Dugway tests, which agrees with the observation that the maximum peak overtakes the first peak earlier than at Dugway. The later disappearance of the first shock is clearly shown in the Appendix records.

Figures 20, 21, 22, and 23 show the maximum peak air-blast pressures as functions of λ for the four tests covered by this report. Increasing the charge depth appears to flatten the curve close to the charge, while all curves ultimately assume a slope corresponding to an inverse 1.4 power attenuation law.

The model law applies very well to the peak air-blast pressure measurements for HE-1 and HE-2, except close to the charge. Measurements of the peak air-blast pressure by the Ballistic Research Laboratories using the velocity method gave good model law behavior close to the charges for these two tests, and agreed very closely with the HE-2 data reported here. The discrepancy between the close-in measurements on HE-1 and HE-2 has not yet been explained by instrument characteristics.

Beyond $\lambda = 10$, HE-1 ($\lambda_c = 0.135$) produced about the same peak air-blast pressures (6 psi at $\lambda = 10$) as HE-4 (surface shot $\lambda_c = -0.135$). The greater charge depth of HE-3 ($\lambda_c = 0.5$) reduced the peak air-blast pressures to about 40 per cent of those from the surface shot (HE-4) in the same region. The effect of the charge depth on air-blast was much more pronounced closer to ground zero, where the earth effects would have greater military significance.

---

* Interim Report, "Underground Explosion Tests at Dugway," by Stanford Research Institute, July 1951.

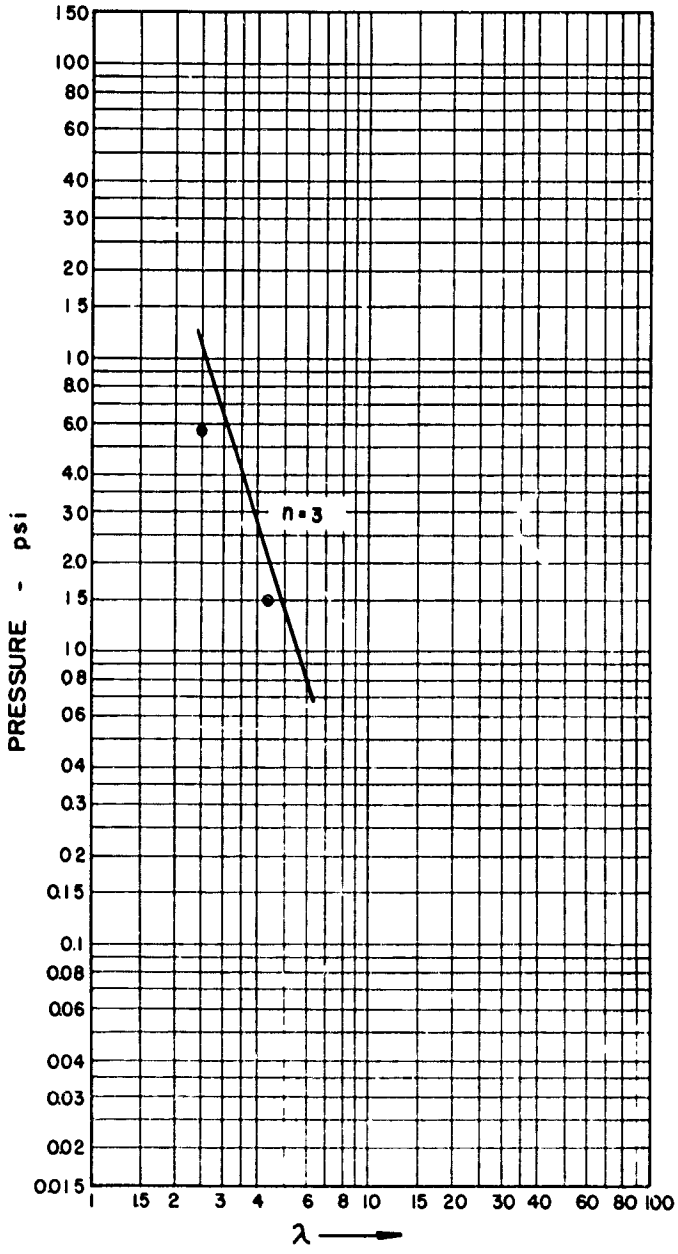

FIGURE 16
EARTH PRESSURE - FIRST PEAK
HE-1

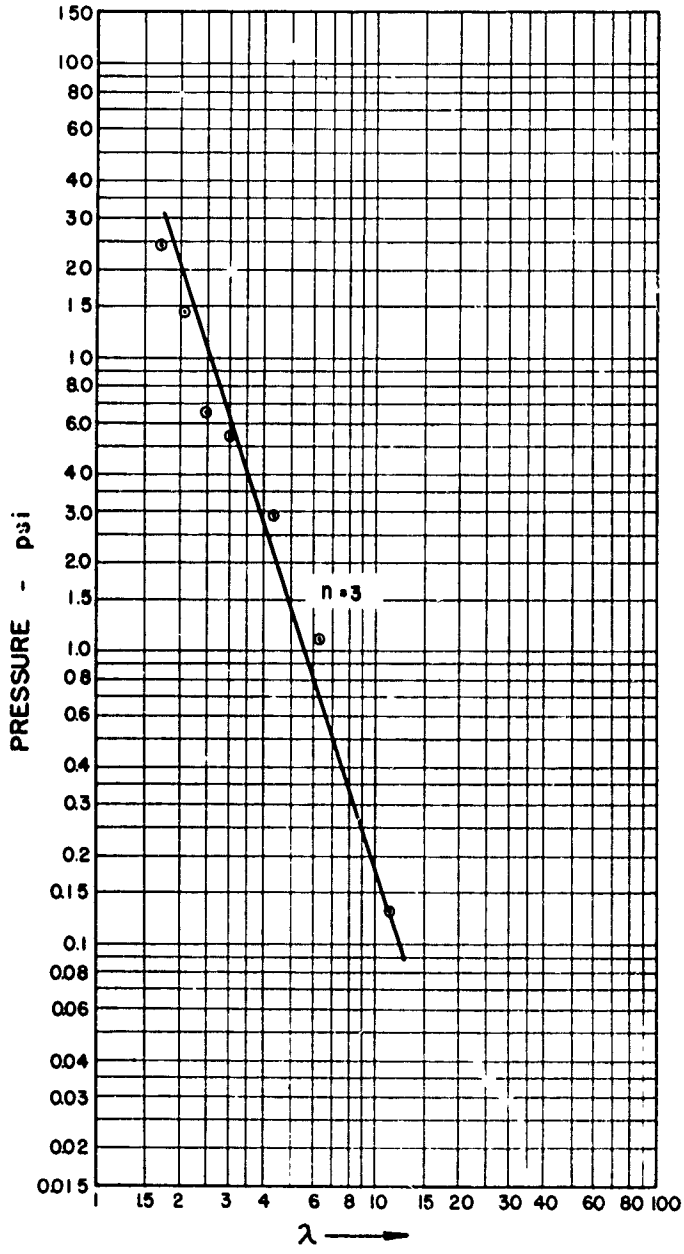

FIGURE
EARTH PRESSURE - FIRST PEAK
HE-2

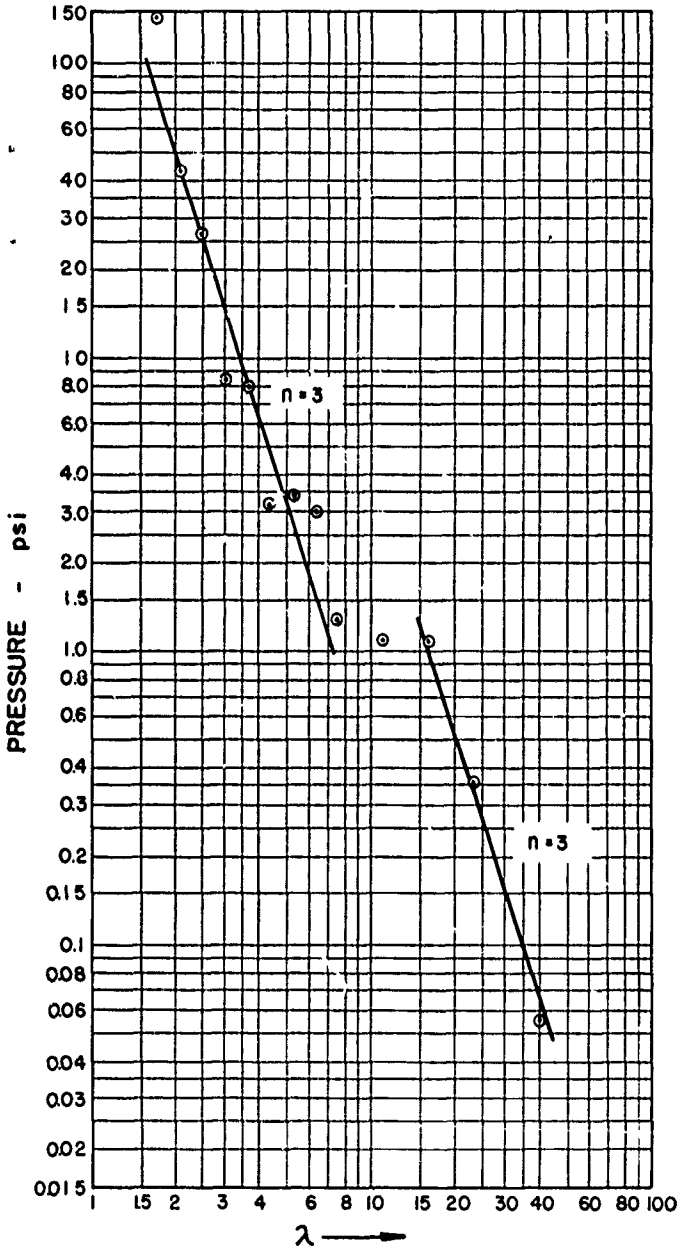

FIGURE 18
EARTH PRESSURE - FIRST PEAK
HE-3

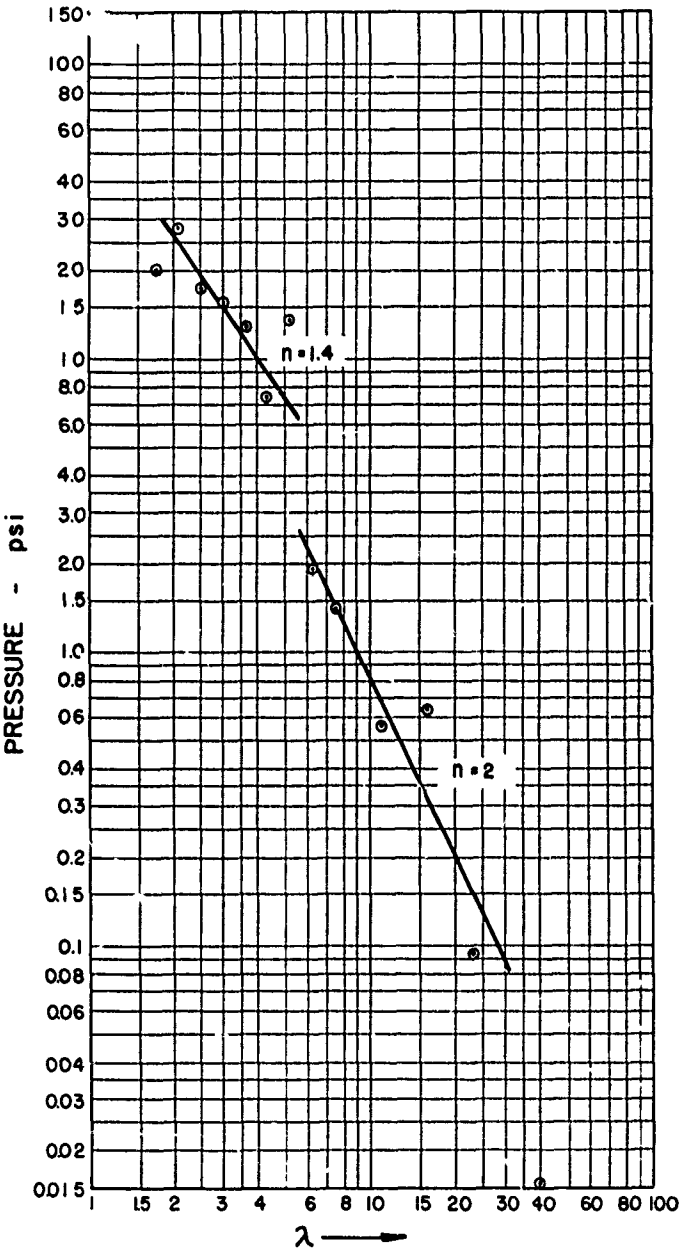

FIGURE 19
EARTH PRESSURE - FIRST PEAK
HE-4

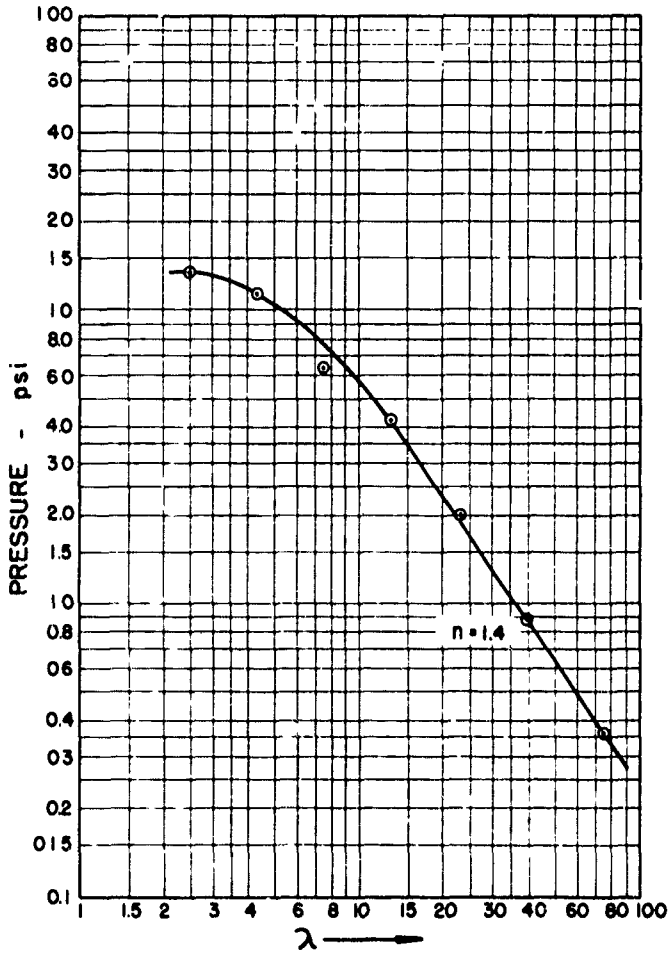

FIGURE 20
AIR-BLAST PRESSURE - MAXIMUM PEAK
HE-1

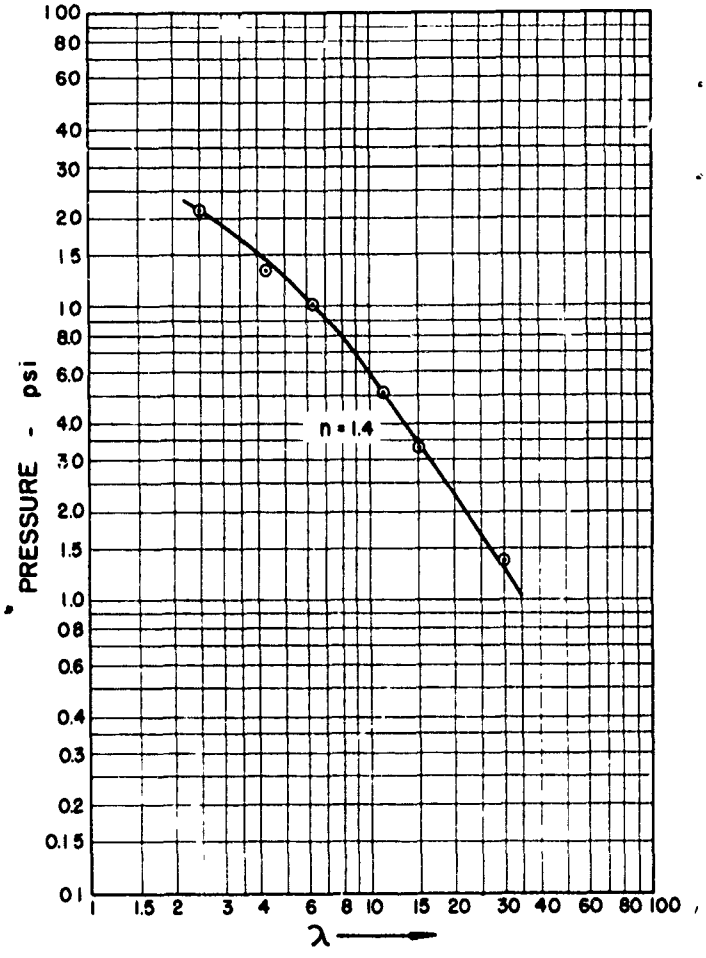

FIGURE 21
AIR-BLAST PRESSURE - MAXIMUM PEAK
HE-2

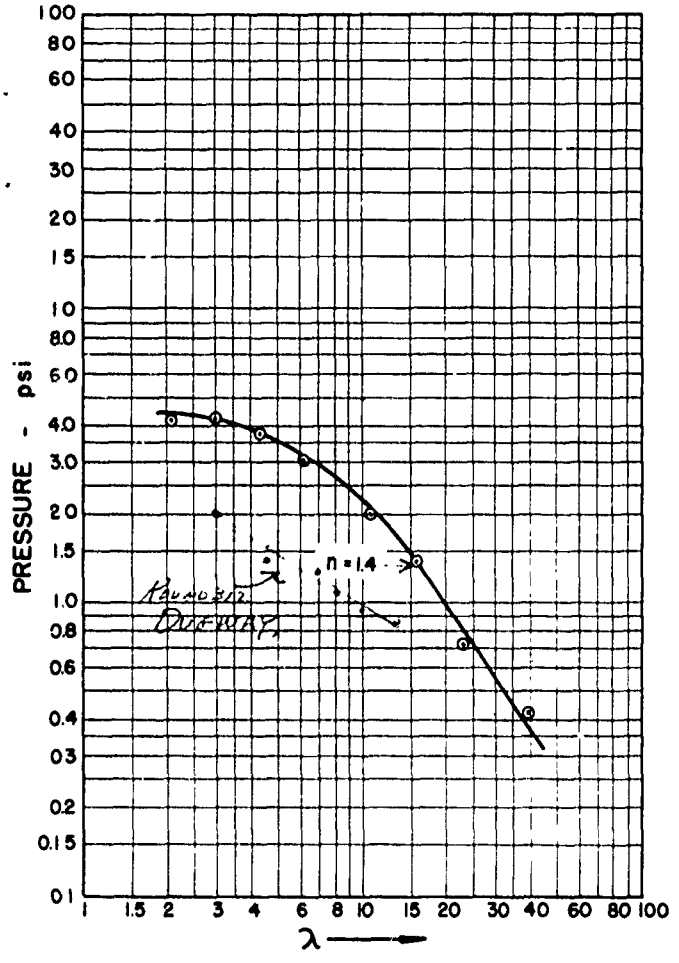

FIGURE 22
AIR-BLAST PRESSURE - MAXIMUM PEAK
HE-3

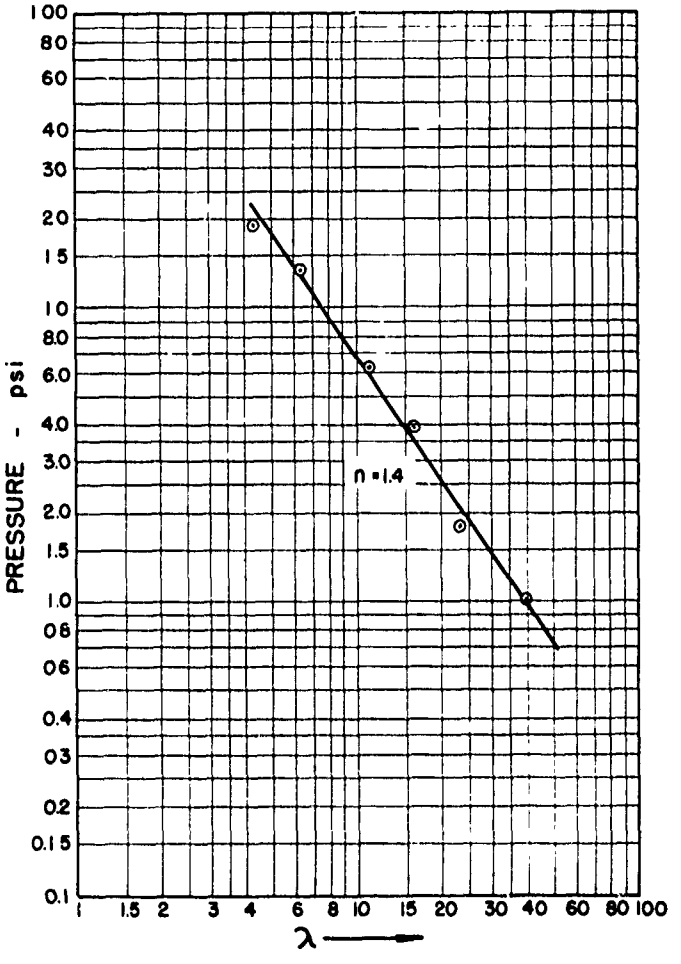

FIGURE 23
AIR-BLAST PRESSURE - MAXIMUM PEAK
HE - 4

[redacted]

F. Composite Data

Figures 24, 25, 26, and 27 present composite curves of the first peaks of horizontal earth acceleration, vertical earth acceleration and earth pressure, and peak air-blast pressure for the four test explosions. These figures use the smooth curves obtained from each test, eliminating the experimental points to avoid confusion. For the sake of simplicity, acceleration is plotted in terms of G units for a one-pound TNT charge. A division of the ordinate value by $W^{1/3}$ gives the corresponding acceleration for a charge containing W pounds of TNT, assuming that the model law holds. The curves for horizontal and vertical earth acceleration for HE-1 and HE-2 are coincident, with departures near the ends, as shown.

G. Time of Arrival

Figure 28 shows the time of the first arrival of the horizontal earth acceleration as a function of the radial distance from the charge for the four test explosions. The horizontal earth-acceleration arrival time was chosen because the greater recorded amplitudes gave better time resolution. In general, however, the arrival times were the same for the horizontal and vertical components of earth acceleration, within reading accuracy.

Essentially identical time of arrival curves were obtained for the three 2560-pound tests, HE-1, HE-3, and HE-4, which were instrumented along adjacent parallel gage lines. The lower velocity between the outer gage stations is quite unusual. However, since it was obtained on all three tests it would appear to be indisputable, possibly indicating an anomaly in the sub-surface geology.

The time of arrival curve for HE-2 is distinctly different from those for the other three tests. The HE-2 curve consists of two unconnected sections, each having the same slope and each yielding a velocity equal to that obtained between the outer gage stations for HE-1, HE-3, and HE-4. It is believed that this effect is not due to the different charge sizes. The gage line for HE-2 made a 30 degree angle to those used for the other three tests, crossing at approximately 1000 feet from the ground zeros for HE-1 and HE-2.* The different time of arrival curve for HE-2 could possibly indicate a local sub-surface variation, detected because of the 30 degree spread between gage lines.

In view of the difference between the HE-1 and HE-2 time of arrival curves, it is interesting to note that the model law applied almost perfectly to both the horizontal and the vertical components of the earth acceleration, with a charge scale ratio of 2.5. This would indicate that the acceleration attenuation characteristics of the transmission paths along the two gage lines crossing at a 30 degree angle were reasonably similar, although the transmission velocity characteristics differed.

---

* See Figure 1, Page 2.

[redacted]

H. Conclusions

With the discussion presented above, the tables of results and the individual gage records in the Appendix, the interested reader can form his own opinion as to the significant conclusions to be drawn from the four explosion tests covered by this report. A limited preliminary analysis of these complex data cannot be expected to lead to a unique set of conclusions. However, the following points seem to be of particular interest:

1. For both the horizontal and the vertical components of the earth acceleration, the two scaled tests, HE-1 and HE-2, obeyed the model law remarkably well, with a scale factor of 2.5.

2. The horizontal earth acceleration showed a step in the attenuation curve, which appeared to follow the model law.

3. The vertical earth acceleration attenuation curve tended to flatten out at large distances. This effect did not follow the model law, occurring at a range of about 500 feet for all tests.

4. As compared to a surface burst (HE-4) a shallow buried charge (HE-1 at $\lambda_c = 0.135$) increased the horizontal earth acceleration by about 40 per cent. Beyond about $\lambda = 10$ air-blast pressures from these two tests were nearly equal.

5. For buried charges the vertical component of the earth acceleration was about one-fifth of the horizontal component.

6. Beyond about $\lambda = 10$ the air-blast pressure attenuation curves were similar for all tests, and the model law applied to the scaled HE-1 and HE-2 tests. Closer to ground zero, the charge depth affected the characteristics of the attenuation curves.

7. The air-blast pressures produced marked ground effects. This was particularly evident on the surface shot (HE-4). However these induced ground effects were of shorter duration than those produced directly by the explosive forces.

8. Time of arrival data indicate the possibility of local anomalies in the sub-surface geology, showing a distinct difference between the HE-1 and HE-2 gage lines, even though the model law held very well for earth acceleration amplitudes and durations. These possible anomalies must be considered when applying these test results to other shot points in the same test area.

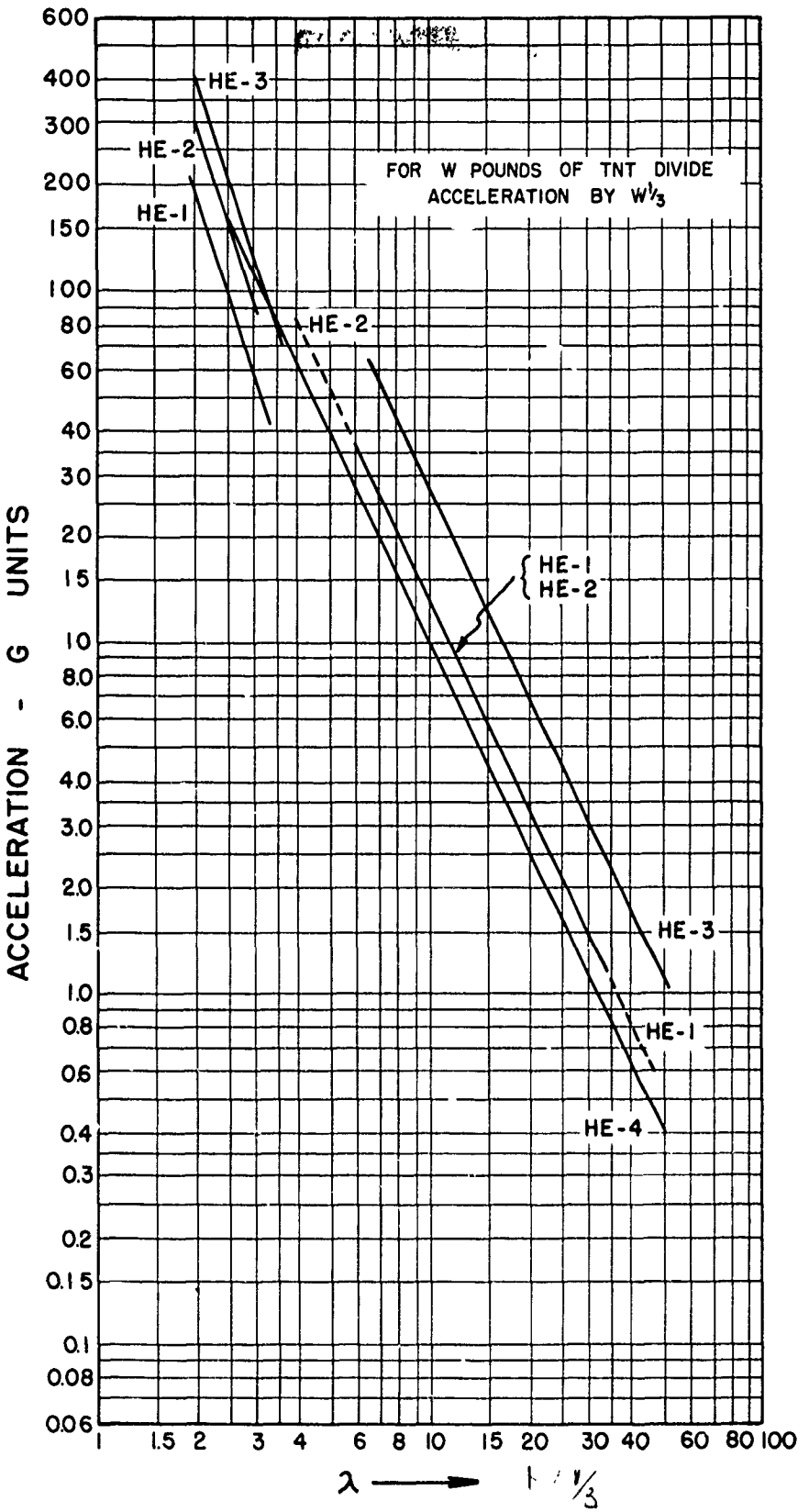

FIGURE 24

HORIZONTAL EARTH ACCELERATION - FIRST PEAK

COMPOSITE FOR EQUIVALENT OF ONE POUND OF TNT

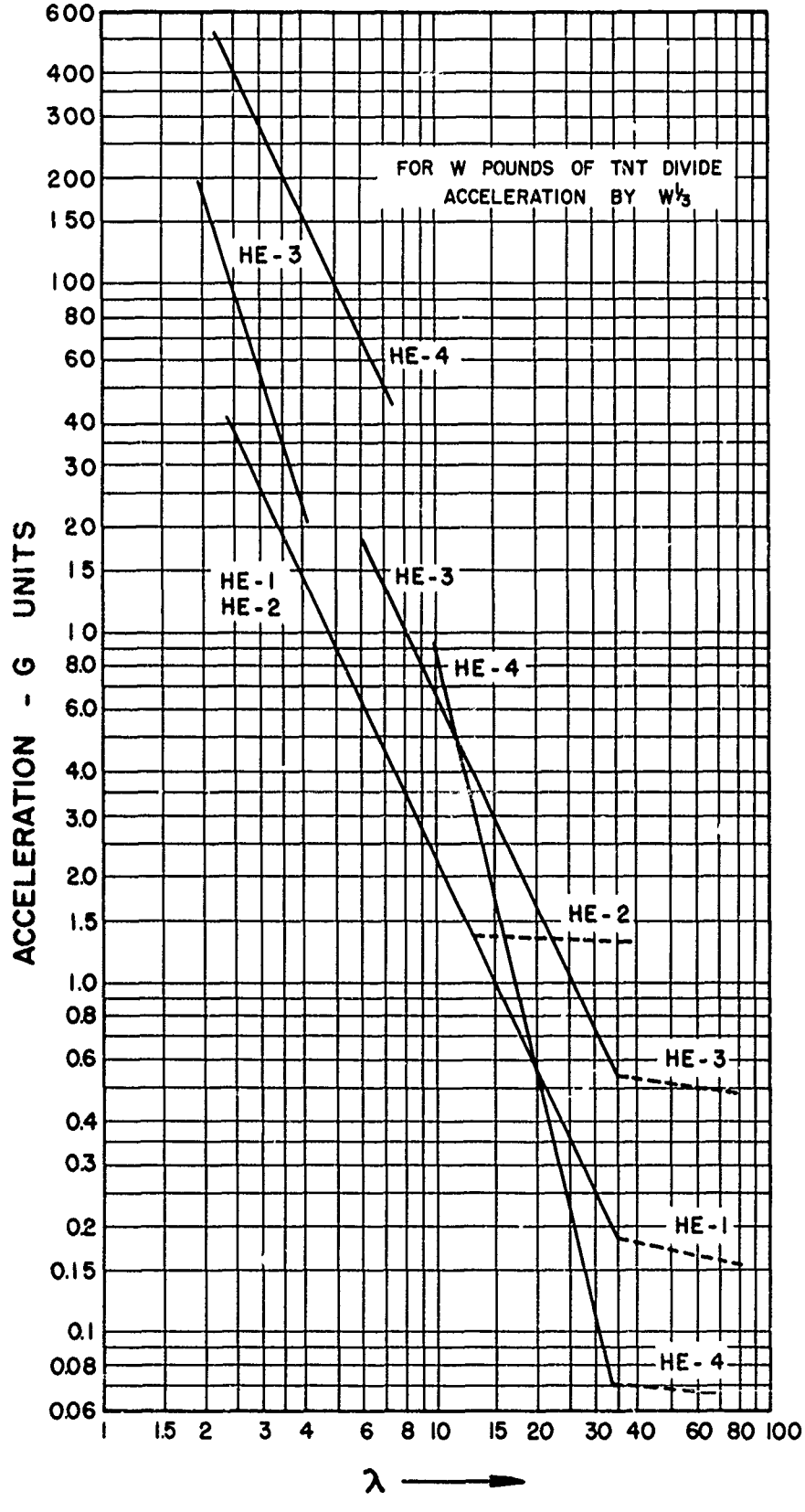

FIGURE 25

VERTICAL EARTH ACCELERATION - FIRST PEAK

COMPOSITE FOR EQUIVALENT OF ONE POUND OF TNT

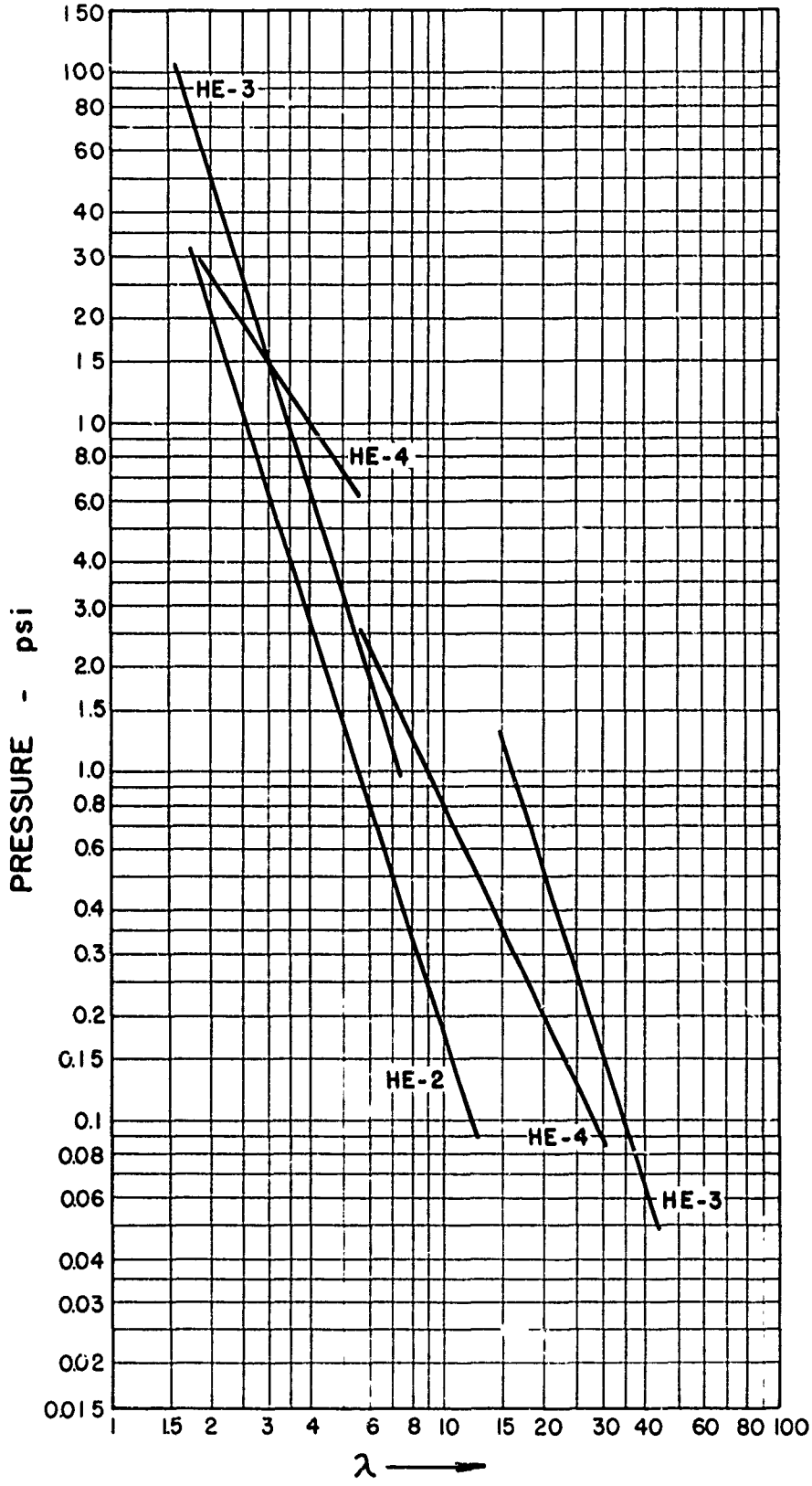

FIGURE 26

EARTH PRESSURE - FIRST PEAK

COMPOSITE

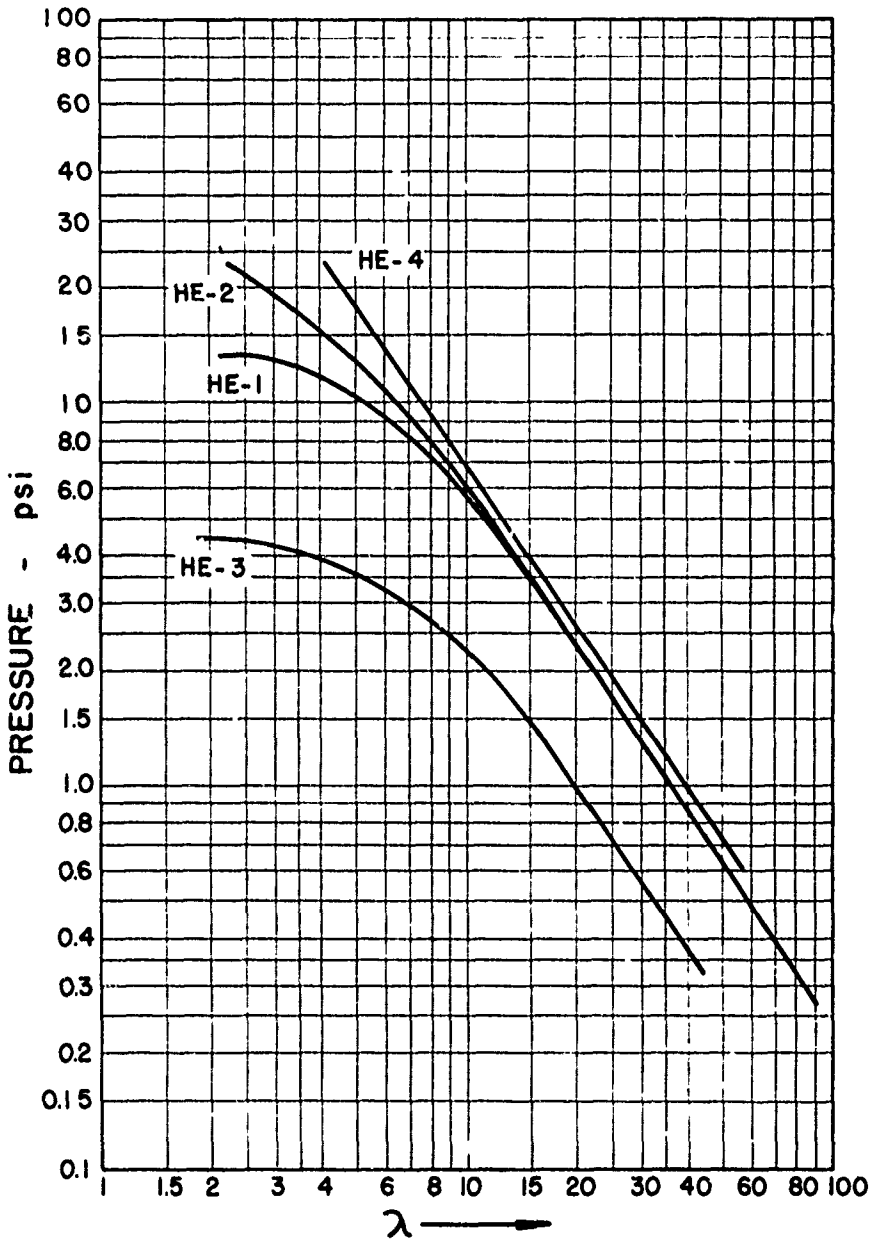

FIGURE 27

AIR - BLAST PRESSURE - MAXIMUM PEAK

COMPOSITE

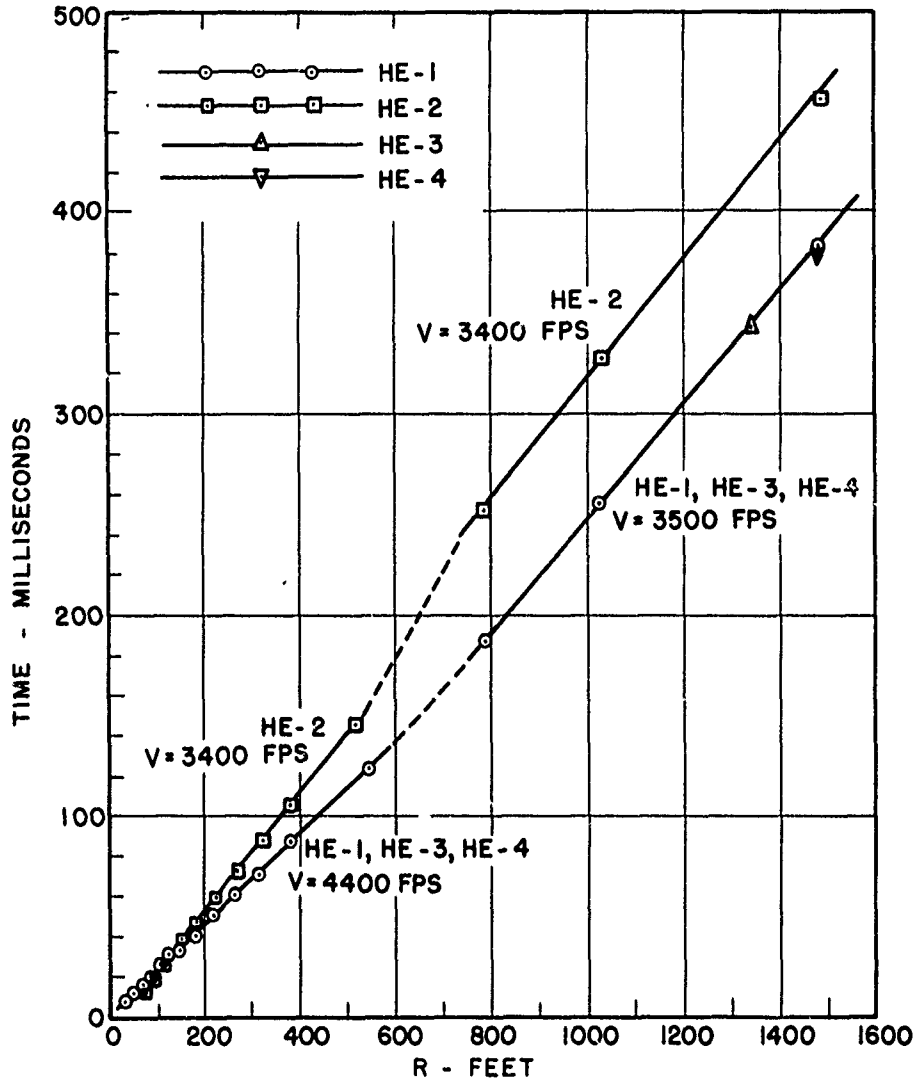

FIGURE 28

TIME OF FIRST ARRIVAL

HORIZONTAL EARTH ACCELERATION

V. APPENDIX

The Appendix contains the individual records obtained on 196 gage channels. These records are direct tracings of the oscillograph records, without editing of any kind. No "smoothing" has been used and the noise or background level is as shown. Each group of traces is identified by the test number and each trace is identified by measurement type, gage code number, gage distance from ground zero in feet and λ, and nominal gage rating. H and V represent horizontal and vertical earth acceleration with the positive directions being outward and upward, respectively. P is for earth pressure and B is for air-blast pressure. The time of incidence of the air-blast shock wave at each gage location is indicated by a single line marked AB on each trace. The traces are grouped so that all records of one phenomenon from a single test can be viewed simultaneously. This presentation clearly shows the change in the wave-form character of the various phenomena as a function of the distance from ground zero.

VI. PERSONNEL

All Stanford Research Institute activities covered by this report on Project 1(9) of OPERATION JANGLE were under the direction of Dr. E. B. Doll. The field party was headed by Mr. L. M. Swift and included L. H. Inman, V. E. Krakow, C. C. Hughes, S. C. Ashton, W. M. Stewart and D. C. Sachs. This report was written by E. B. Doll and D. C. Sachs with the assistance of Miss Jane Crawford and Mrs. Ann Heyer. PFC Mike Johnson of Program One of OPERATION JANGLE also served as a member of the working field party.

APPENDIX

HE - 1

HORIZONTAL EARTH ACCELERATION

HE - 1

HORIZONTAL EARTH ACCELERATION

W 2560
$W^{1/3}$ 13.8

D_g 5.0
D_c 1.9
λ_c 0.135

OPERATION JANGLE

25 August 1951

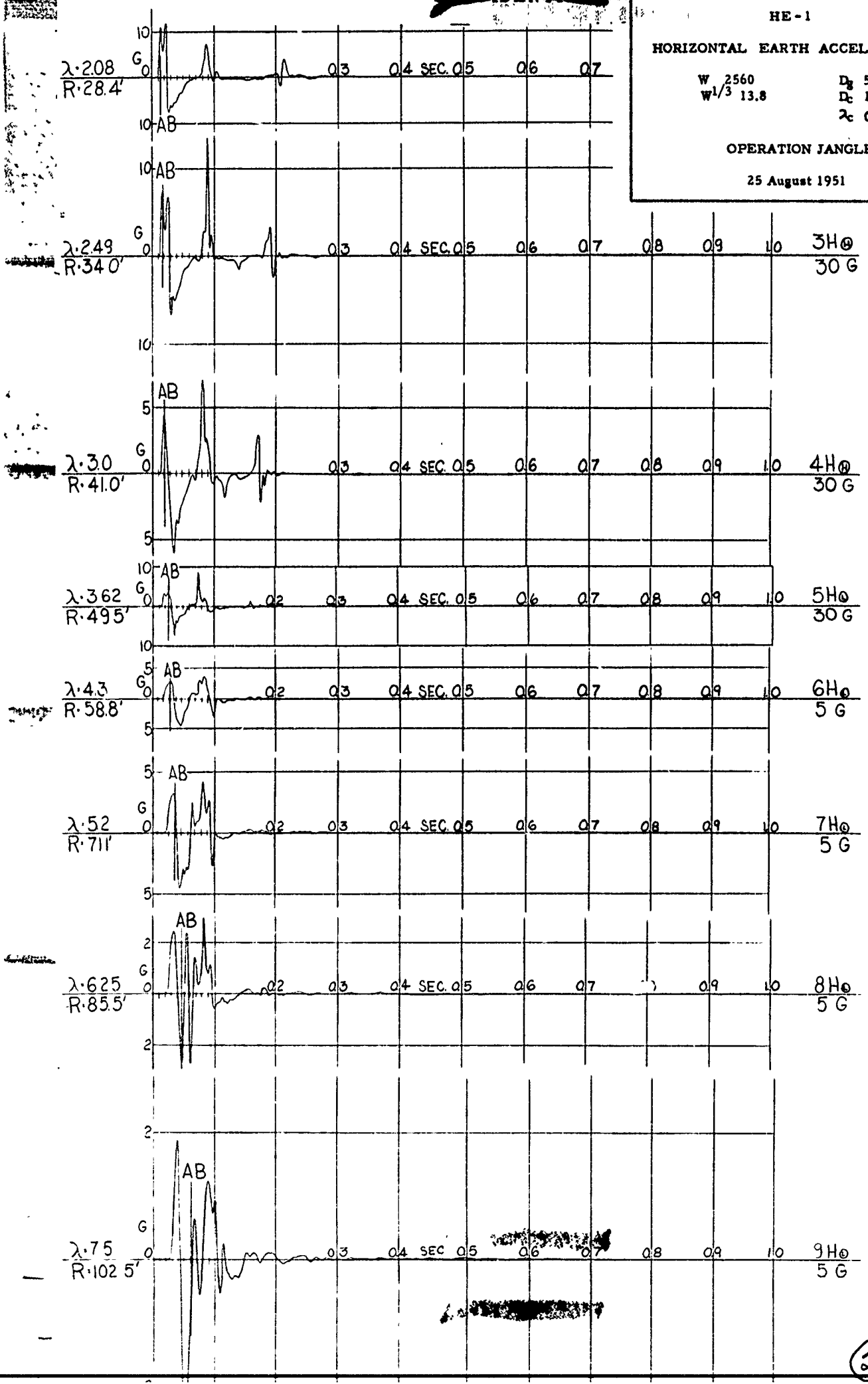

(2)

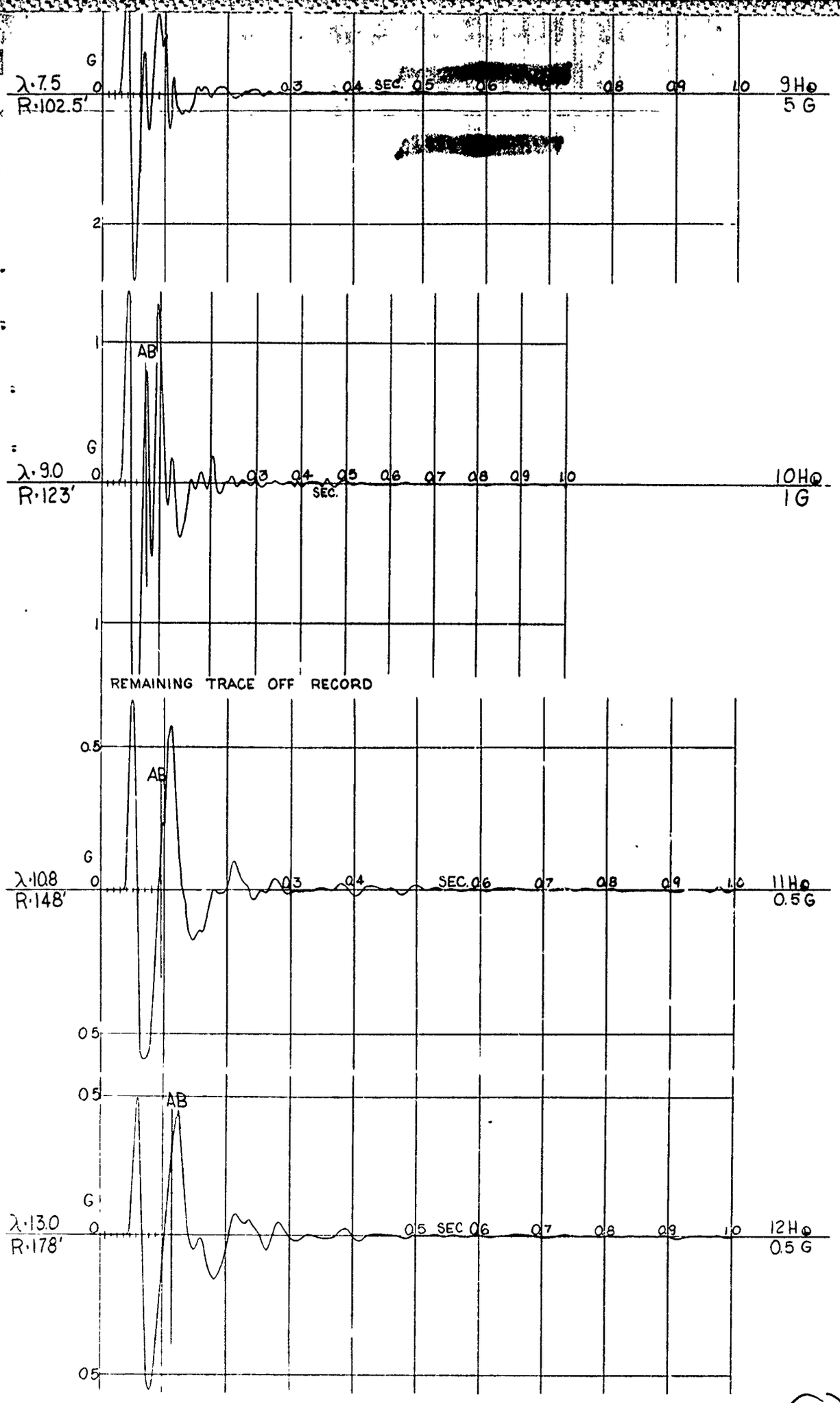
λ·7.5
R·102.5'
G
0
2
0.3
0.4 SEC.
0.5
0.6
0.8
0.9
1.0
9 H⊕
5 G
AB
1
λ·9.0
R·123'
0.3
0.4
0.5
0.6
0.7
0.8
0.9
1.0
SEC.
10 H⊕
1 G
REMAINING TRACE OFF RECORD
0.5
λ·10.8
R·148'
0.3
0.4
SEC.
0.6
0.7
0.8
0.9
1.0
11 H⊕
0.5 G
λ·13.0
R·178'
0.5 SEC
0.6
0.7
0.8
0.9
1.0
12 H⊕
0.5 G

HE-1

HORIZONTAL EARTH ACCELERATION

W 2560
$W^{1/3}$ 13.8

D_g 5.0
D_c 1.9
λ_c 0.135

OPERATION JANGLE

25 August 1951

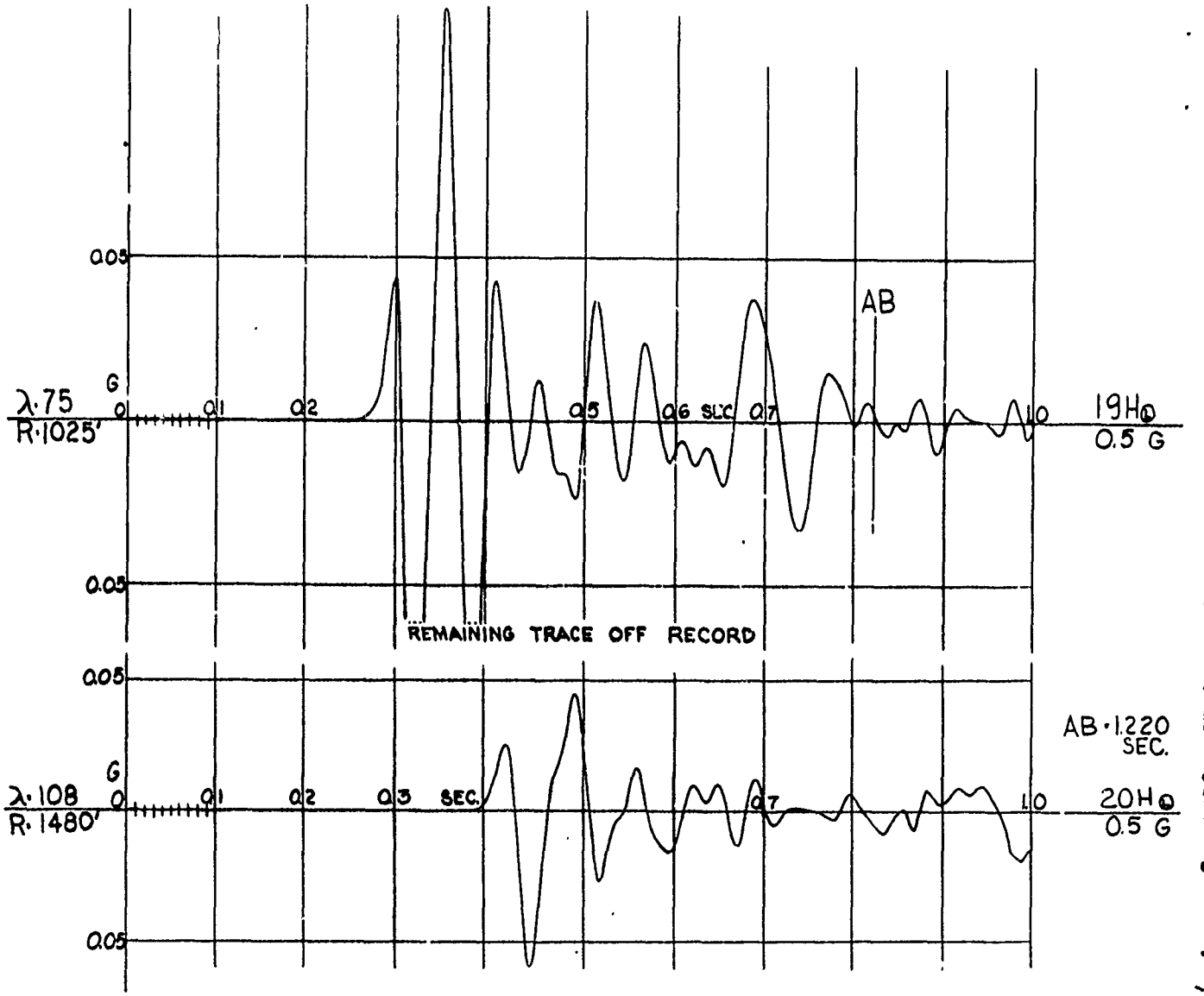

[redacted]

HE - 1

HORIZONTAL EARTH ACCELERATION

(continued)

[redacted]

HE-1

HORIZONTAL EARTH ACCELERATION

W 2560 D_g 5.0
$W^{1/3}$ 13.8 D_c 1.9
α_c 0.135

OPERATION JANGLE

25 August 1951

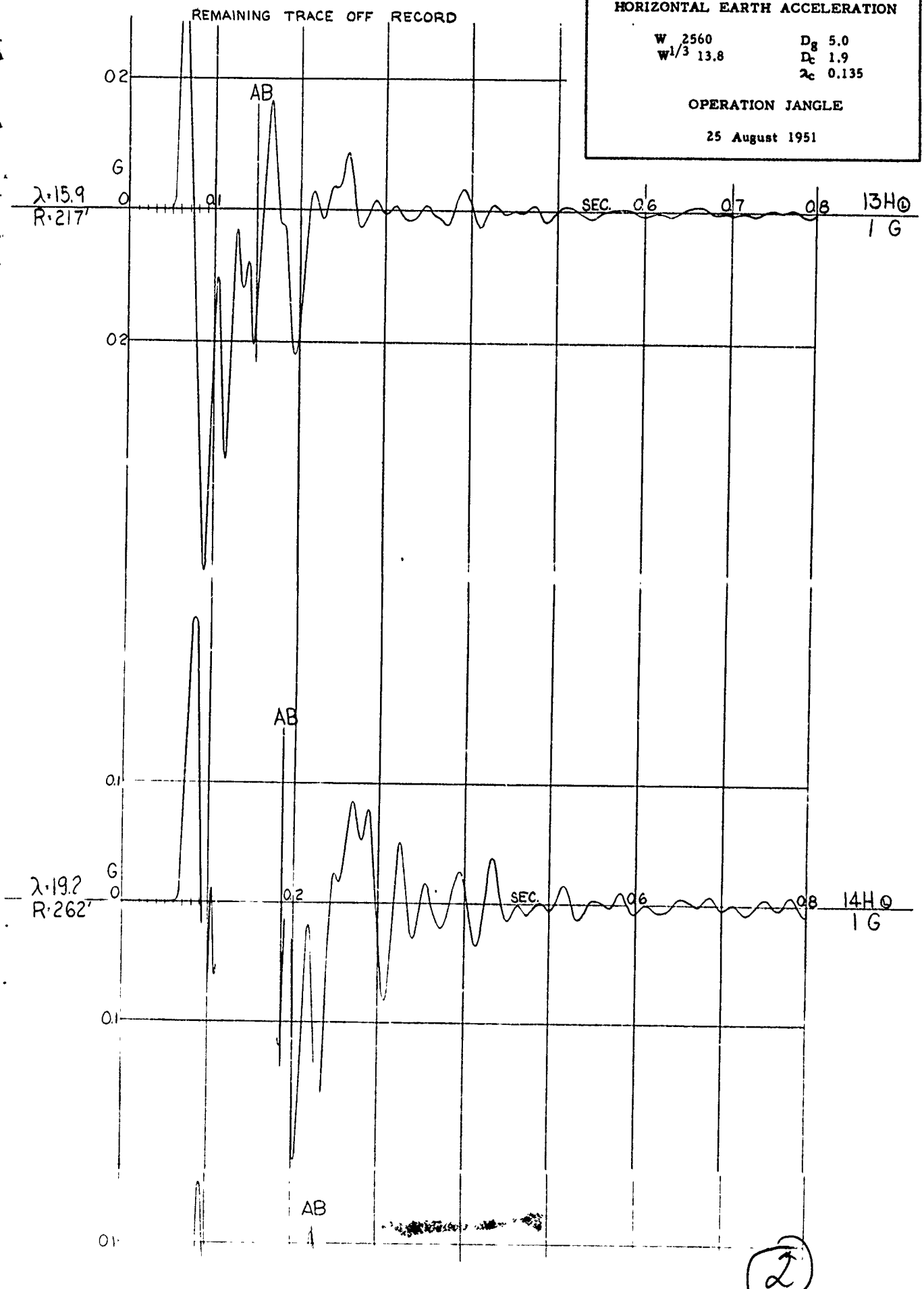

(2)

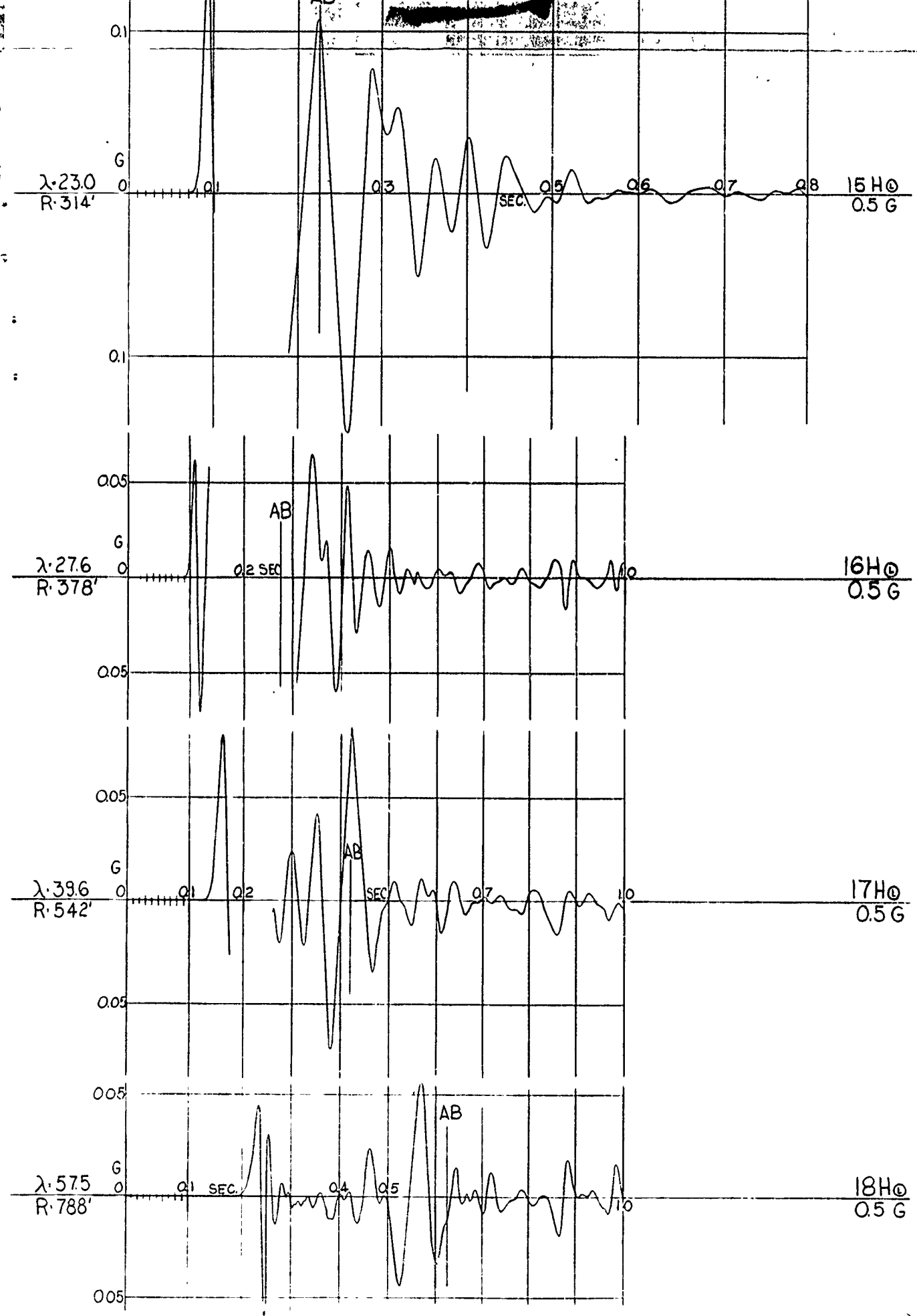

[redacted]

(3) of (3)

HE - 1

VERTICAL EARTH ACCELERATION

HE-1

VERTICAL EARTH ACCELERATION

W 2560 | D_g 5.0
$W^{1/3}$ 13.8 | D_c 1.9
λ_c 0.135

OPERATION JANGLE

25 August 1951

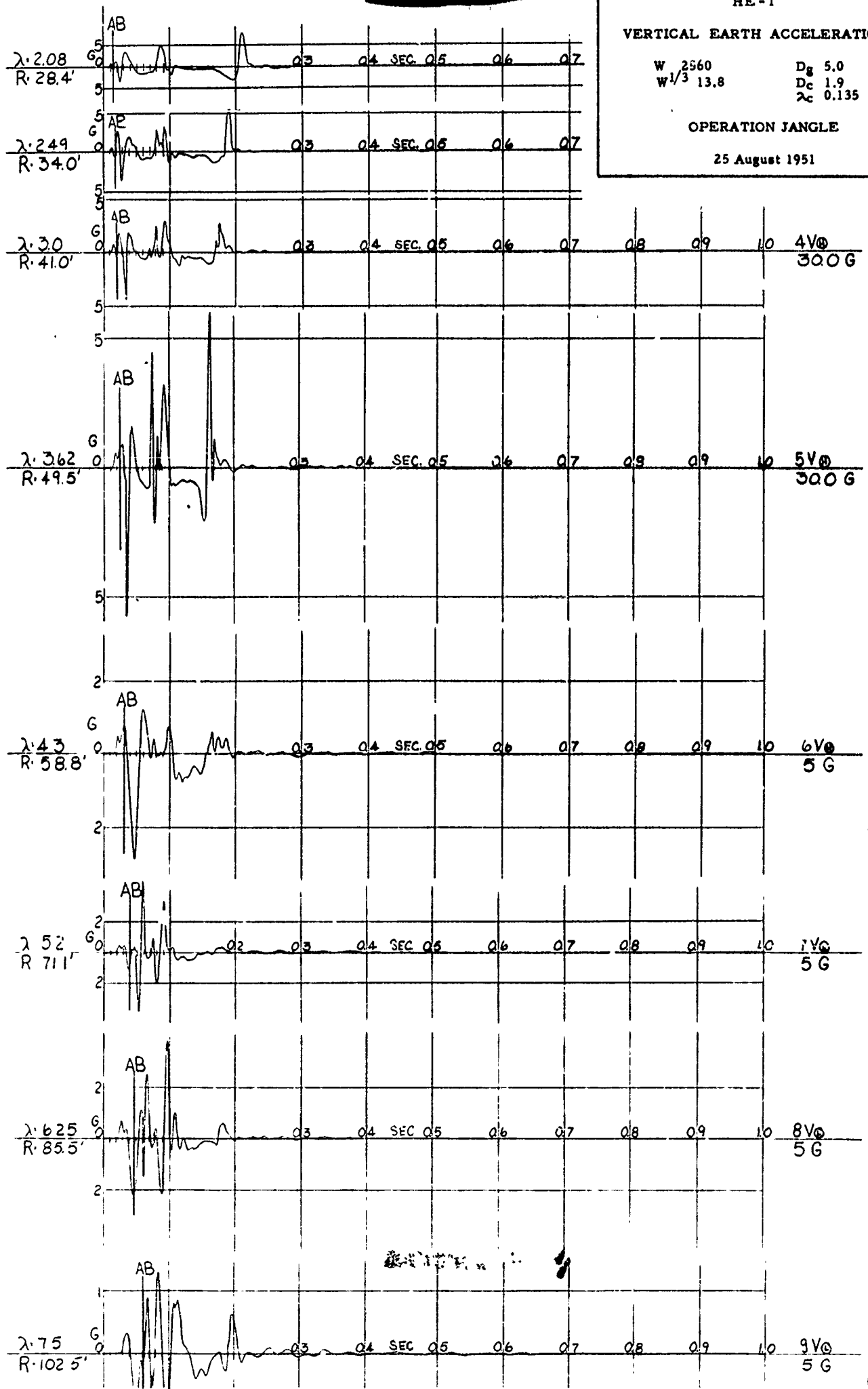

(2)

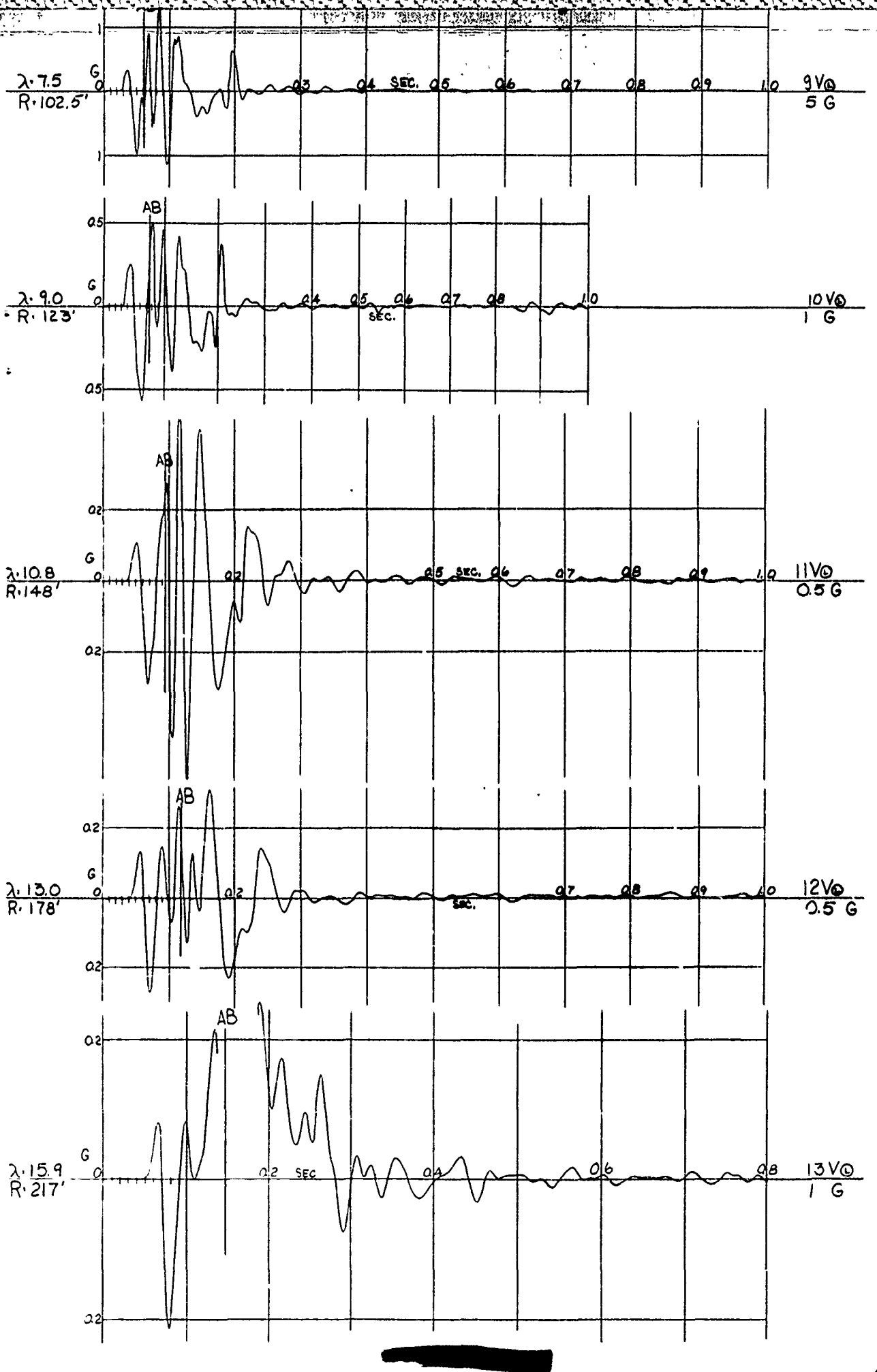
λ·7.5
R·102.5'
G
0
SEC.
9V@
5 G
AB
λ·9.0
R·123'
10V@
1 G
λ·10.8
R·148'
11V@
0.5G
λ·13.0
R·178'
12V@
0.5 G
λ·15.9
R·217'
13V@
1 G

[redacted]

HE - 1

VERTICAL EARTH ACCELERATION

(continued)

[redacted]

HE-1

VERTICAL EARTH ACCELERATION

W 2560	D_g 5.0
$W^{1/3}$ 13.8	D_c 1.9
	λ_c 0.135

OPERATION JANGLE

25 August 1951

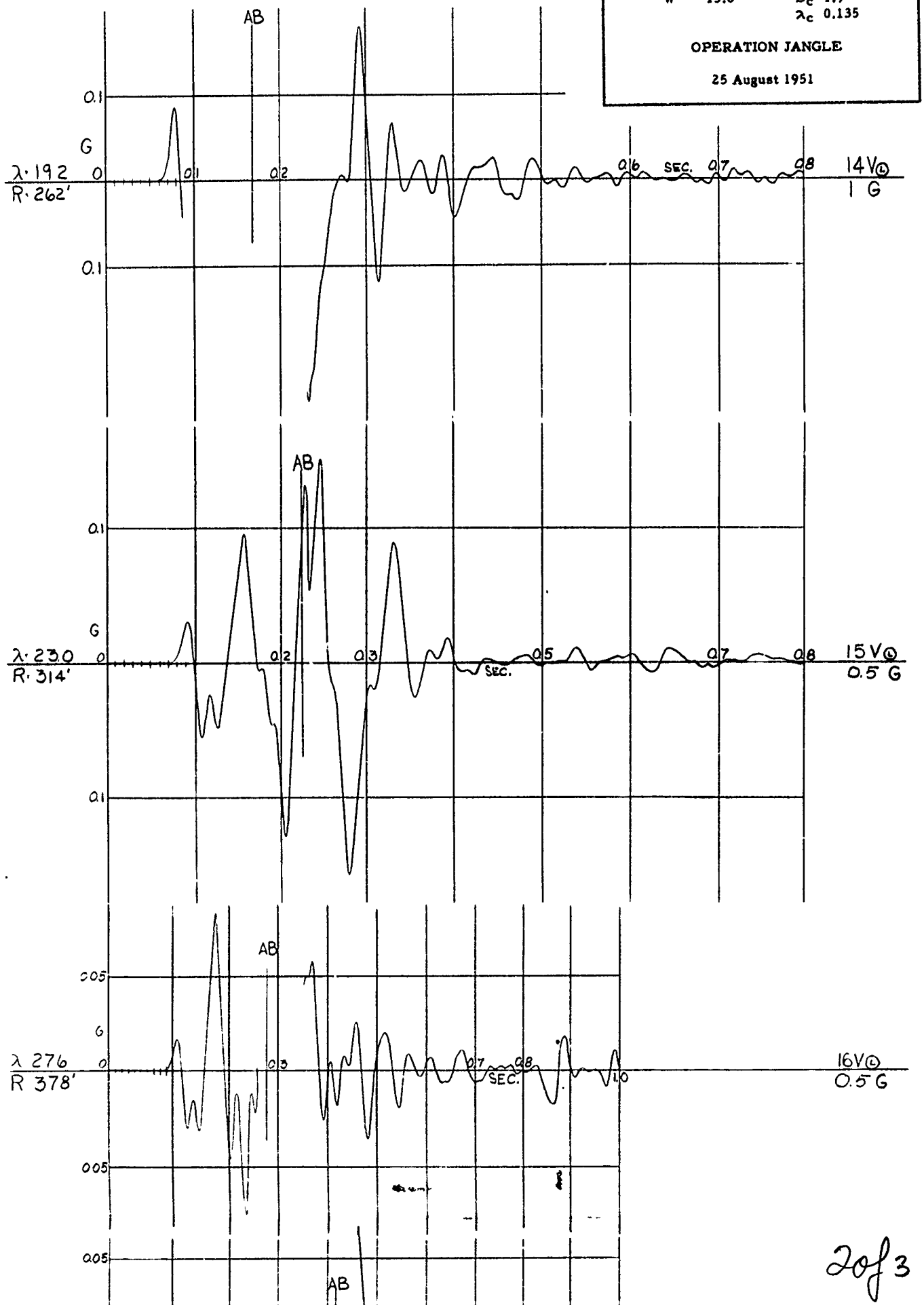

2 of 3

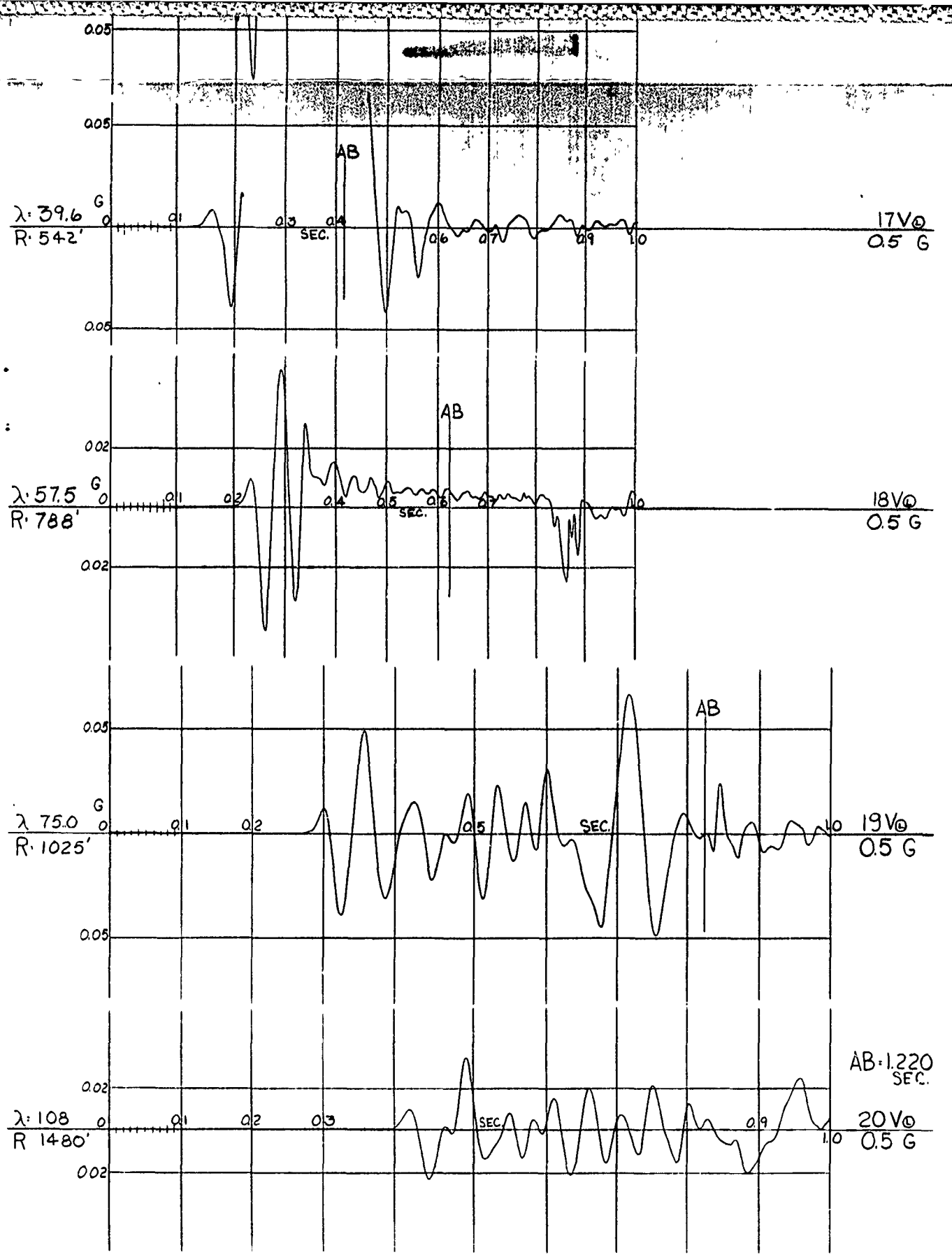

[redacted]

(3) of (3)

HE-1

EARTH PRESSURE

W 2560 D_g 5.0
$W^{1/3}$ 13.8 D_c 1.9
λ_c 0.135

OPERATION JANGLE

25 August 1951

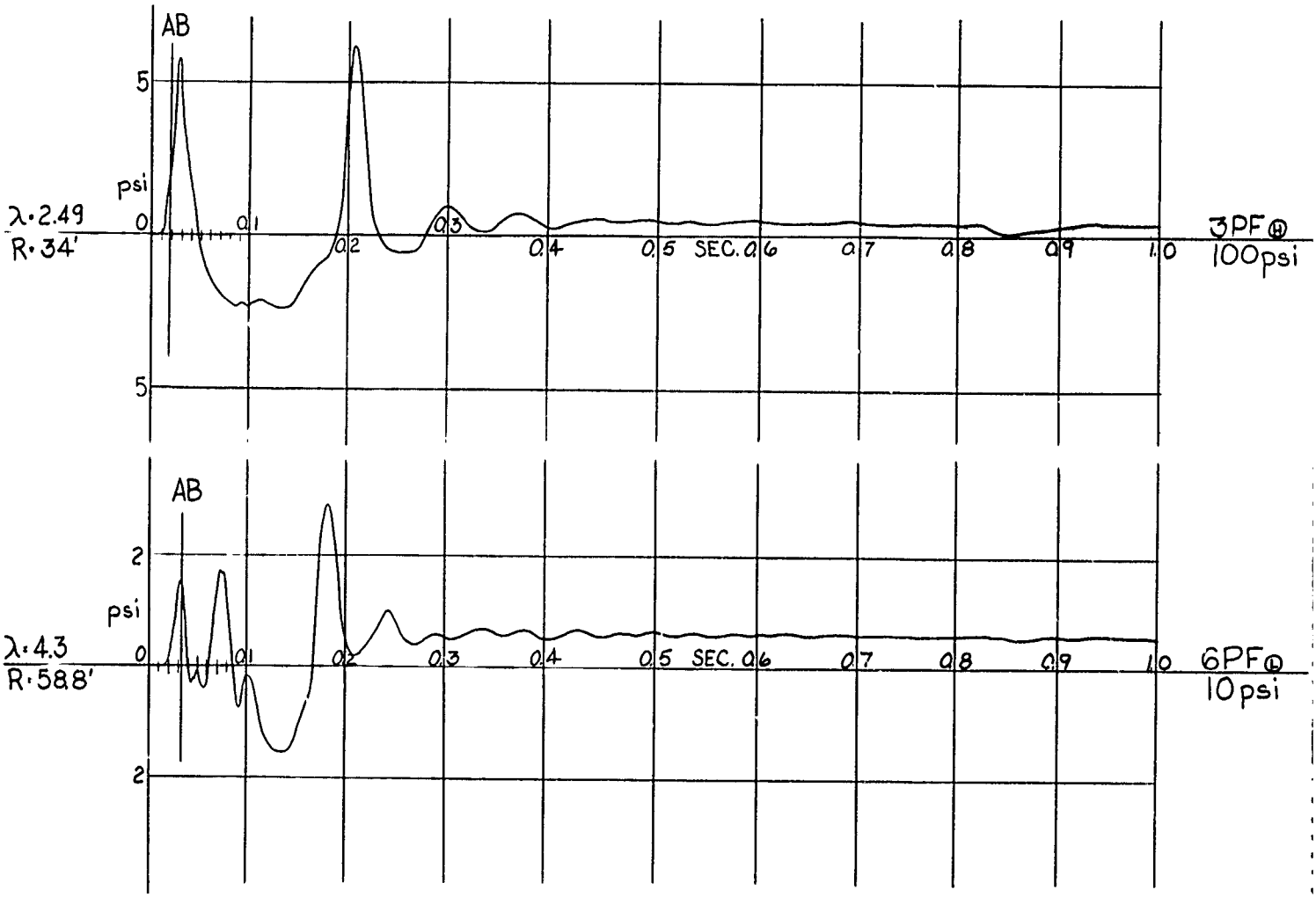

HE - 1

AIR-BLAST PRESSURE

W 2560 D_c 1.9
$W^{1/3}$ 13.8 λ_c 0.135

OPERATION JANGLE

25 August 1951

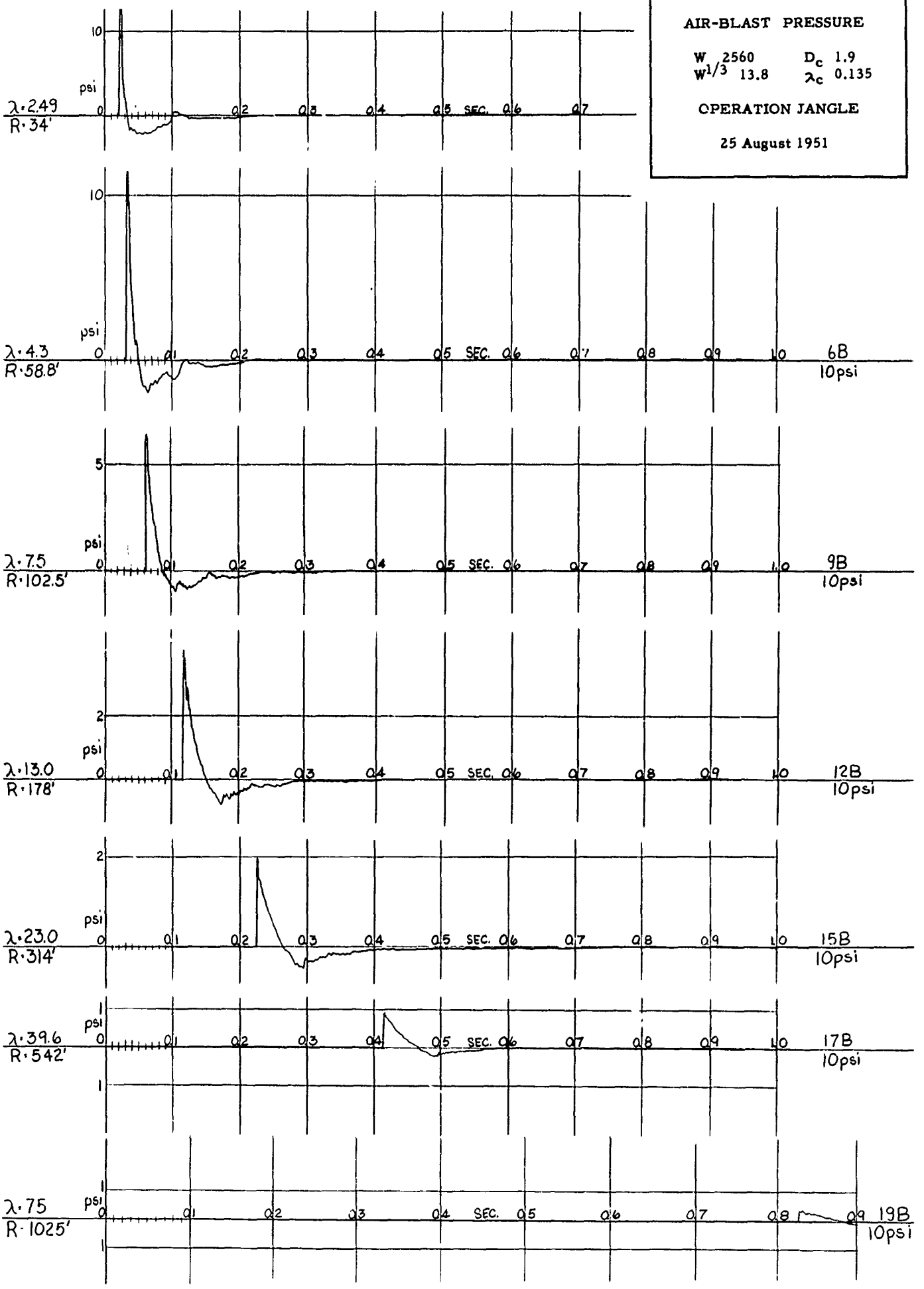

HE - 2

HORIZONTAL EARTH ACCELERATION

HE-2

HORIZONTAL EARTH ACCELERATION

W 40,000 | D_g 5.0
$W^{1/3}$ 34.2 | D_c 4.7
λ_c 0.135

OPERATION JANGLE

3 September 1951

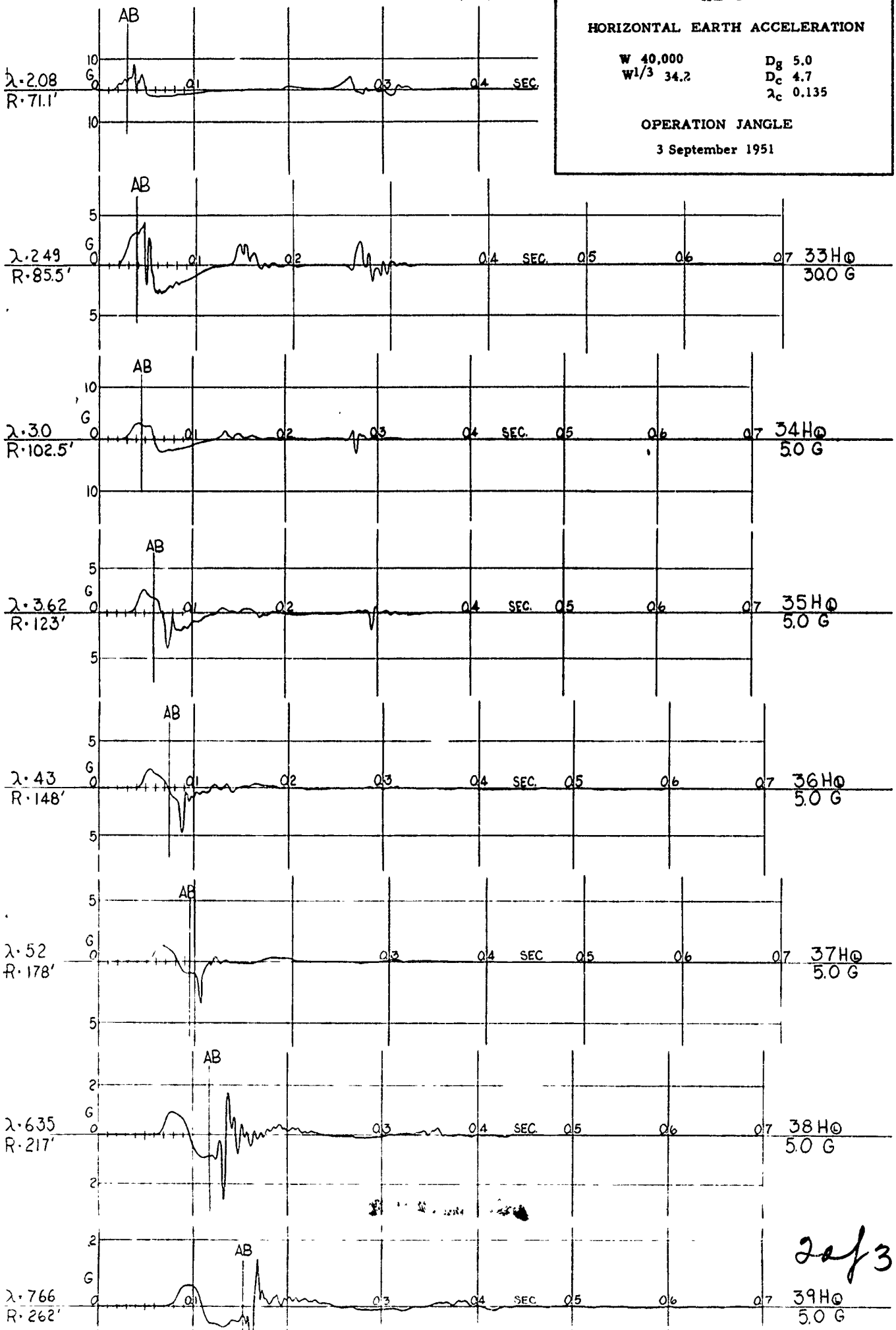

2 of 3

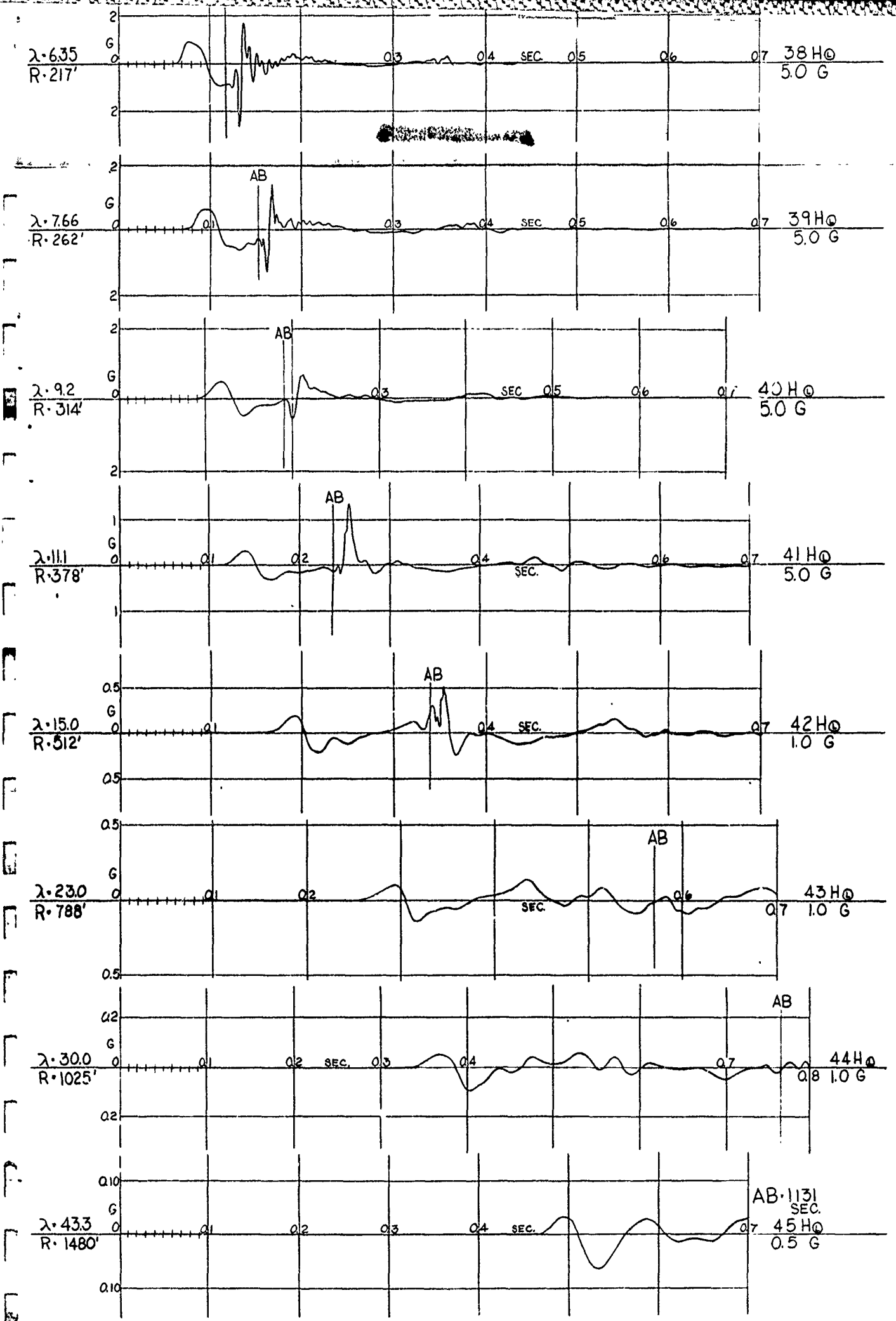
λ·6.35
R·217'
38 H①
5.0 G
λ·7.66
R·262'
AB
39 H①
5.0 G
λ·9.2
R·314'
AB
40 H①
5.0 G
λ·11.1
R·378'
AB
41 H①
5.0 G
λ·15.0
R·512'
AB
42 H①
1.0 G
λ·23.0
R·788'
AB
43 H①
1.0 G
λ·30.0
R·1025'
AB
44 H①
1.0 G
λ·43.3
R·1480'
AB·1131 SEC.
45 H①
0.5 G
SEC.

HE - 2

VERTICAL EARTH ACCELERATION

HE-2

VERTICAL EARTH ACCELERATION

W 40,000 D_g 5.0
$W^{1/3}$ 34.2 D_c 4.7
λ_c 0.135

OPERATION JANGLE

3 September 1951

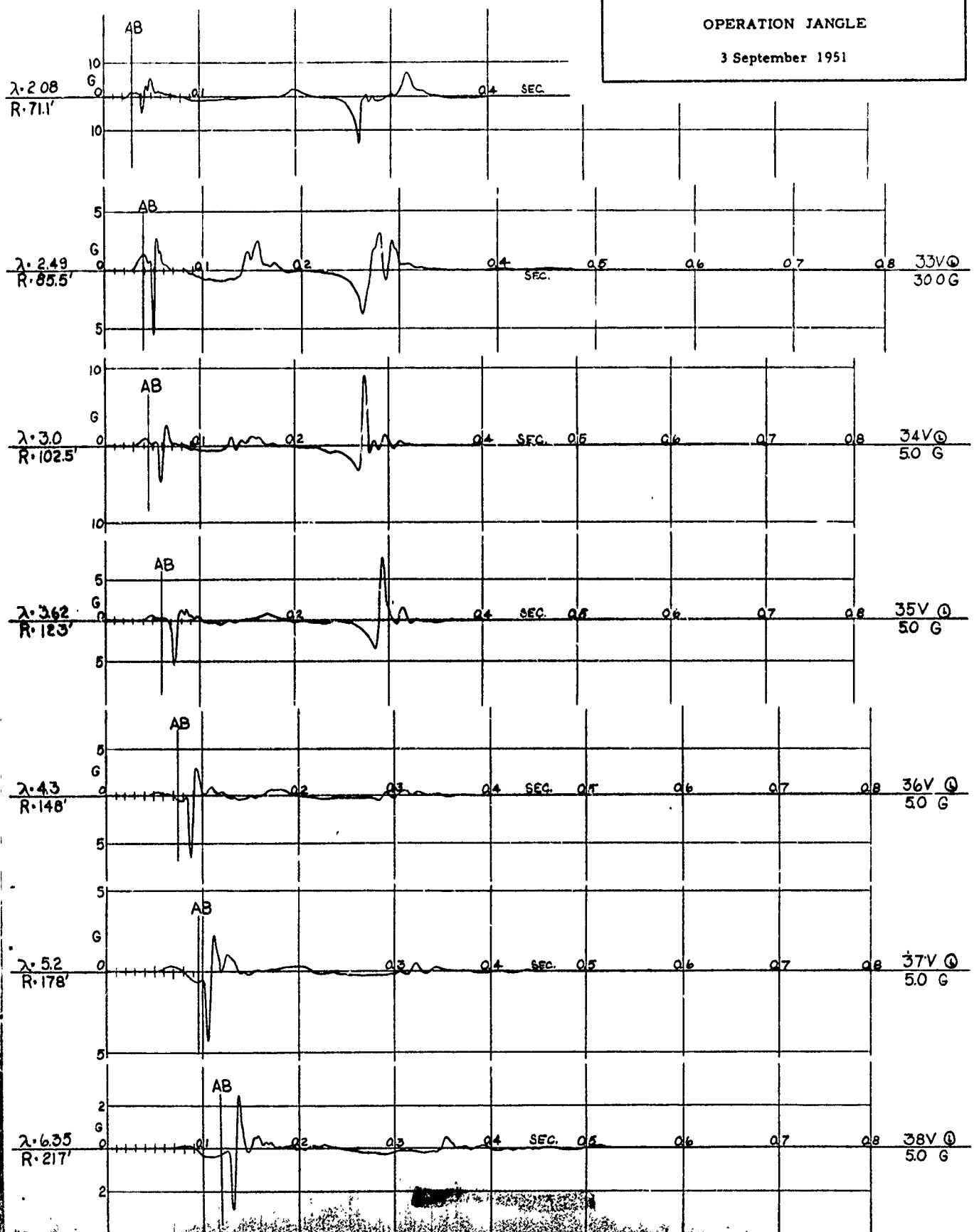

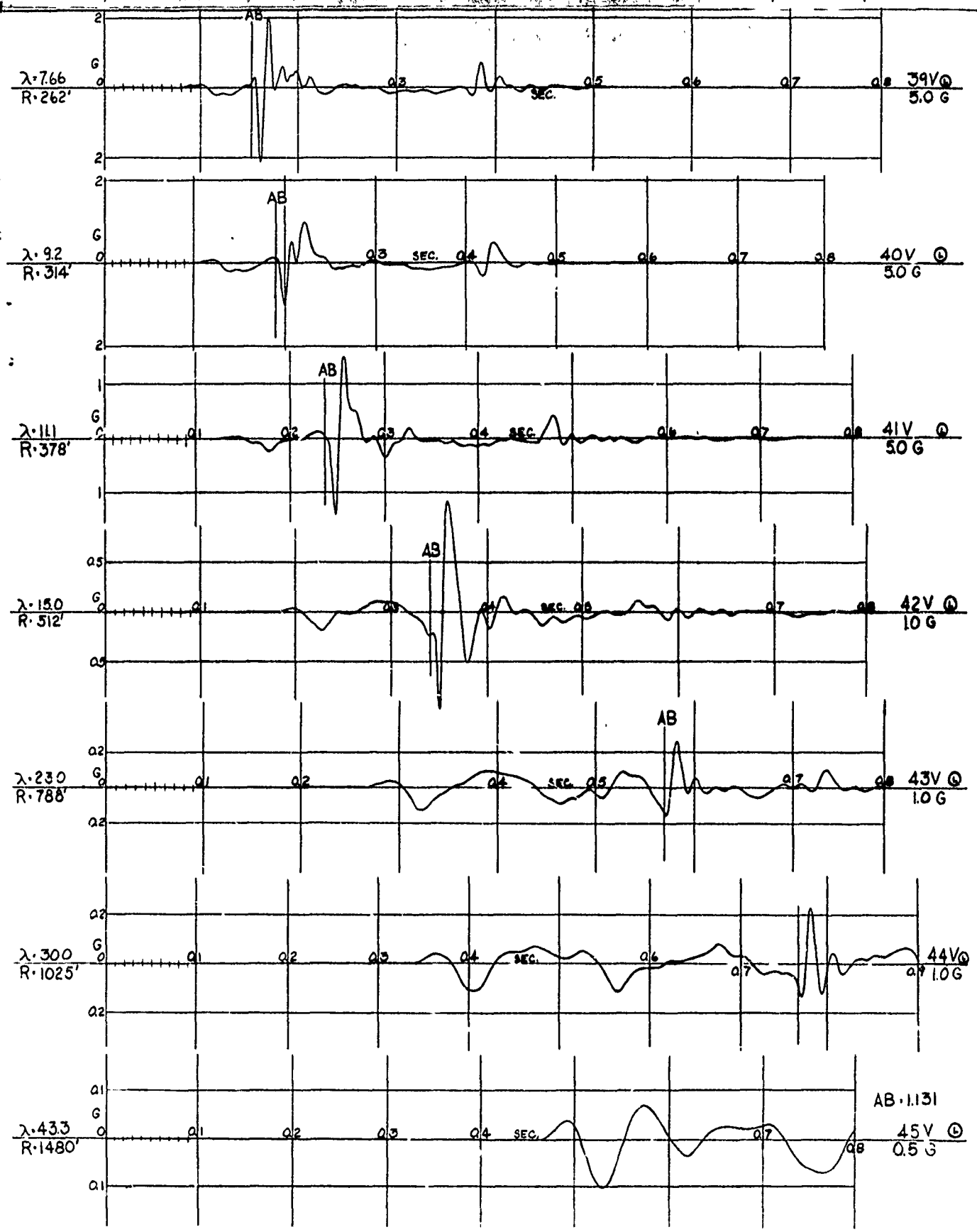
λ·7.66
R·262'
AB
SEC.
39V
5.0 G
λ·9.2
R·314'
AB
SEC.
40V
5.0 G
λ·11.1
R·378'
AB
SEC.
41V
5.0 G
λ·15.0
R·512'
AB
SEC.
42V
1.0 G
λ·23.0
R·788'
AB
SEC.
43V
1.0 G
λ·30.0
R·1025'
SEC.
44V
1.0 G
λ·43.3
R·1480'
AB·1.131
SEC.
45V
0.5 G

[redacted]

HE - 2

EARTH PRESSURE

HE-2

EARTH PRESSURE

W 40,000 D_g 5.0
$W^{1/3}$ 34.2 D_c 4.7
λ_c 0.135

OPERATION JANGLE

3 September 1951

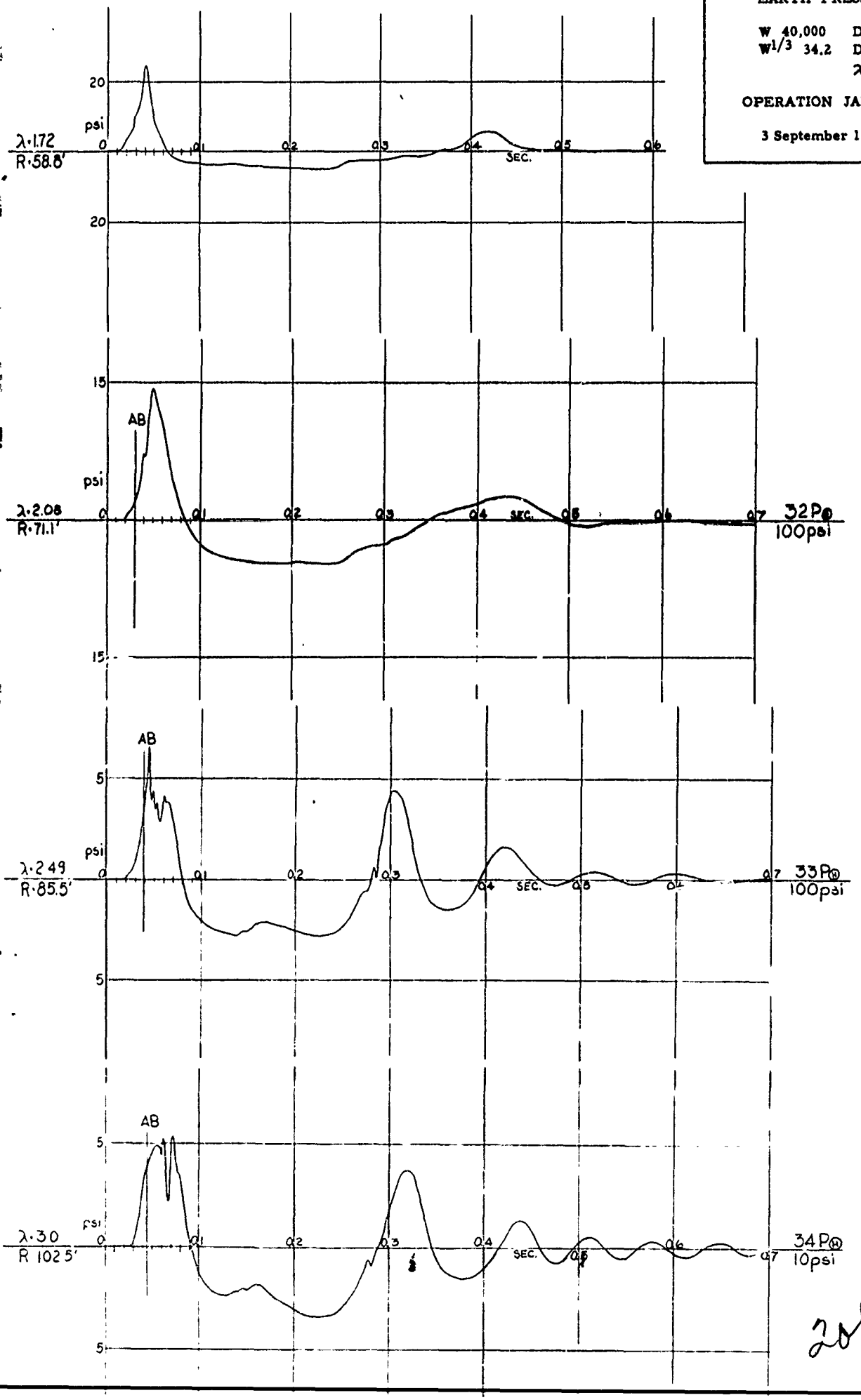

2 of 3

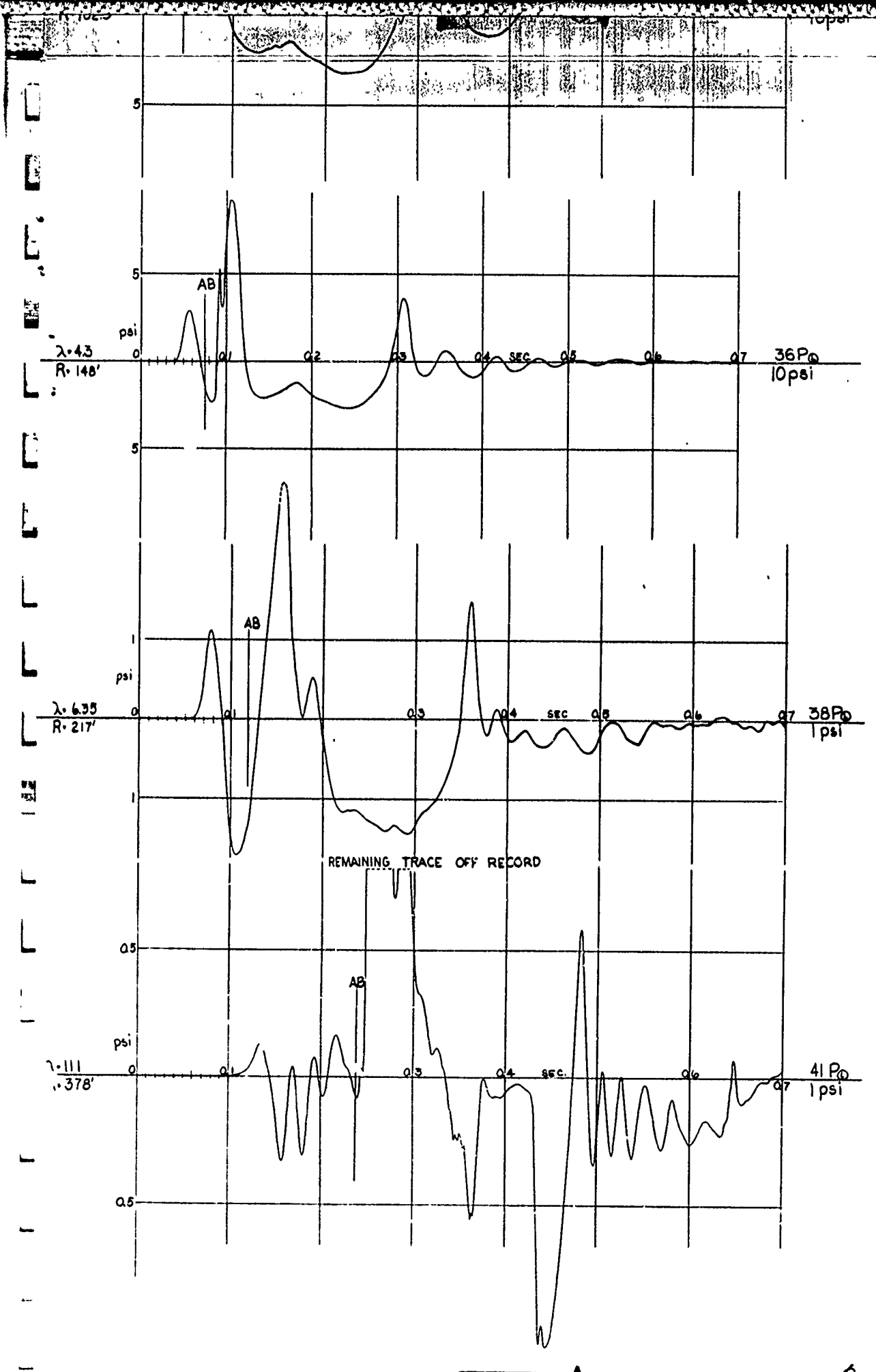
5
AB
psi
0
λ•4.3
R• 148'
0.1
0.2
0.3
0.4
SEC
0.5
0.6
0.7
36P①
10psi
5
1
AB
psi
0
λ• 6.35
R• 217'
0.1
0.3
0.4
SEC
0.5
0.6
0.7
38P①
1psi
1
REMAINING TRACE OFF RECORD
0.5
AB
psi
0
λ•111
•378'
0.1
0.3
0.4
SEC.
0.6
0.7
41P①
1psi
0.5

3 of 3

HE-2

AIR-BLAST PRESSURE

W 40,000 D_c 4.7
$W^{1/3}$ 34.2 λ_c 0.135

OPERATION JANGLE

3 September 1951

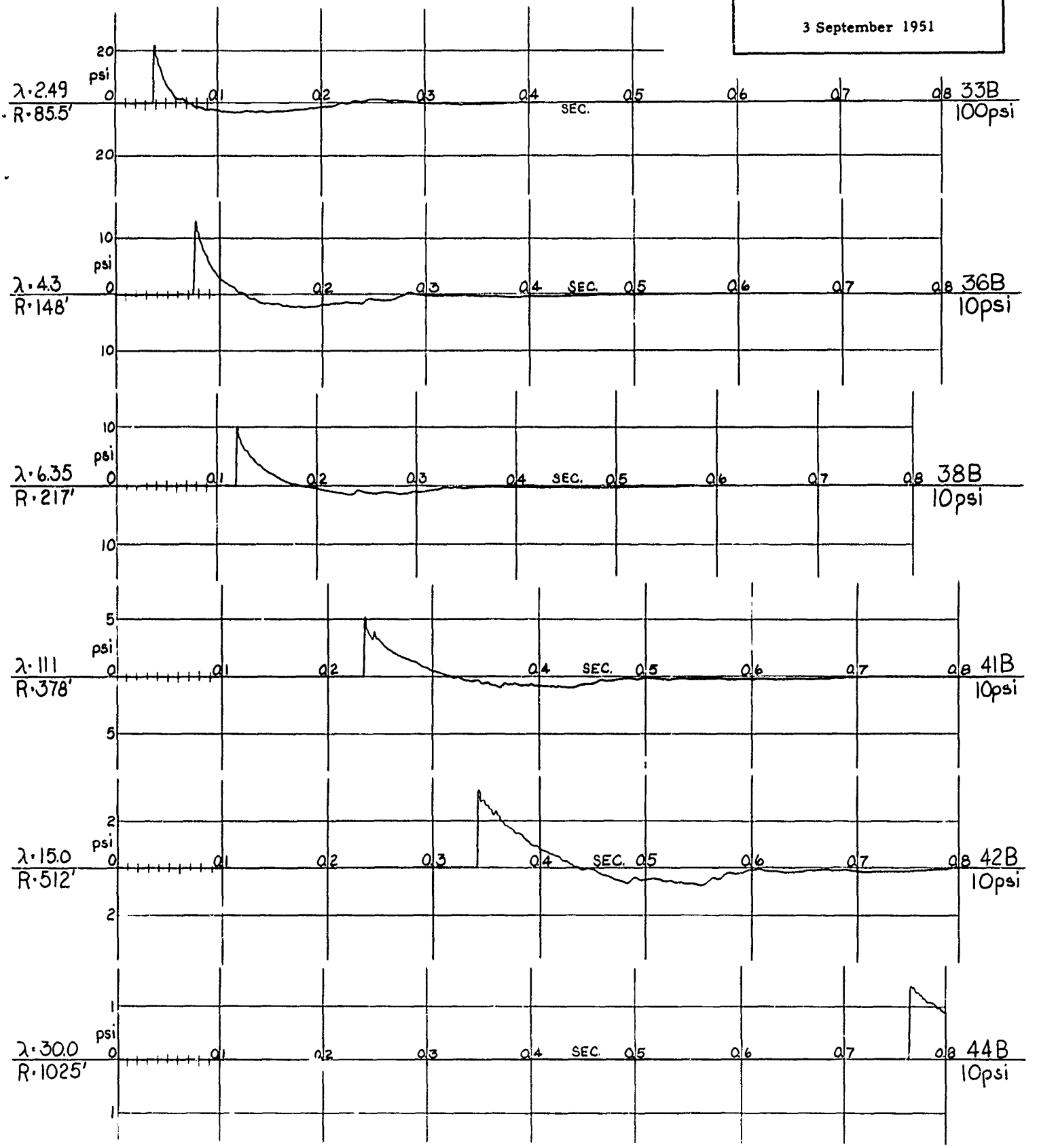

HE - 3

HORIZONTAL EARTH ACCELERATION

HE-3

HORIZONTAL EARTH ACCELERATION

W 2560 D_g 5.0
$W^{1/3}$ 13.8 D_c 6.9
λ_c 0.5

OPERATION JANGLE

15 September 1951

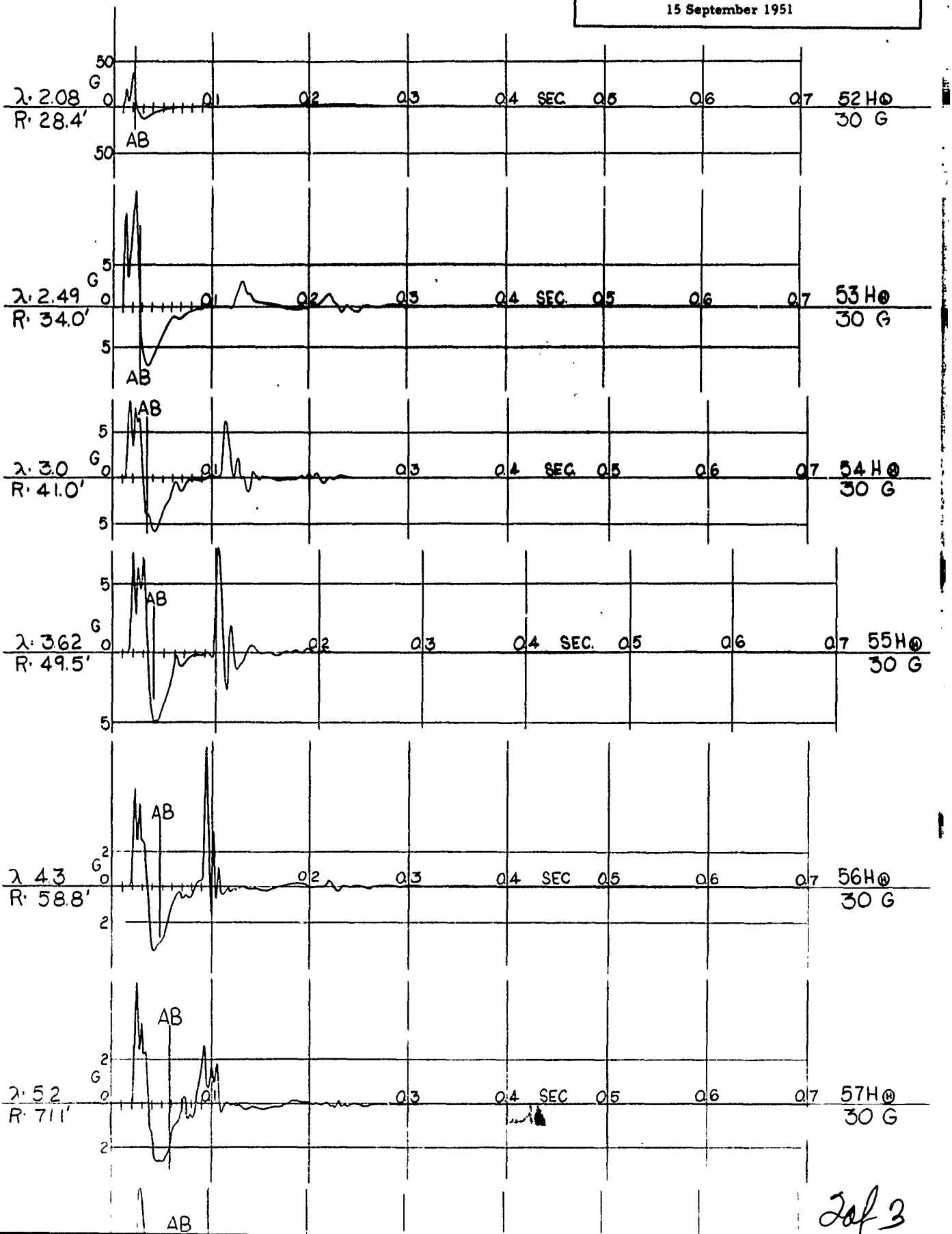

2 of 3

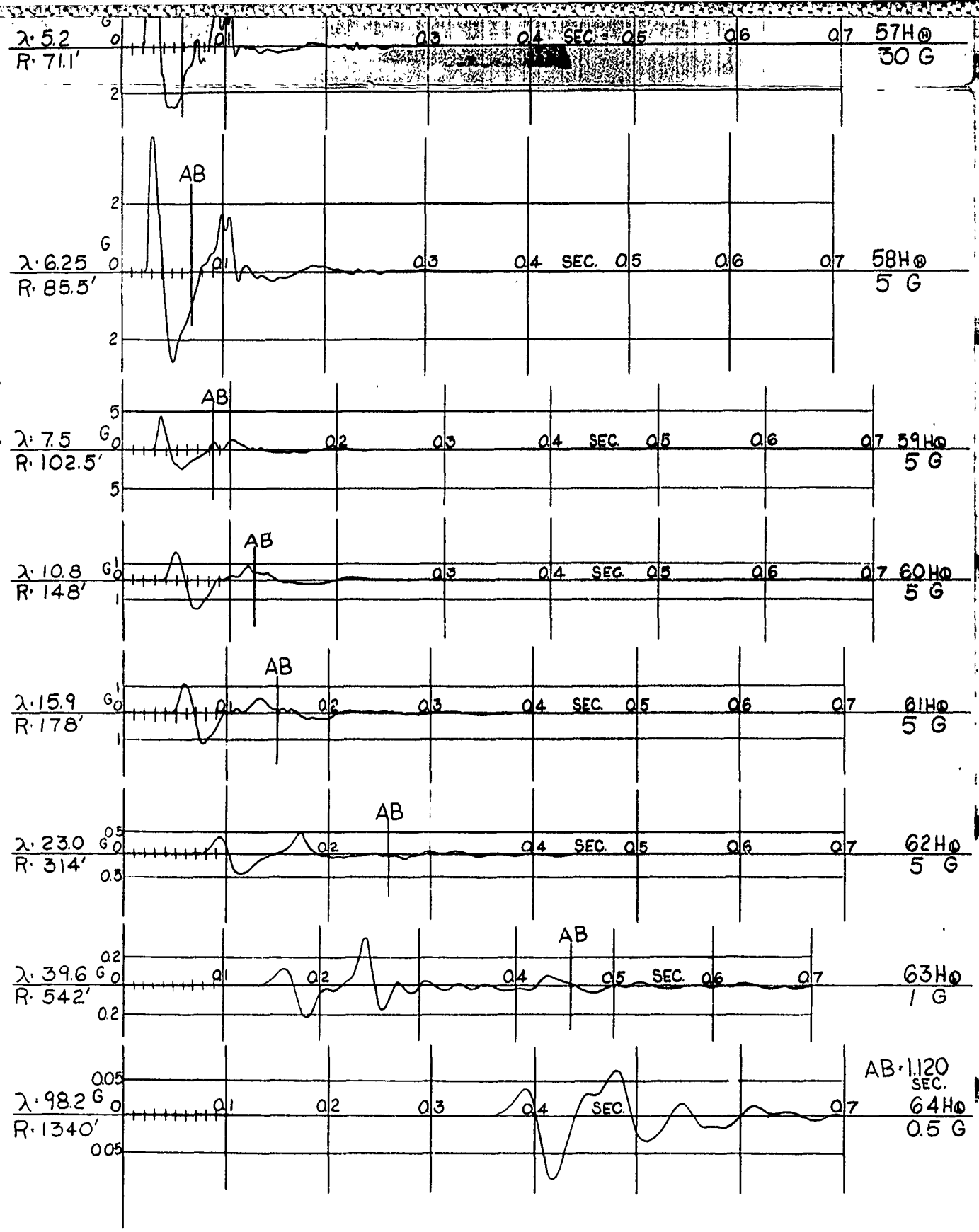
λ·5.2
R·71.1'
G
0
2
0.1
0.3
0.4
SEC.
0.5
0.6
0.7
57H⊗
30 G
AB
λ·6.25
R·85.5'
58H⊗
5 G
λ·7.5
R·102.5'
5
0.2
59H⊗
5 G
λ·10.8
R·148'
1
60H⊗
5 G
λ·15.9
R·178'
61H⊗
5 G
λ·23.0
R·314'
0.5
62H⊗
5 G
λ·39.6
R·542'
0.2
63H⊗
1 G
λ·98.2
R·1340'
0.05
AB·1.120
SEC.
64H⊗
0.5 G

3 of 3

HE - 3

VERTICAL EARTH ACCELERATION

HE-3

VERTICAL EARTH ACCELERATION

W 2560
$W^{1/3}$ 13.8

D_g 5.0
D_c 6.9
λ_c 0.5

OPERATION JANGLE

15 September 1951

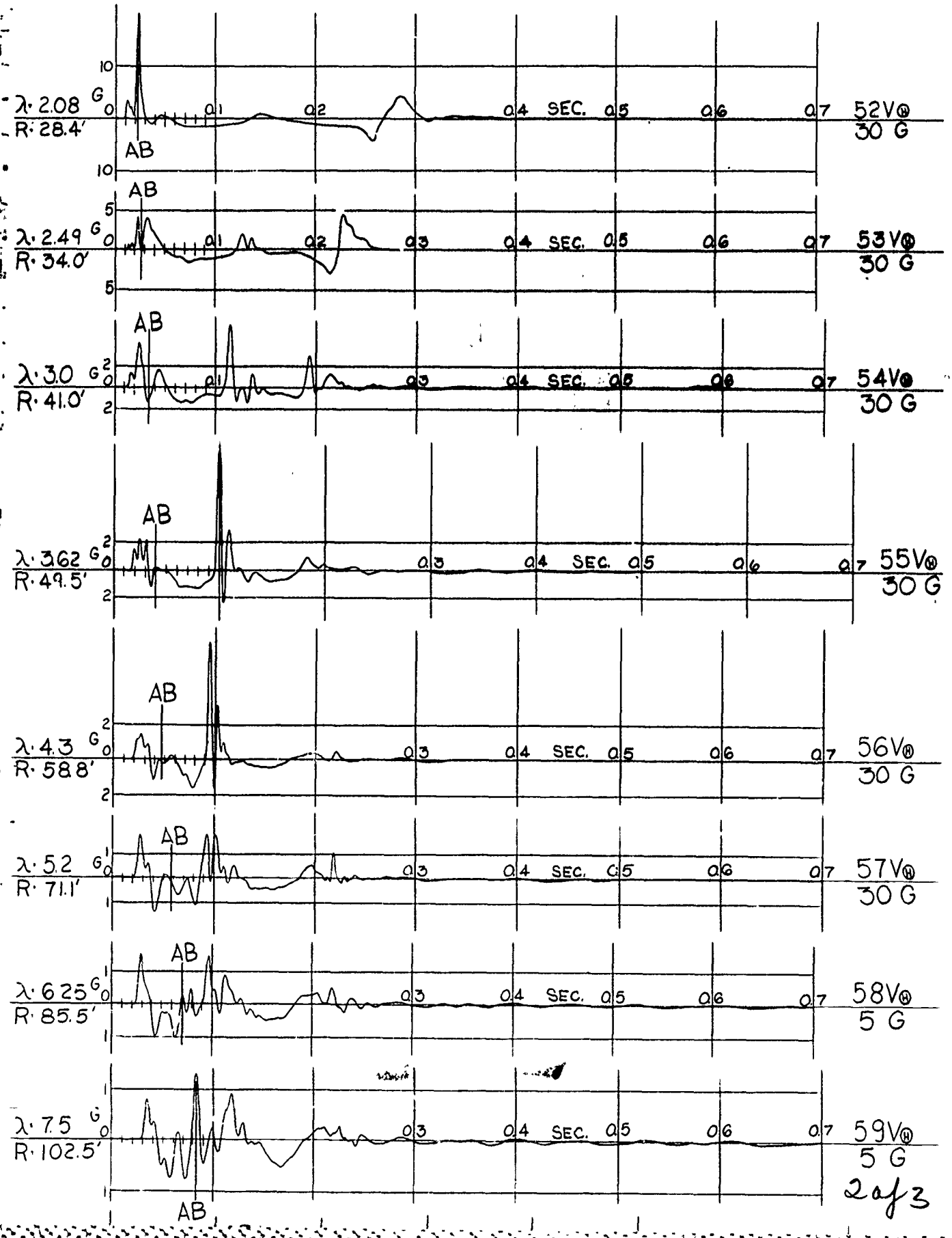

2 of 3

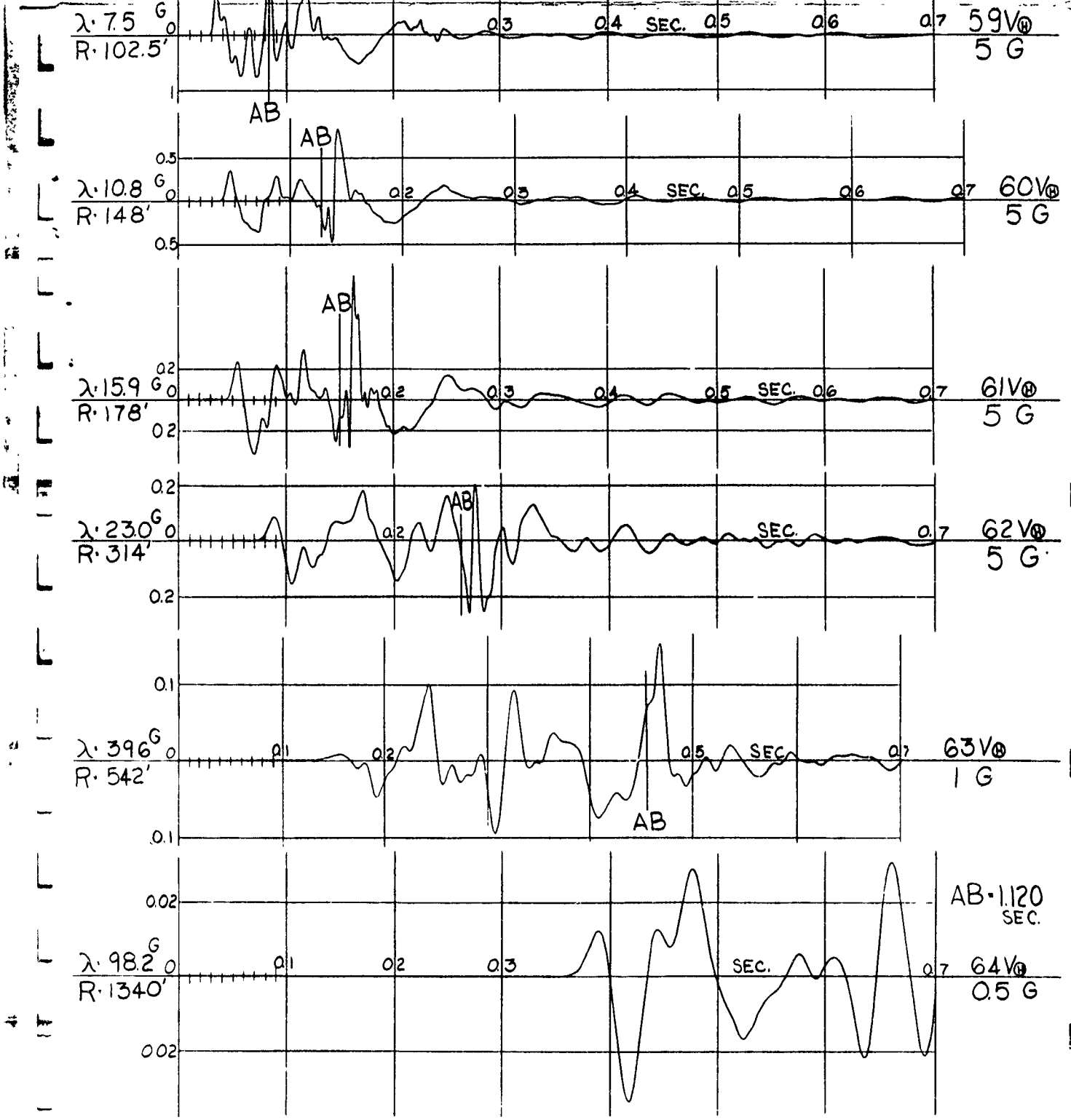
λ·7.5 G
R·102.5'
0.3
0.4 SEC. 0.5
0.6
0.7
59V⊗
5 G
AB
AB
0.5
λ·10.8 G
R·148'
0.2
0.3
0.4 SEC. 0.5
0.6
0.7
60V⊗
5 G
0.5
AB
0.2
λ·15.9 G
R·178'
0.2
0.2
0.3
0.4
0.5 SEC. 0.6
0.7
61V⊗
5 G
0.2
λ·23.0 G
R·314'
0.2
AB
0.2
SEC.
0.7
62V⊗
5 G
0.1
λ·396 G
R·542'
0.1
0.1
0.2
0.5 SEC.
0.7
AB
63V⊗
1 G
0.02
λ·98.2 G
R·1340'
0.02
0.1
0.2
0.3
SEC.
0.7
AB·1.120
SEC.
64V⊗
0.5 G

3 of 3

HE - 3

EARTH PRESSURE

HE-3

EARTH PRESSURE

W 2560 D_g 5.0
$W^{1/3}$ 13.8 D_c 6.9
λ_c 0.5

OPERATION JANGLE

15 September 1951

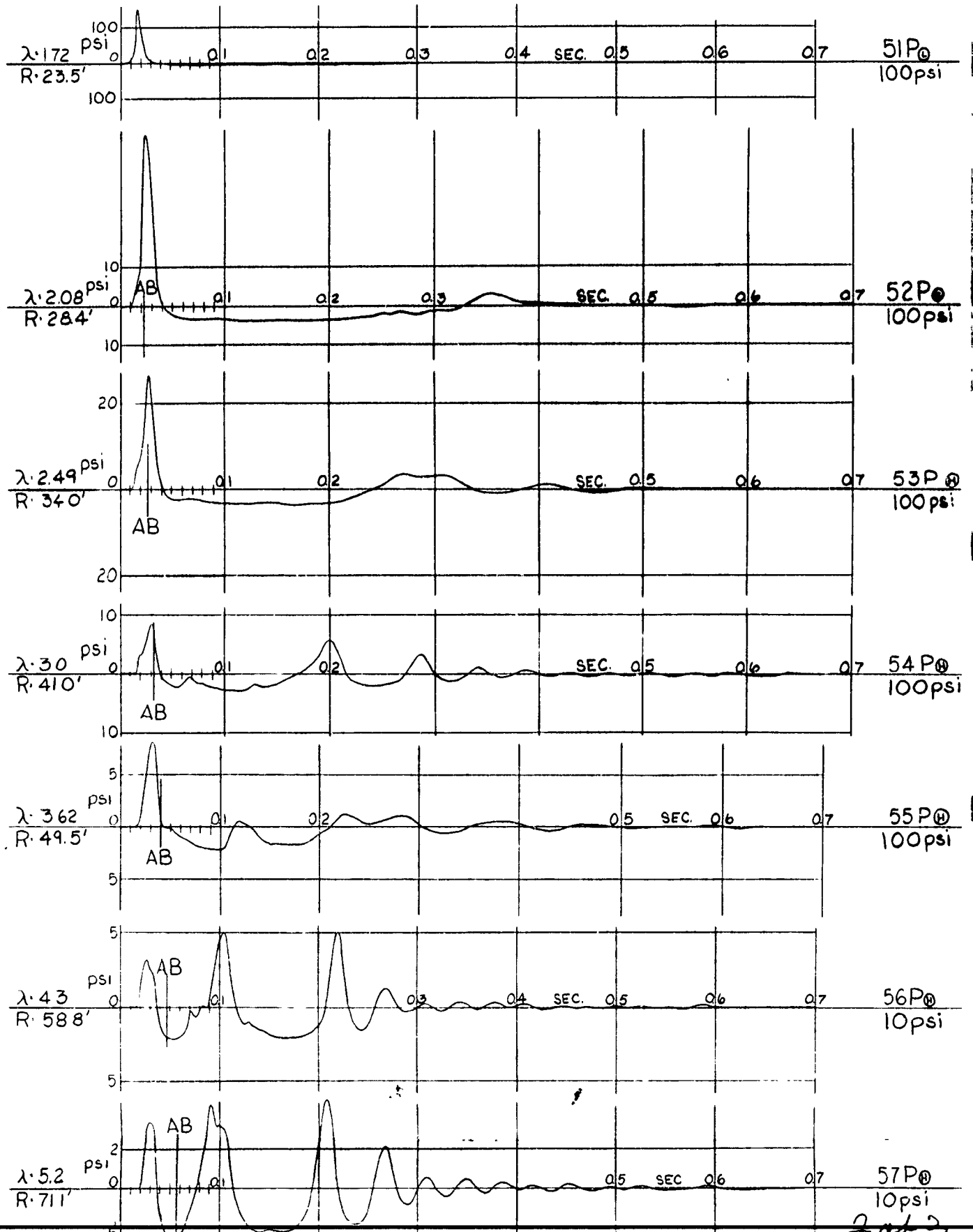

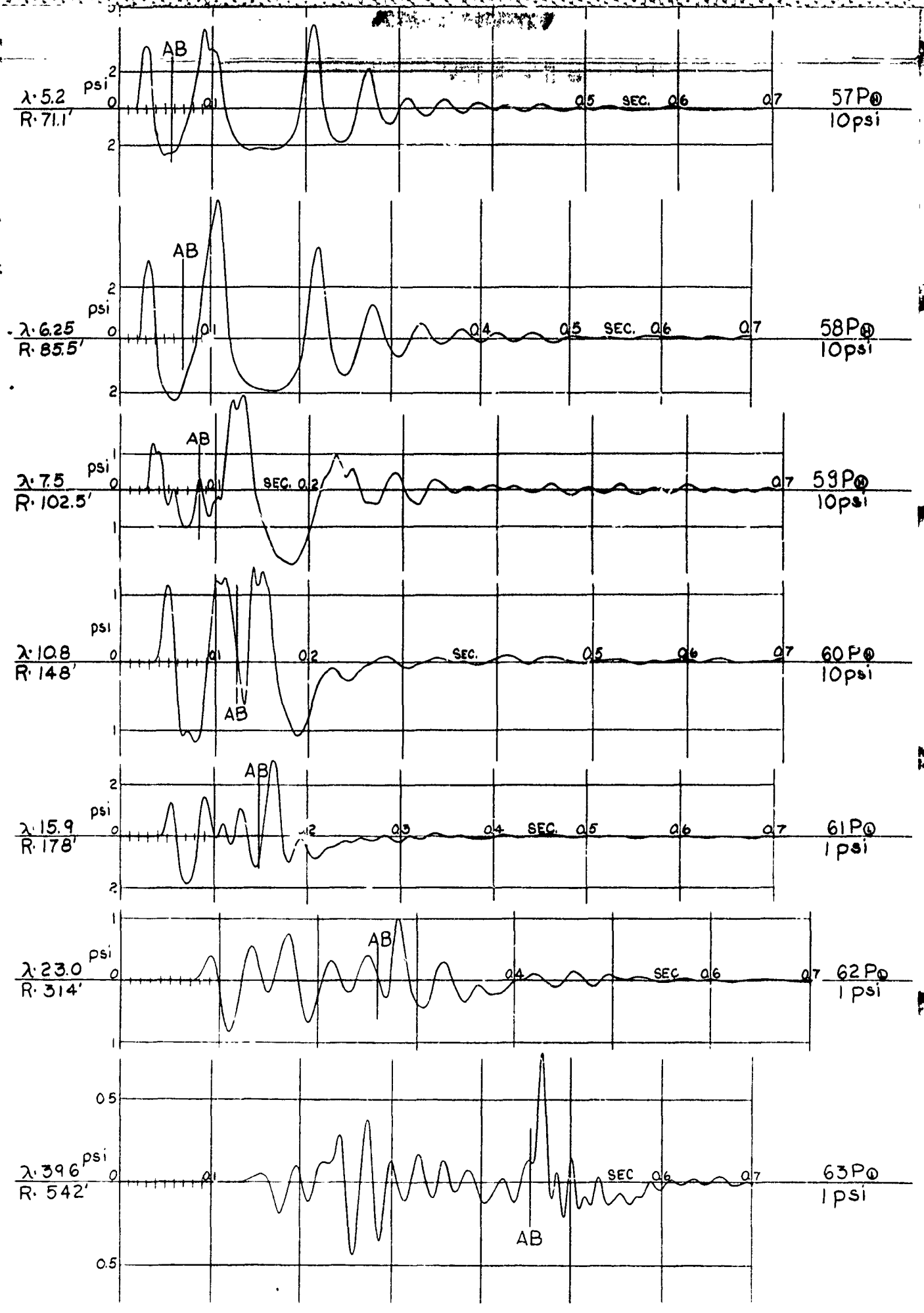

[redacted]

3 of 3

HE-3

AIR-BLAST PRESSURE

W 2560 D_c 6.9
$W^{1/3}$ 13.8 λ_c 0.5

OPERATION JANGLE

15 September 1951

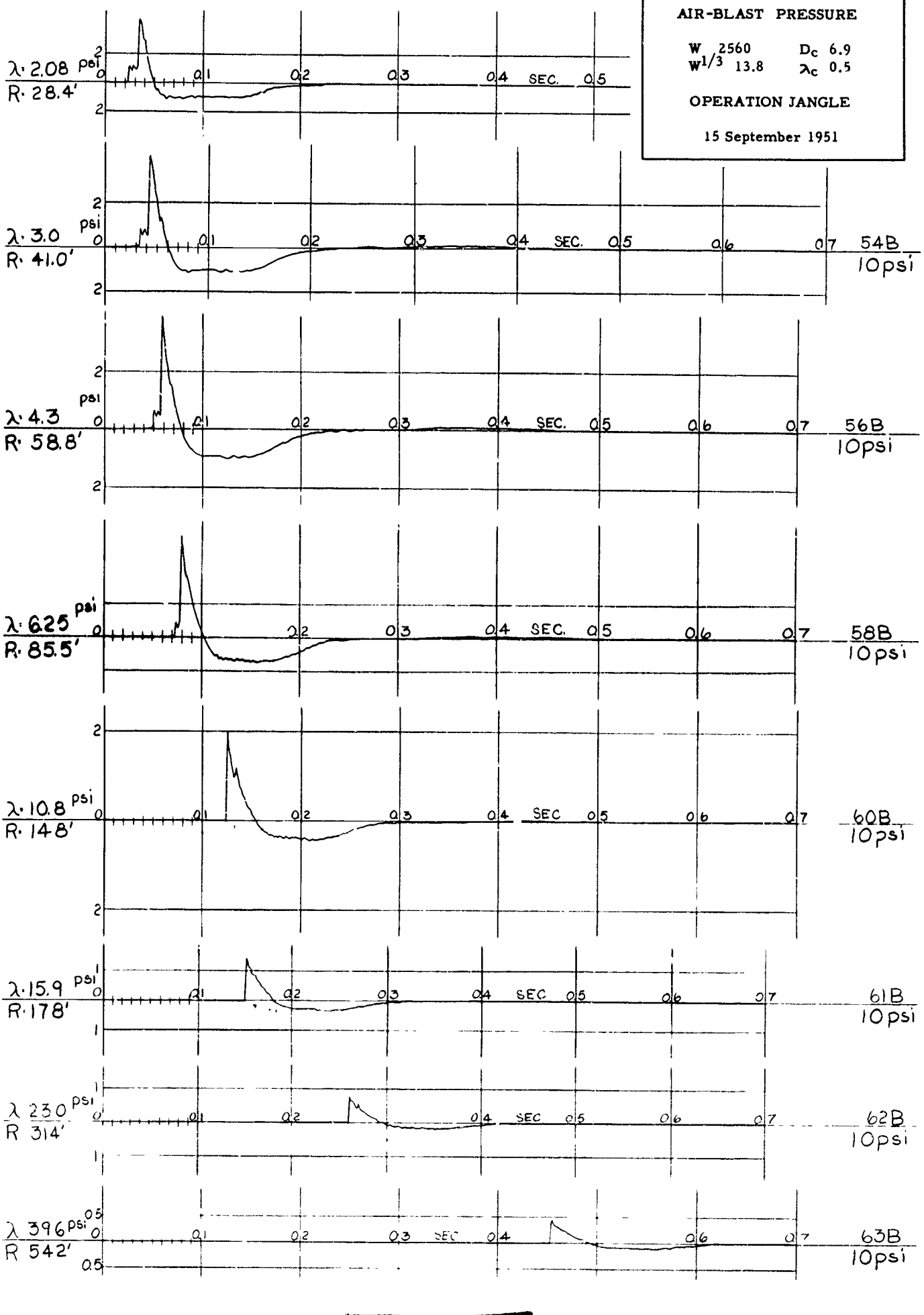

HE - 4

HORIZONTAL EARTH ACCELERATION

HE-4

HORIZONTAL EARTH ACCELERATION

W 2560
$W^{1/3}$ 13.8

D_g 5.0
D_c -1.9
λ_c -0.135

OPERATION JANGLE

9 September 1951

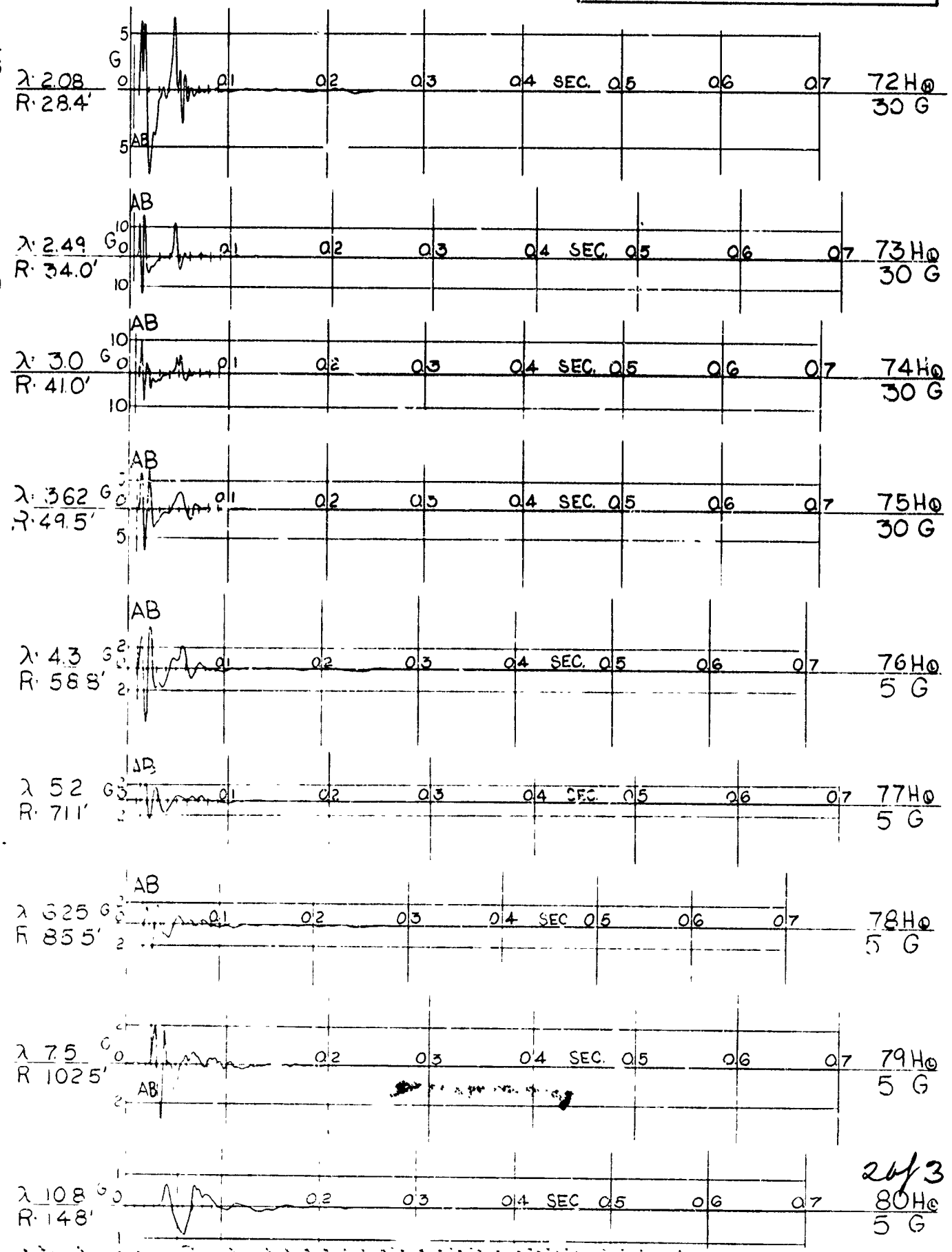

2 of 3

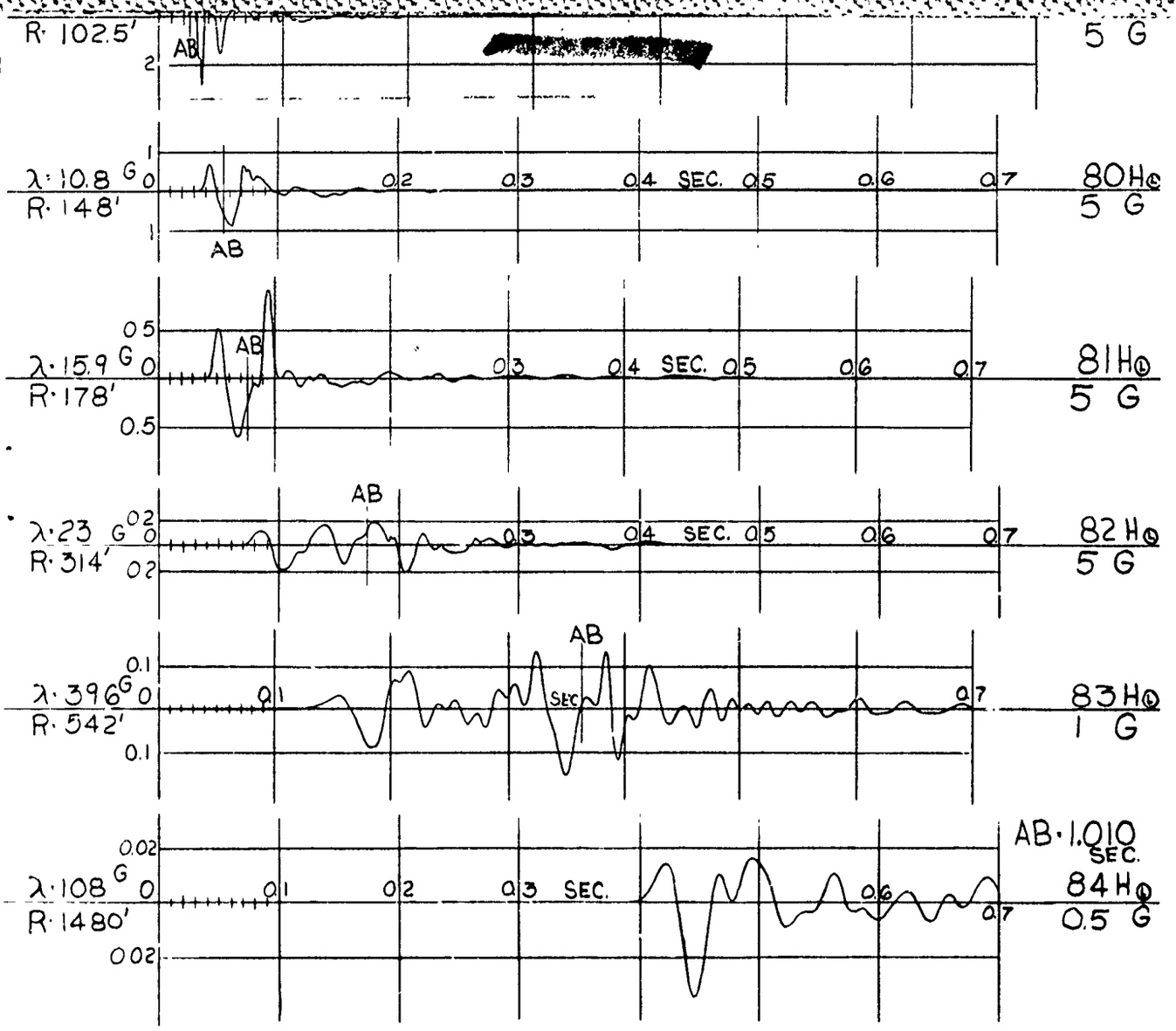

[redacted]

(3 of 3)

HE - 4

VERTICAL EARTH ACCELERATION

HE-4

VERTICAL EARTH ACCELERATION

W 2560	D_g 5.0
$W^{1/3}$ 13.8	D_c -1.9
	λ_c -0.135

OPERATION JANGLE

9 September 1951

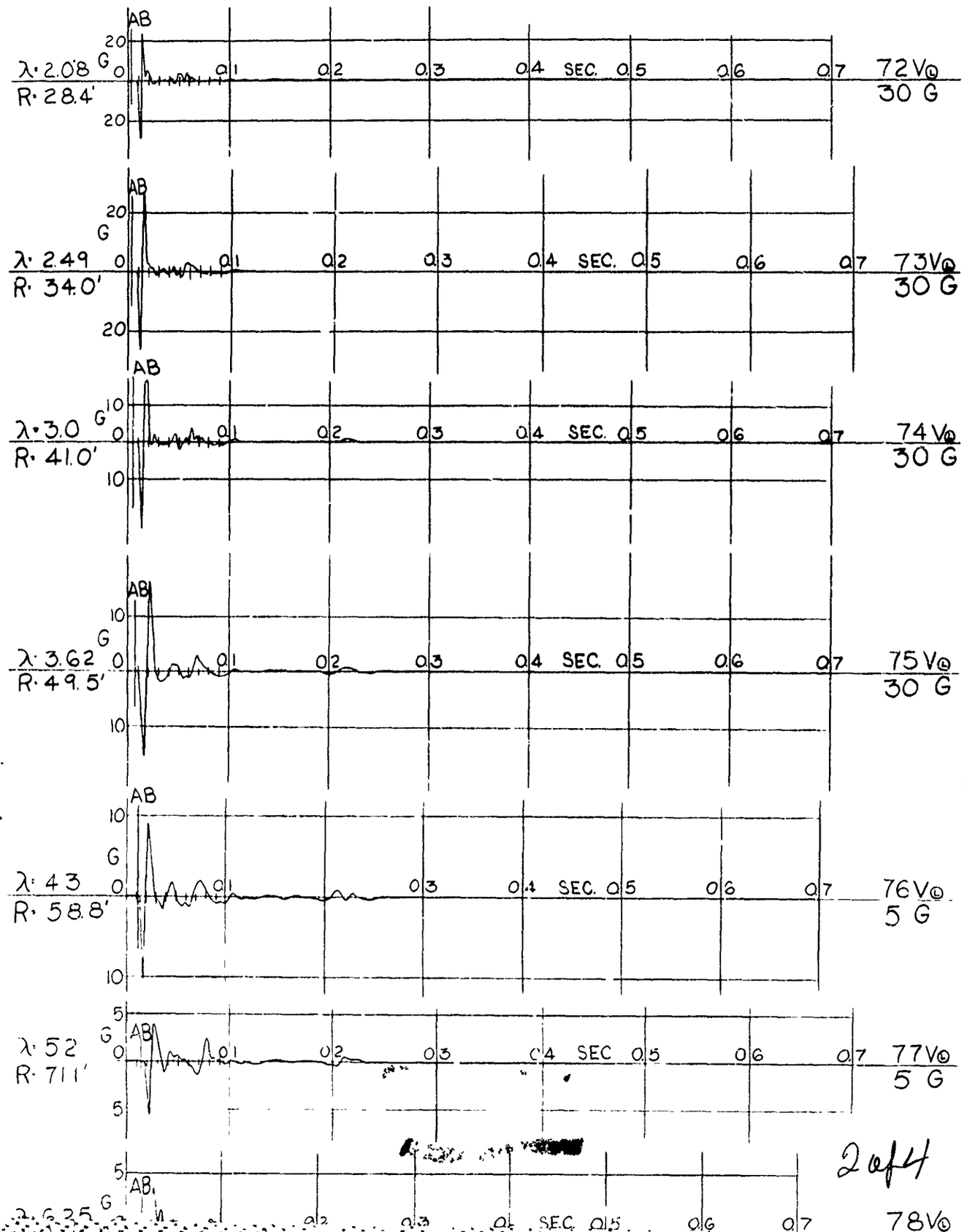

2 of 4

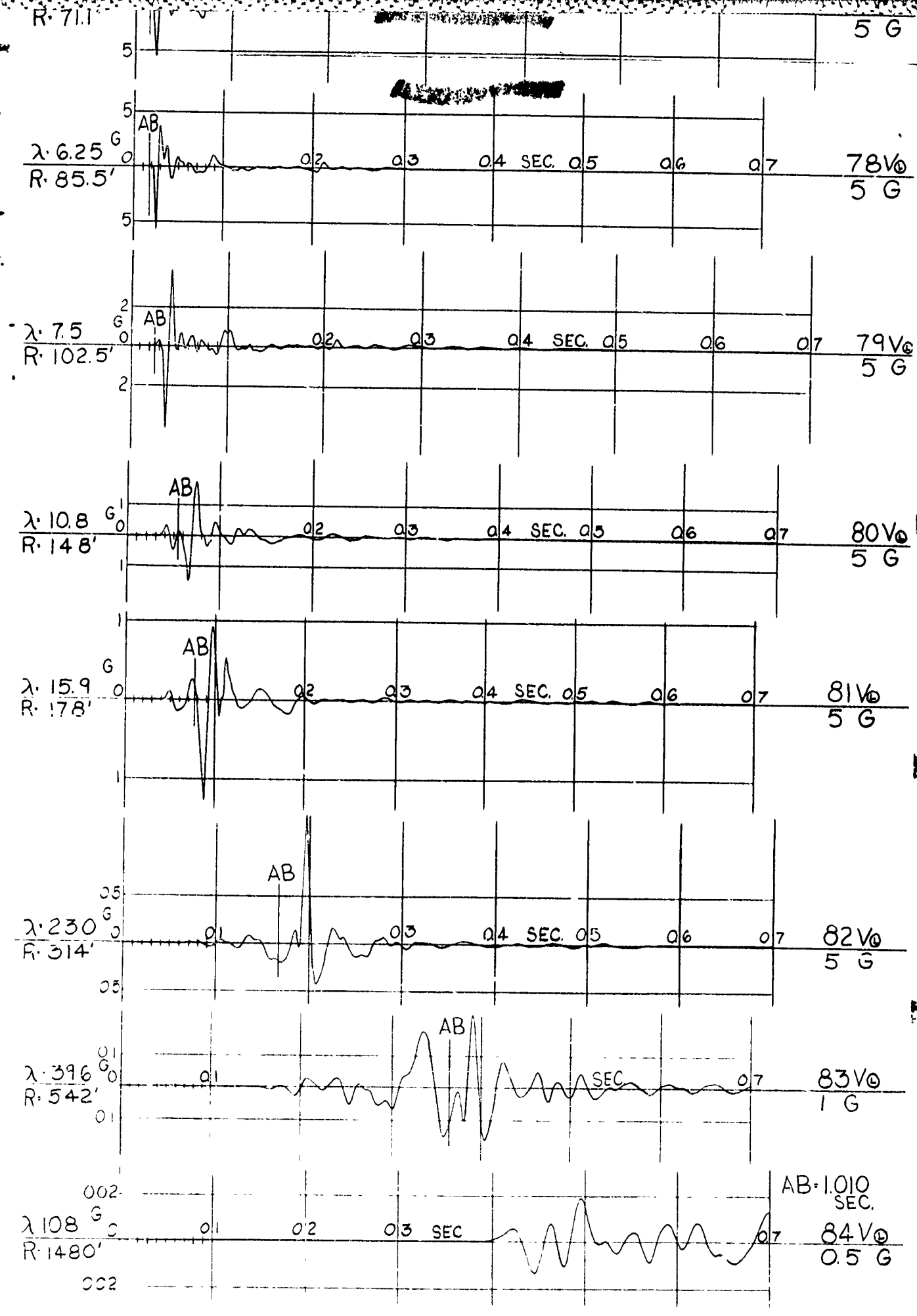
R· 71.1
5
5 G
λ· 6.25
R· 85.5'
AB
0 2 0 3 0 4 SEC. 0 5 0 6 0 7
78V
5 G
λ· 7.5
R· 102.5'
2
AB
79V
5 G
λ· 10.8
R· 148'
1
AB
80V
5 G
λ· 15.9
R· 178'
AB
81V
5 G
λ· 230
R· 314'
0 5
AB
82V
5 G
λ· 396
R· 542'
0 1
AB
SEC
83V
1 G
λ 108
R· 1480'
0 0 2
0 1 0 2 0 3 SEC
AB· 1.010 SEC.
84V
0.5 G

3 of 4

[redacted]

HE-4

EARTH PRESSURE

W 2560 D_g 5.0
$W^{1/3}$ 13.8 D_c -1.9
λ_c -0.135

OPERATION JANGLE

9 September 1951

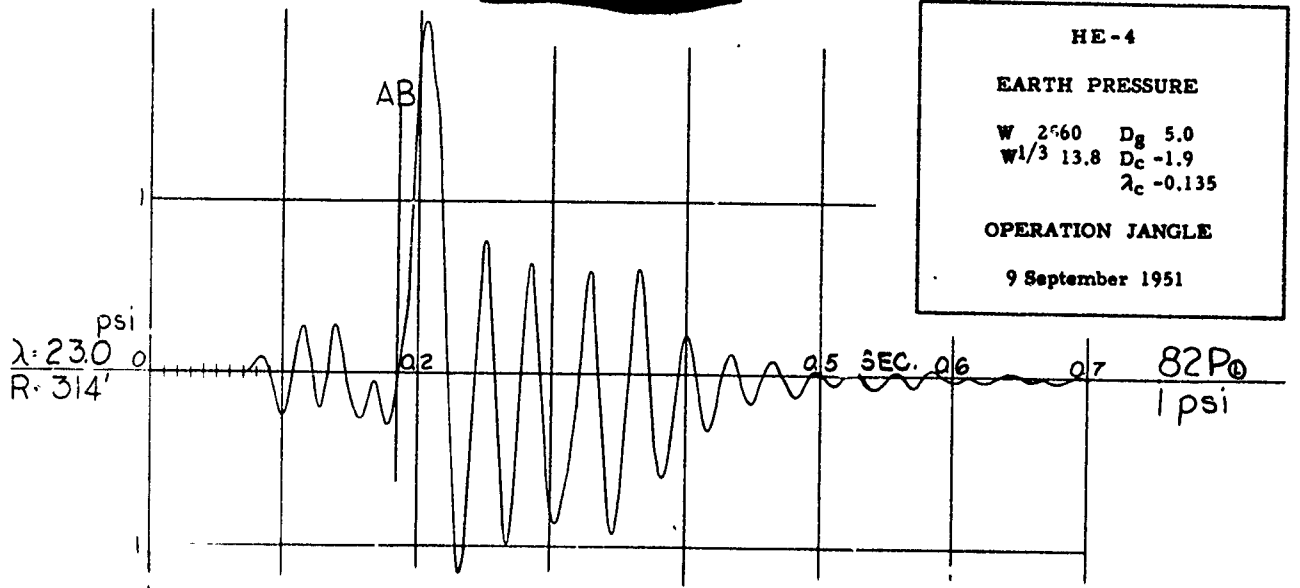

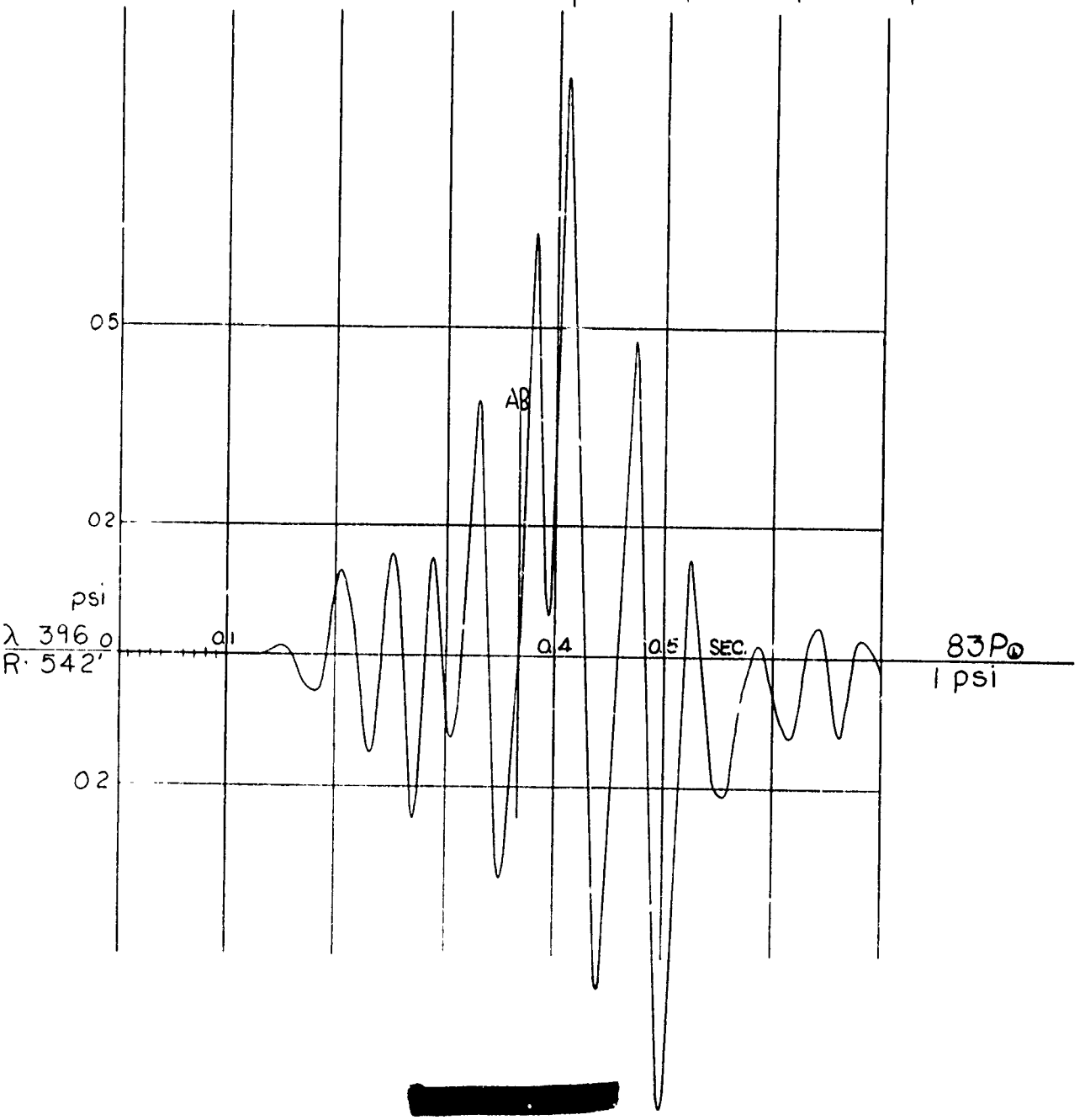

[redacted]

HE - 4

EARTH PRESSURE

HE-4

EARTH PRESSURE

W 2560 D_s 5.0
$W^{1/3}$ 13.8 D_c -1.9
λ_c -0.135

OPERATION JANGLE

9 September 1951

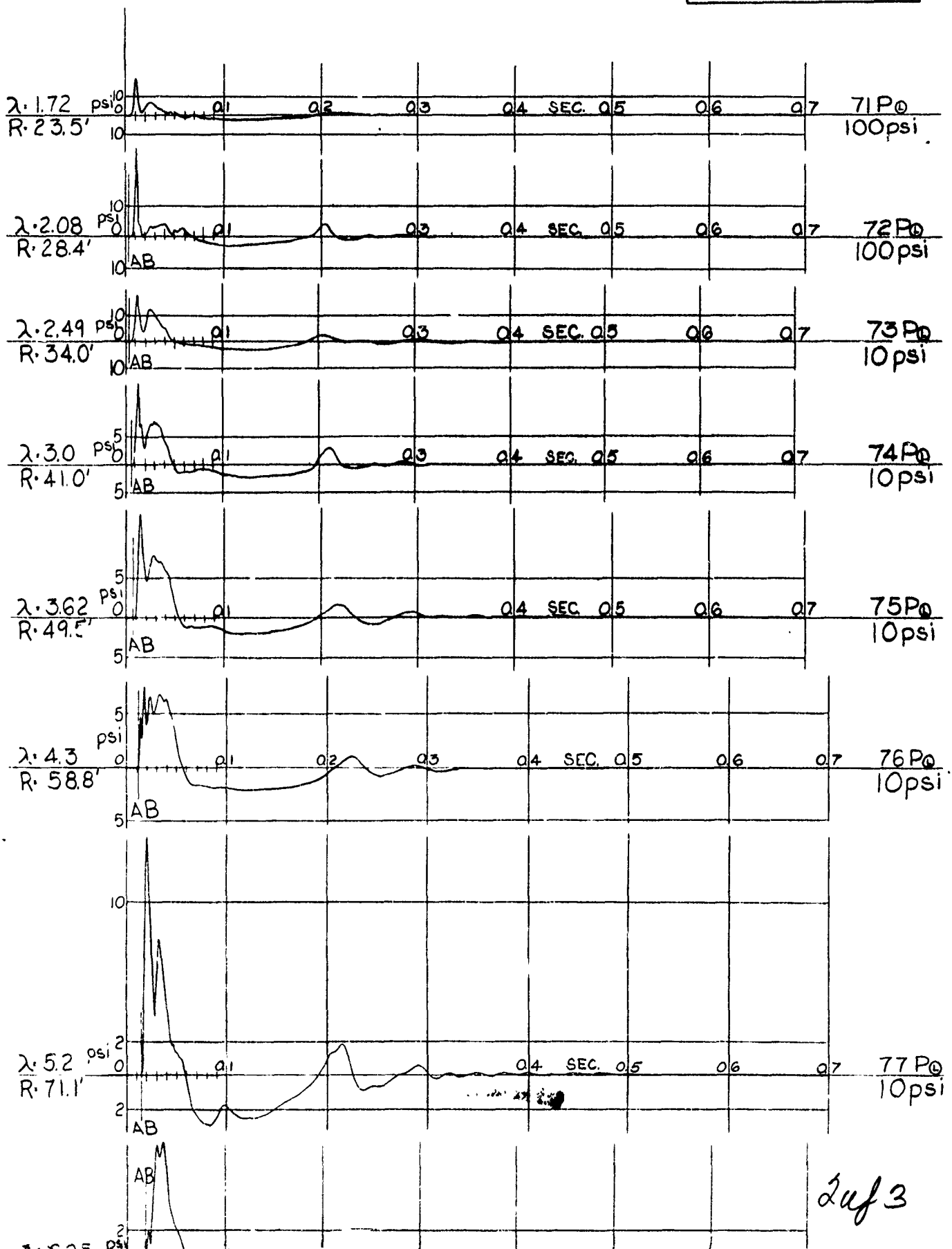

2 of 3

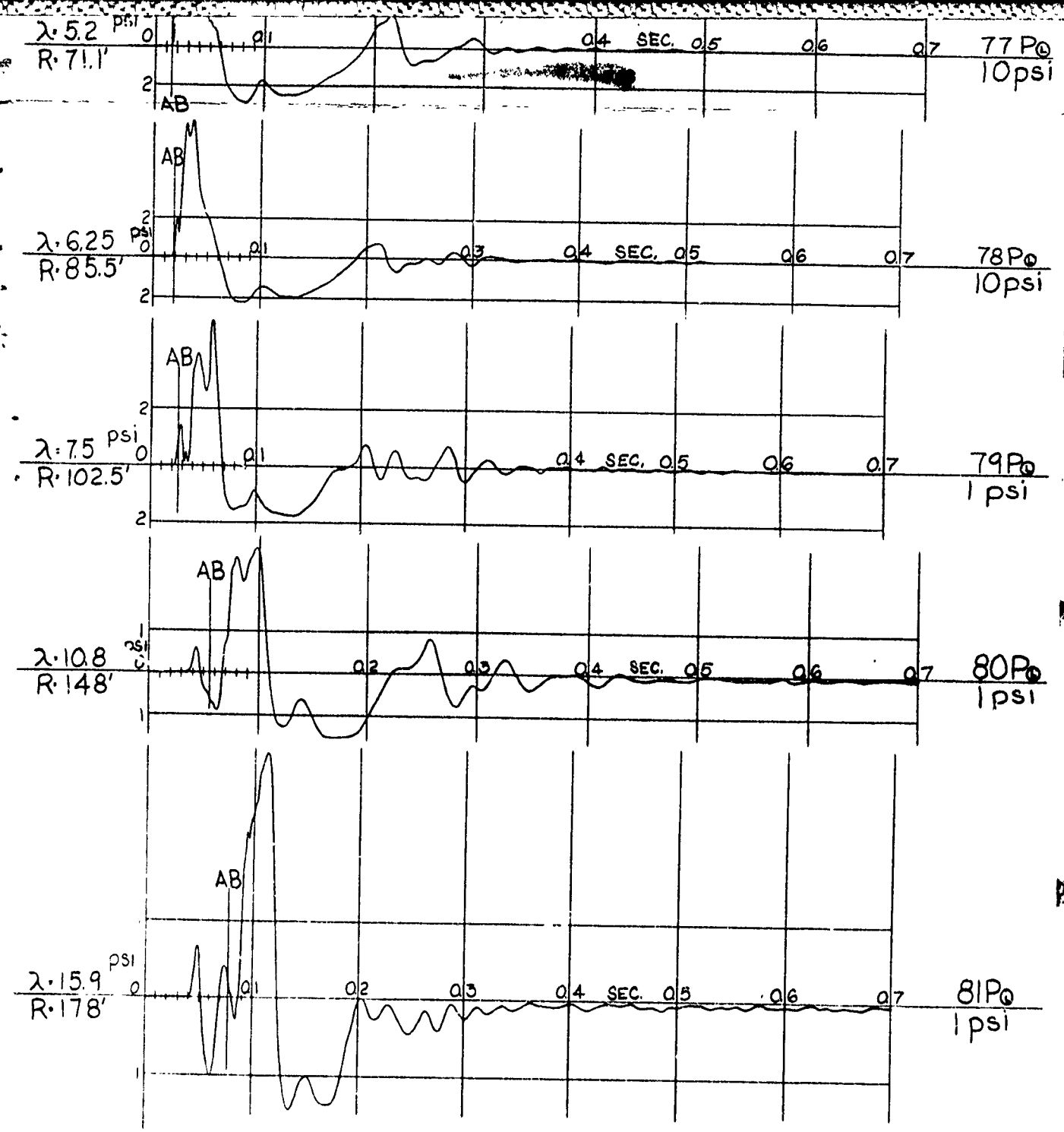

[redacted]

3 of 3

HE-4

AIR-BLAST PRESSURE

W 2560 D_c -1.9
$W^{1/3}$ 13.8 λ_c -0.135

OPERATION JANGLE

9 September 1951